Commissioning of a GafChromic EBT film dosimetry protocol at Ionizing Radiation Standards group of National Research Council

Ling Bin Xu

Medical Physics Unit

McGill University, Montreal

Submitted on June 2009

A thesis submitted to Mcgill University in partial fulfillment of the requirements of the degree of master of Science

Abstract

A GafChromic EBT film dosimetry protocol was established at the Ionizing Radiation Standards group of National Research Council. After a literature view, several aspects of EBT film dosimetry were investigated. The energy and radiation modality independence of EBT film was confirmed at the 2 % level. A calibration curve was established using a 32 point calibration curve described by a four-parameter polynomial. The darkening of EBT film is found to be significant after the first 24 hours, and up to 5 % darkening was observed over three months, which rules out the use of EBT film as an audit dosimeter. We confirmed the need for scanner uniformity correction and devised a single equation correction technique. The film homogeneity was found to be the dominant factor in dose measurement uncertainty. After establishing the film dosimetry protocol, the EBT film was used as a two-dimensional dosimeter in Monte Carlo benchmarking experiments.

Un protocol dosimétrie utilisant du film Gafchromic EBT a été établi d'en le groupe des Étalons de rayonnements ionisants du Conseil national de recherches. Après une vue de la littérature, plusieurs aspects de la dosimétrie du film EBT ont été étudiés. L'indépendance de l'énergie et le tipe de rayonnement du film EBT a été confirmé avec une precision de 2%. Une courbe d'étalonnage a été établie en utilisant une courbe d'étalonnage de 32 point décrite par un polynôme a quatre paramètres. Le noircissement du film EBT a ete jugée significative après les premières 24 heures, et jusqu'à 5% a été observé au cours d'assombrissement de trios mois, ce qui exclut l'utilisation du film EBT comme un dosimètre audit. Nous avons confirmé la nécessité de faire un correction pour l'uniformité du scanner et concu une seule equation pour la correction. L'homogénéité du film a été le facteur dominant dans l'incertitude de la mesure du dose. Après avoir établi le protocole du film, le film EBT a été utilisé comme un dosimètre à deux dimensions pour des experiences de confirmation des techniques Monte Carlo.

Acknowledgements

I would like to thank my supervisors, Dr. Malcolm McEwen and Dr. Jan Seuntjens, for their guidance in this M.Sc. thesis project. I would like to thank Dr. Carl Ross and Dr. Claudiu Cojocauru for their collaboration in the Vickers measurements and for providing Monte-Carlo simulation results. Prior to starting my project at NRC, I received EBT dosimetry training with Dr. Slobodan Devic. Dr. Erwin Podgorsak's dosimetry classes provided academic preparation for this project. Brad Downton performed Cobalt Junior irradiation. David Marchington constructed various equipments essential to his project. David Marchington and Matt Kosaki were vital in keeping the Vickers accelerator running. Stewart Walker provided electronic support in the Vickers experiment. Feridoun Farahvash provided computer support during this project. Dr. David Lewis provided useful comments on the properties of EBT film. During this project, I received financial support from the National Research Council of Canada. This project is partially funded by a CIHR Master's award.

Chapter 1 Introduction

Ionizing radiation has been used in the treatment of cancer for more than 100 years. The ability of ionizing radiation to kill cells was recognized almost immediately and within two years of the discovery by Roentgen in 1895, x-rays were being used for therapeutic purposes. Advances in radiotherapy have concentrated on accurately delivering the prescribed tumor dose while sparing surrounding healthy tissue. Advances in imaging techniques have allowed accurate location of the tumor, while improved dose delivery techniques such as Intensity Modulated Radiotherapy (IMRT) have enabled highly conformal dose delivery. In conventional radiotherapy employing simple field setups, quality assurance (QA) can be performed with single point dose measurements by measuring the dose delivered at a representative point in the treatment volume, usually with an ionization chamber. As imaging and dose delivery techniques advance, increasingly complex treatment plans are employed, and therefore rigorous quality assurance programs of both the treatment machines and individual patient treatment plans are required. The complexity means that single-point dose measurements are not adequate for QA purposes.

Since the goal of contemporary radiotherapy is to deliver uniform and conformal dose to the target volume while sparing nearby critical organs, it would be ideal to obtain three-dimensional dose information for each treatment plan. Three-dimensional dosimeters such as dosimetry gels have been developed for this purpose, but they have not progressed beyond the research phase. When a three-dimensional dosimeter is not available, one and two-dimensional dose profile measurements are needed. For this purpose, various dose profile measurement devices have been commercially introduced, and GafChromic® EBT[1], which stands for External Beam Therapy, film is one of them.

Besides radiotherapy clinics, research institutes such as National Research Council (NRC) also have needs for two-dimensional dosimeters. For routine QA of machines, it is desirable to obtain complete two-dimensional dose profiles of

[1] ISP corp, Wayne, NJ

high energy beams produced by the Cobalt-60 teletherapy machine or the Elekta clinical linear accelerator (Linac). Compared to ionization chamber based detectors, EBT films can obtain complete dose profiles in one irradiation, instead of scanning the entire field with a scanning water tank. For Monte-Carlo benchmarking, various dose profile measurement devices have been employed to measure both relative and absolute dose profiles in one and two dimensions, in order to validate predictions made by Monte Carlo simulations. For such measurements, it is desirable to employ different types of dosimetry detectors, in order to shed light on any discrepancies between experimental measurements and theoretical predictions. In this case, EBT film's chemistry-based dose measurement mechanism can provide a valuable alternative to ionization chambers traditionally employed in such investigations.

Since GafChromic EBT's introduction in 2005, more than 100 peer-reviewed articles have been published about this detector, and it is now a relatively mature field. Unfortunately, as a dosimeter designed for clinical applications, most investigations on EBT film have been clinically oriented. Currently, film dosimetry protocols described in literature tend to focus on ease of use and high patient throughput rather than higher accuracy, with IMRT QA as the primary purpose of the protocols. Currently, clinical protocols generally result in 3 % in dose measurements, while lower uncertainties are desired in a research environment. Unlike a clinical environment, IMRT QA is not the purpose of an EBT film dosimetry protocol at NRC. Instead, it is desirable to have low uncertainties (1 % or less) in absolute dose measurement, even if that means a more cumbersome and labor-intensive film dosimetry protocol. In a standards lab, it is also desirable to have higher confidence on the results of our measurements. Therefore it would be necessary to verify the claims made by the vendor of the film, rather than taking them at face value. For reasons listed above, it is necessary to establish a film dosimetry protocol unique to NRC, with every step geared towards higher accuracy rather than shorter experiment time.

This M.Sc. thesis will describe the commissioning of a highly accurate GafChromic EBT film dosimetry protocol at Ionizing Radiation Standards of

NRC. A thorough literature review will present most aspects of EBT film dosimetry reported in the literature, and the results section will describe our experimental verification of claims made in the literature and our approaches in implementing the protocol. The applications section will present sample applications of our EBT film dosimetry protocol.

The commissioning of the EBT film dosimetry protocol is my work under the guidance of my supervisor. The Cobalt Junior work presented in the applications section is a collaboration with Brad Downton. The Vickers accelerator work presented in the applications section is a collaboration with Dr. Claudiu Cojocaru and Dr. Carl Ross.

Chapter 2 Literature Review

2.1 Background and characteristics of EBT film

2.1.1 The need for a two dimensional dosimeter

Other than primary dosimeters used in primary standards labs, the gold standard of measuring dose in high-energy radiation is the ionization chamber. In high energy beams, a Farmer type or parallel plate ionization chamber calibrated at a primary or secondary standards lab is usually the instrument that links all other dosimeters to a primary dose standard. The reference-class ionization chambers provide highly accurate dose measurements at the 0.5 % level, but they can only measure dose at one point. When dose distribution measurements are desired, reference class ionization chambers can be used in a scanning water tank, but their relatively large measurement volume and the high cost of replacing them make them unattractive for scanning work. Instead, smaller ionization chambers not designed for reference dosimetry are often used. In addition, diodes can also be used with a scanning tank to achieve high spatial resolution. Whether a scanning chamber or diode is used in a water tank, the sequential measurement leads to long measurement time when measuring two dimensional dose profiles. The difficulties in setting up a water tank also makes chamber or diode scans undesirable in routine clinical application or everyday research.

2.1.2 The drawbacks of chamber and diode based 1-D and 2-D arrays.

One and two-dimensional arrays based on multiple ionization chambers or diodes are a popular choice for measuring dose profiles in high energy radiation. Compared to water tank based solutions, detector arrays such as SunNuclear[2] Profiler™ or DoseMap™ can be used in plastic phantoms, making the experimental setup easier. The simultaneous measurement of doses at multiple positions leads to much smaller monitor unit (MU)'s required for sufficient statistics, therefore reducing measuring time significantly. The detector arrays, however, suffer their own setbacks. Since all detectors are fixed in position, the

[2] SunNuclear

spatial resolution of detector arrays is limited by the detector spacing. Moving the entire array by a small offset helps improve spatial resolution, but such an approach is limited by mechanical positioning accuracy. For chamber based arrays, the need for a relatively large air volume means that high spatial resolution can only be achieved in one dimension. These large detectors also make dose measurements in high gradient two-dimensional fields difficult. Due to the cost of producing each individual detector, detector arrays either have high 1-D resolution and limited number of lines, such as the PTW[3] Starcheck, or have a complete Cartesian grid but lower spatial resolution, such as the SunNuclear MapCheck™ or PTW Seven-29. Therefore, a dosimetry device that provides high resolution two-dimensional dose distribution in a field is desired. Currently, film is the only option available.

2.1.3 Brief history of radiochromic films

Radiographic films used in diagnostic radiology were used widely before affordable radiochromic films were introduced. Based on silver halide film technology of the photographic industry, radiographic films were designed primarily for detecting low energy kilovoltage radiation. The drawbacks of radiographic films are the need for dedicated developers and darkrooms and the presence of silver which causes strong energy dependence in film response. For quantitative dose measurements in megavoltage beams, radiochromic films were developed. Radiochromic films change color when exposed to ionizing radiation, and do not require a developer or a darkroom facility. Earlier versions of radiochromic films required dose levels of 1000 Gy, and were limited to industrial irradiation facility use (Lewis, 2009). As film production technology improved, radiochromic films like the MD-55 were introduced to clinical and research environment for megavoltage beams, as they required doses in the 50-100 Gy range. However, across a sheet of MD-55 film, the sensitivity varies by up to 15 %. Such sensitivity variation makes MD-55 unattractive for accurate dose distribution measurement. The latest model of radiochromic film, GafChromic

[3] PTW Freiburg GmbH

EBT claims high sensitivity at the 2 to 8 Gy level, uniformity at 1.5 % level, and energy independence from Co-60 to megavoltage Linac beams.

2.1.4 Introduction of EBT film

Introduced in 2005, GafChromic EBT (External Beam Therapy) film is the latest generation of radiochromic film. Since radiochromic film dosimetry is a relatively small field, ISP is the only provider at the time of writing. ISP's previous models of RCF include HD-810, MD-55, and HS. Such models have been used in 2-D dose distribution measurements, but their low sensitivity prevented their routine use in the clinical environment. With the introduction of model EBT, clinical applications such as patient-specific IMRT verification became feasible and extensive literature has been published on the characteristics and applications of EBT film.

2.1.5 Current state of EBT film dosimetry

Unlike the radiographic films conventionally used in the clinical environment, irradiated EBT film does not absorb the visible light spectrum uniformly. As it turns blue after irradiation, the strongest absorption occurs in the red part of the spectrum. Therefore, conventional radiographic scanners such as the Vidar scanner have been shown to be inferior for EBT film dosimetry, while flatbed scanners such as the Espon 1680Pro and 10000XL have been recommended by ISP. Currently EBT film is primarily used for IMRT plan verification, with the gamma index set to 3 % in dose, 3 mm distance to agreement for most clinical environment (Saur *et al* 2008, Chung *et al* 2008). Lower uncertainties have been claimed by various authors, but the published results have been limited to one dimensional comparisons between film and ionization chamber scans. Averaging of multiple films irradiated in the same field have been shown to reduce uncertainty significantly, as the film uniformity is the dominating factor in measured dose uncertainty (Battum *et al*, 2008). Due to the water-equivalent nature of EBT films, multiple film pieces can be stacked to obtain 3-D dose distributions (Chiu-Tsao *et al*, 2008).

2.1.6 Composition of EBT film

Unlike silver-halide based radiographic films, the active component of EBT film is based on a low-Z material and has an estimated effective atomic number, Z_{eff}, of 6.98 (Lewis, 2009). This makes EBT film water-equivalent for dosimetry purposes, as water has an effective atomic number of 7.3. The elemental composition of the active layer of EBT film has been reported by the manufacturer as: Carbon (42.3 %), Hydrogen (39.7 %), Oxygen (16.2 %), Nitrogen (1.1 %), Lithium (0.3 %), and Chlorine (0.3 %). Note that Chlorine has an atomic number of 17 and is not desirable in a water-equivalent dosimeter. Small amounts of Chlorine was added to improve energy independence in film's response to beams with lower energies. (Devic, private conversation). Due to its low Z_{eff}, EBT film has shown much lower energy dependence than silver-halide based Kodak[4] EDR-2 radiographic film. (Fuss *et al*, 2007) In fact, no literature to date has reported a significant energy dependence of EBT film. The expected energy independence of EBT film in photon beams is based on the relative contributions of photoelectric effect and Compton interaction. For high-Z materials such as silver used in radiographic films, the photoelectric effect is the dominant interaction in the kV energy range, while Compton interaction is the dominant interaction in the MV energy range. The changing dominance of the two interactions from low to high energy photons for high-Z materials causes significant energy dependence of radiographic films. For low-Z materials, on the other hand, Compton interactions are dominant in both kV (30 keV and up) and MV energy ranges. Therefore little energy dependence is expected for EBT film. Note that the water equivalent design of EBT film causes it to have relatively low sensitivity compared to radiographic films, especially in the kilovoltage range. Therefore, EBT film is not suitable for radiology purposes, as it requires a very large dose to form an image. For such applications, ISP offers another line of film, the XR-QA, where high-Z materials are added to the sensitive layer composition to enhance film sensitivity in the kilovoltage range. XR-QA film will not be discussed further in this thesis.

[4] Eastman Kodak Company, Rochester, NY

Structurally, EBT film contains two active layers of 34 μm each separated by a 6 μm surface layer. A Polyester base of 97 μm was added to each side to protect the active layer and provide mechanical rigidity. EBT film has a reported density of 1.1 g/cm^3 (Chiu-Tsao *et al*, 2005), which is close to the density of water. The film was designed with two active layers to achieve maximum sensitivity without compromising uniformity. Note that such design may potentially cause problems in very high spatial resolution dosimetry work, as the point of measurement is not at the center of film in a radiation field with steep dose gradients. At time of writing, this dual-layer feature of EBT film has not been a limiting factor in spatial resolution of film dosimetry, as most authors in literature report spatial resolutions of 1 mm or worse.

2.1.7 Comparison of EBT and MD-55

Before the model EBT, MD-55 provided by ISP was the dominant radiochromic film used in both industrial and clinical environments. Its primary drawback was the low sensitivity, slow development, and poor uniformity. MD-55 and EBT are both based on monomer crystals that turn into polymer crystals upon radiation, which have different light absorption properties (Rink *et al*, 2005). As shown in Figure 2.1, the MD-55 crystals are sand-like structures while EBT crystals are stick-like structures. The elongated crystals found in EBT films are responsible for the much shorter development time compared to MD-55. The non-circular crystals are also the cause of the polarizing nature of EBT film. When used in a film reading device with a polarized light source or detector such as a flatbed scanner, the orientation of EBT film becomes critical.

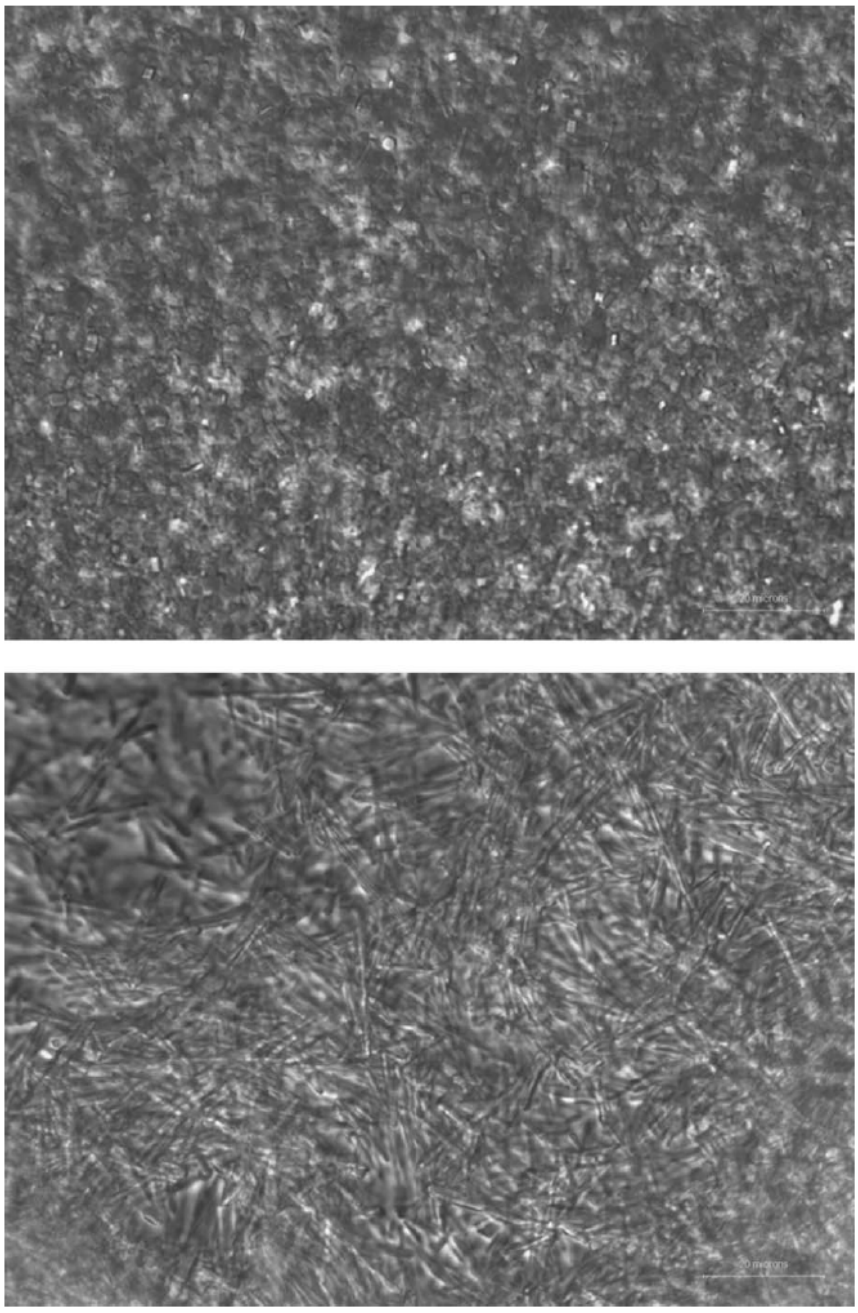

Figure 2.1. Microscope images of MD-55(top) and EBT (bottom) films, published by Rink *et al* (2005).

2.2 General EBT dosimetry work flow

2.2.1 Calibration phase

The calibration phase of EBT dosimetry refers to establishing the sensitivity curve of a batch of EBT films. EBT film does not respond linearly to radiation, requiring an empirical calibration that produces a non-linear calibration curve. No consensus has been reached on the ideal equation, but a second or higher order polynomial is often used as the calibration equation, based on Taylor's theorem (Devic *et al* 2005, Battum *et al* 2008, and Saur *et al* 2008). Since there is no physical reason for the film to have a dose threshold, the constant term of the calibration equation is generally assumed to be zero. With that in mind, the general calibration procedure as described in the literature comprises the following steps:

1. Cut a sheet of film into multiple pieces. Standard clinical practice uses eight, but research work often uses ten or more pieces.
2. Deliver a known dose to each piece. This is usually done in a solid phantom, using either Linac MU reading or Farmer-type chamber to measure the dose delivered.
3. Wait a fixed length of time, read the film with scanner. Correct for scanner artifacts such as scanner fluctuation and light scattering effect. Get the change of optical density in the film due to each specific dose.
4. Obtain a calibration data set consisting of multiple dose-optical density (OD) pairs.
5. Fit the calibration data with an equation containing two to four parameters. There is considerable difference between authors in the number of parameters and the particular equations used. This will be investigated further in this thesis.

2.2.2 Measurement phase

In the measurement phase, a blank EBT film is irradiated in the radiation field of interest, and scanned in the same scanner as used for calibration. Since this

film needs to be larger than the field being investigated, a large sheet of film is usually used. The large size of the film requires further corrections due to the scanner lamp light scattering effect. This effect will be discussed in detail in subsequent sections of the literature review. The steps in the measurement phase are as follows:

1. Irradiate the experimental film in the unknown radiation field.
2. Wait the same time, and then scan the film.
3. Correct the image for any scanner artifacts. Note that different types of scanner artifacts need to be addressed in measurement phase compared to calibration phase.
4. Convert the corrected image into a dose distribution, by converting optical density values into dose, and pixel index into spatial position.

2.2.3 The topics of interest in this literature review.

In this literature review, I will focus on the steps and choices that influence the accuracy of EBT film dosimetry. The following topics will be introduced:

- Choice of scanner
- Darkening due to scanner lamp
- Scanner fluctuation
- Scanner noise and pre-scanning
- Calibration curves and the equations used to describe them in literature
- Energy and beam modality dependence of EBT film
- Scanner uniformity effect (light scattering effect)
- EBT film development after irradiation
- Humidity effect
- Application of EBT film in one-dimensional dose measurement
- Application of EBT film in two-dimensional dose measurement

2.3 Scanners used in literature

Although the currently recommended scanner for EBT film is a flat bed scanner designed for professional photographic use, other film optical density measuring devices have been investigated in the literature. Within the realm of flat bed scanners, various models have been investigated by various authors before the Epson 1680Pro and its successor 10000XL were recommended as the ideal scanner for EBT film dosimetry. In this chapter, we will review the various types of film readers reported in the literature.

2.3.1 Film readers other than linear CCD-array based scanners.

Unlike radiographic films, radiochromic films such as GafChromic EBT do not absorb all visible light uniformly. Even more importantly, the absorption spectra of radiochromic films change significantly after exposure to ionizing radiation. This effect means an ideal film reader should be most sensitive to the absorption peak of the EBT film. Figure 2.2 illustrates the absorption spectrum of EBT film before and after exposure to radiation, where a strong peak in the red visible light region suggests that the ideal EBT film reader should have maximum sensitivity in the red region.

In Devic *et al*'s 2004 paper, seven film digitizers were compared for use in reading the GafChromic HS model film, which is a radiochromic film similar to the EBT model. The film digitizers investigated were LKB Pharmacia UltroScan XL, Molecular Dynamics Personal Densitometer, Nuclear Associates Radiochromic Densitometer Model 37-443, Photoelectron Corporation CMR-604, Laser Pro 16, Vidar VXR-16, and AGFA Arcus II document scanner. Of these seven, the four digitizers including Victoreen, LaserPro16, Molecular Dynamics, and LKB pharmacia were non-CCD based digitizers. These detectors are more expensive than a CCD based scanner and are cumbersome to use. The investigation showed that non-CCD based film readers show similar or inferior performance to CCD based scanners in spatial resolution, sensitivity, and measurement accuracy. The conclusion is that CCD based film readers are

the better choice for film digitization than non-CCD based readers. There has been no further literature that challenges this conclusion.

CCD based film readers can be grouped into linear CCD array based film scanners and two-dimensional CCD camera based film readers. Chiu-Tsao *et al* (2005) used a CCD camera based densitometer with interchangeable red and green light boxes, but the red light employed missed the absorption peak of EBT film, causing the green channel to be more sensitive than the red channel. The drawback of such a system is the high cost of the instrument and the low resolution due to limits of the CCD camera. Keller *et al* (2008) demonstrated the use of a digital microscope in very high resolution EBT film dosimetry, by mounting the film of interest on a translational stage. Even though very high spatial resolution can be achieved, the high cost of such a system and extremely long time required for reading large films makes such a technique unfeasible at most institutions. Therefore, linear CCD array based scanners are the most appropriate choice for EBT film dosimetry. In the next section, we will examine the comparison between film scanners designed for radiographic purposes and film scanners designed for photographic purposes.

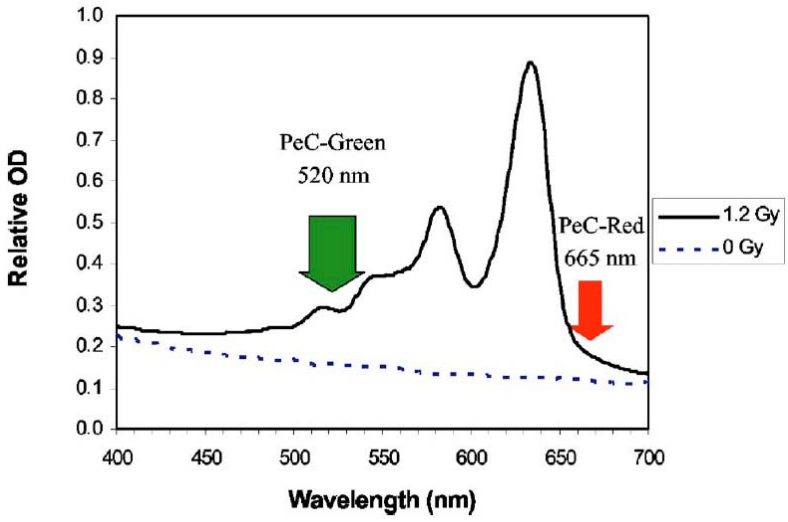

Figure 2.2. Absorption spectra of EBT film (Chiu-Tsao *et al*,2005). Note that the authors used CCD based densitometers with interchangeable red and green light source, which is different from broad spectrum light source of photographic scanners used today.

2.3.2 Scanners designed for radiographic films

Before the introduction of affordable and sensitive radiochromic films, radiographic films such as the Kodak EDR2 were used for dose measurement in clinical environments. Specially designed clinical film scanners such as the Vidar VXR-16 were used to read the black and white radiographic films. Compared to color scanners, greyscale scanners such as the Vidar VXR-16 offer superior performances in measuring black and white films. For radiochromic films, however, clinical scanners do not offer any advantage compared to inexpensive flatbed scanners such as the Epson 1680Pro. In Devic *et al*'s 2004 paper comparing seven scanners, the Vidar VXR-16 was shown to be inferior to the AGFA Arcus II photo scanner. Various other papers have confirmed that the Vidar VXR-16 is inferior to flatbed color scanners such as the Epson 1680Pro (Wilcox *et al*, 2007). The primary drawback of greyscale scanners such as the Vidar VXR-16 are their broad spectrum sensitivity. By averaging over the entire visible light spectrum, radiographic scanners are far less sensitive than the red channel of color scanners, which use red filters in front of CCD elements to selectively capture red light. This lack of spectrum sensitivity can be improved by installing a red filter in front of the Vidar's scanner lamp, as suggested by ISP (www.isp.com). For institutions that do not already own a radiographic scanner, however, buying a flat bed color scanner is a far more economical solution. The Vidar VXR-16 costs more than $20,000, while the best flat bed color scanner, the Epson 10000XL, presently costing $3000.

Another drawback of the Vidar scanner is the use of rollers instead of a glass bed in the scanning mechanism. The mechanical movement of film produces additional artifacts (www.isp.com). Given the high cost and various issues associated with radiographic scanners, they are not recommended for EBT film dosimetry.

2.3.3 General design of flatbed scanners

Given the drawbacks of radiographic scanners, the recommended scanner for EBT film dosimetry is a flat bed photo scanner. Flatbed scanners record an image by moving both a light source and a linear CCD array along the scanner bed to record the object on the glass bed. All flatbed scanners are capable of reflection mode, in which a light source is located next to the CCD array and light reflected from an opaque object is recorded by the CCD array. For film measurements, however, canners capable of transmission mode are preferred, since scanning in transmission mode reduces light scattering due to the white reflection backing. In this case, the scanner is equipped with a light source above the glass bed, while the CCD array is underneath the glass bed. The light source and the CCD array are moved along the scanner bed, and light transmitted through the film is recorded by the CCD. This requirement rules out scanners in the $100 range, as they do not have transmission mode capability. For the image produced, it is desirable to have as little image processing done by the scanner software as possible. Therefore flatbed scanners will need to have a "professional mode", where all image enhancement and manipulation can be turned off manually. The image file need to be saved in uncompressed format to avoid compression artifacts, and "positive film" scanning mode is used to avoid artifacts introduced in the image inversion process. Such requirements limits the scanners used in EBT film dosimetry to the "photo scanner" class, which starts at around $500 and goes up to $3000.

2.3.4 Flatbed scanners recommended in the literature - Epson 1680Pro and 10000XL

Among the many models of flat bed photo scanners available, the Epson 1680Pro is the most commonly used in literature, as it was recommended by ISP. Currently the Epson 10000XL is the scanner recommended by ISP, as the 1680Pro has been discontinued. Both scanners are designed for professional photographic purposes, and offer the capability of scanning an entire 8 ×10 inch EBT film at once in transmission mode. The difference between such high-end

scanners and cheaper consumer models is that a cold Xenon lamp is used in professional models while a fluorescent lamp is used in consumer models. (www.epson.com) Even though most articles in literature use the 1680Pro model, recent literature have shown similar performance for the 10000XL. Chung *et al* (2008) established a basic EBT protocol using both 1680Pro and 10000XL, but did not address most of the artifacts presented in the literature. The results were comparable within experimental uncertainty. Martisikova *et al* (2008) reported a more comprehensive GafChromic EBT dosimetry protocol utilizing the 10000XL, and the characteristics of the scanner are similar to that of 1680Pro reported in the literature. Therefore, reported characteristics of the 1680Pro when used in EBT dosimetry can be expected of the 10000XL. In this literature review, most results were obtained using 1680Pro, as the 10000XL was only recently introduced by Epson and not enough literature is available at the time of writing. Note that even though HP is a prominent manufacturer of office scanners, its scanners often lack the transmission scan capability. However, Epson's Expression line of photographic scanners has been very popular among professional photographers who need to scan negatives of color films. This may be why Epson scanners are the only ones reported in literature for EBT film dosimetry.

Compared to the Epson 1680Pro and other scanners, the Epson 10000XL has a significantly larger scanning area. The 10000XL has scanning bed of 310 mm by 437 mm, while the Epson's other photo scanner, the V700, has a scanning bed size of 216 mm by 297 mm. Such large scanning area offers greater potential in ignoring scanner uniformity corrections, as the film edges are far away from the edge of scanning bed. In clinical environments, this is desirable because it offers a simplified protocol and saves time.

2.3.5 More economical scanners

Other than the Epson 1680Pro and 10000XL, other photo scanners have also been reported in the literature, often due to their availability at a particular institution or low cost. Devic *et al* (2006) reported an EBT protocol using the

AGFA Arcus II, while Menegotti *et al* (2008) reported a comparison of Epson 1680Pro and V750 scanners when used in EBT film dosimetry. In Menegotti *et al*'s report, the V750 and 1680Pro both resulted in 98 % passing pixel for 3 %, 3 mm gamma index of less than 1 %. The AGFA scanner has been discontinued for a few years, but the V750 represents a class of photo scanners designed for non-professional use. These scanners are inexpensive compared to professional models, but the fluorescent lamp used in these scanners is a major drawback for EBT dosimetry. Prolonged exposure to indoor fluorescent light is also not recommended (Devic, private conversation). Even though radiochromic films are designed to be insensitive to visible light, they have been found to be sensitive to direct sunlight. The sensitivity to sunlight is due to the UV component of sunlight. Scanner lamps that contain UV components are not suitable for EBT film dosimetry. The next section is devoted to the scanner lamp darkening effect of professional class scanners.

2.4 Scanner lamp darkening

Since EBT film is known to be sensitive to sunlight and prolonged indoor fluorescent light exposure, the effect of scanner light on the EBT film is a valid concern. Various authors have acknowledged the potential darkening effect of the scanner lamp when reporting their EBT film dosimetry protocol utilizing the Epson 1680Pro (Battum *et al,* 2008), but few have investigated this effect in detail.

In Paelinck *et al*'s 2006 paper, increasing optical density as a piece of EBT film is successively scanned was reported. The scanner used in this case is the 1680Pro. This result has been quoted by some authors as the reason to avoid scanning EBT film multiple times. The reported effect is shown in Figure 2.3, where increasing optical density in each successive scan is evident. The conclusion that the film is darkened by the scanner lamp, however, has been challenged by Lynch *et al* (2006) .

Lynch *et al* also reported increasing optical density with successive scans, but they investigated this effect in more detail by measuring the scanner bed temperature during each scan. The result is shown in Figure 2.4, where optical density and scanner bed temperature show a linear relationship. The authors noted that this effect is temporary, and repeated scanning of up to 1000 times does not result in permanent film optical density change. This project also investigated the multiple scanning and the scanner temperature effect for the 10000XL.

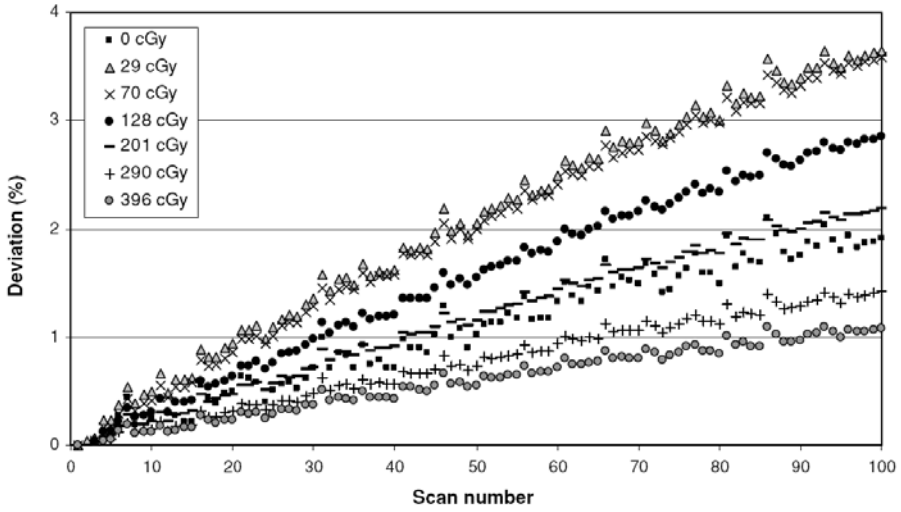

Figure 2.3. Increasing optical density in successive scans reported by Paelinck *et al* (2006).

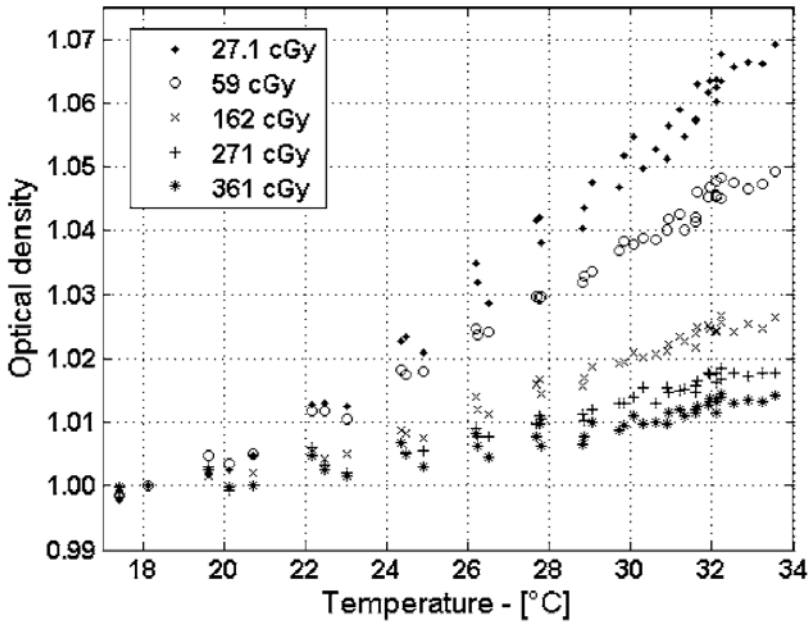

Figure 2.4. Increasing optical density in successive scans due to increasing scanner temperature (Lynch *et al,* 2006) .

2.5 Scanner warm-up and fluctuation

2.5.1 Scanner warm-up

When the scanner lamp is first turned on, it is expected that the lamp requires a finite time to reach a stable temperature, as the heat accumulation from the scanner lamp reaches an equilibrium with heat loss into surrounding air. In certain models of scanners such as the AGFA Arcus II, the scanner lamp can be kept on by leaving the scanner cover up at all times. For newer scanners however, the supplied scanner software does not allow the lamp to be kept on all the time. Therefore, the first few scans after a scanner has been idling for a few hours could be unstable. Various authors have reported scanner warm-up effect and implemented corresponding procedures in their protocols. For scanners based on fluorescent lamps, up to three scans were required for the lamp to become stable (Devic *et al*, 2004). For the Epson 1680Pro, it has been shown that the lamp warm-up effect can be reduced to negligible level by performing a preview before actual scanning. Figure 2.5 provides an example (Paelinck *et al*, 2007). Given that a preview is already required to verify the positioning of the film, scanner warm-up effects for the Epson 1680Pro can be ignored. Other authors have confirmed that scanner warm-up effect for Epson 1680Pro is not significant (Battum *et al*, 2008). Recent literature using 10000XL have shown similar behavior, as shown in figure 2.6 (Martisikova *et al*, 2008).

2.5.2 Scanner fluctuation

Various authors have reported scan-to-scan stability of the 1680Pro, with values ranging from 0.2 %(Martisikova *et al*, 2008) to 0.7 %. Note that the larger fluctuations are reported for day to day scanner fluctuations (Fuss *et al*, 2007). It is interesting to note that Fuss *et al* reported 0.03 % fluctuation over the time scale of a few minute, but 0.7 % fluctuation over the time scale of days. This suggests that scanner fluctuation may not be a Gaussian process, and detailed characterization of scanner fluctuation is necessary. This project will study the

fluctuation of scanner in detail, and devise a correction to account for the lack of scanner stability over many days.

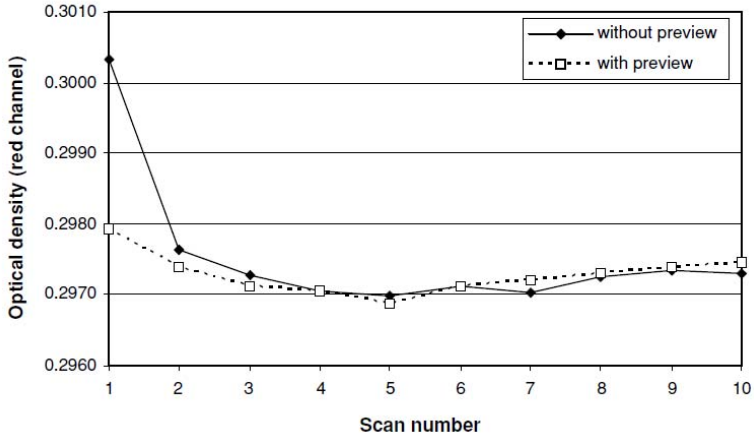

Figure 2.5. Scanner warm-up effect reported by Paelinck *et al* (2007). A preview action reduces the scanner warm-up effect to less than 0.2 %, when 1680Pro is used.

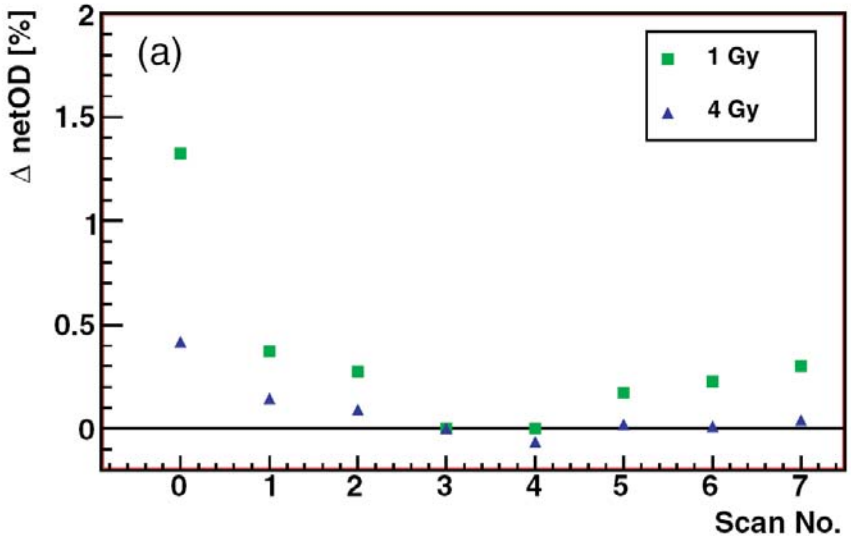

Figure 2.6. Scanner warm-up effect reported by Martisikova *et al* (2008), using 10000XL. Note that the authors did not perform a preview. Even though the scanner response reaches a minimum after four scans, the difference between second and fourth scans is less than 0.5 %.

2.6 Scanner noise and pre-scanning

2.6.1 Scanner noise and multiple scans

At the single pixel level, noise determines the limiting spatial resolution of a film dosimetry protocol. Unlike artifacts, noise can not be corrected because it is unpredictable. Noise in measured dose using radiochromic film has two sources: noise due to scanner electronics and noise due to film grain. Noise due to scanner refers to electronic noise inherent to CCD detectors, and can potentially be reduced through repeated scanning. Noise due to film grain, on the other hand, cannot be reduced by repeated scanning. Note that today's flatbed scanners natively scan at extremely high resolution, on the order of 4800 DPI (dot per inch). Scanning at such high resolution, however, is very slow. Therefore most protocols reported in the literature scan at between 72 to 100 DPI, or about 0.2 to 0.3 mm pixel size. Such resolution implies inherent averaging of raw data from CCD. Earlier protocols utilizing older scanners have demonstrated the significance of scanner electronic noise and incorporated repeated scanning to reduce uncertainty due to noise (Devic *et al*, 2005). Researchers using the Epson 1680Pro scanners, however, have not demonstrated significant scanner electronic noise at the 100 DPI resolution. Some protocols utilizing the 1680Pro do employ multiple scanning techniques due to previously published protocols utilizing older scanners. Most recent protocols utilizing 1680Pro or 10000XL, however, do not average multiple scans to lower scanner electronic noise. Battum *et al* (2009) scanned multiple neutral density filters using a 1680Pro scanner at 72 dpi, and reported single pixel scan accuracy of 0.5 % (2 SD) for filters whose optical density are between 0.3 and 2.5. Since EBT film's optical density is generally less than 1, this result indicates that scanner electronic noise can be neglected for 1680Pro, and likely for 10000XL as well. Note that the Epson 1680Pro and 10000XL are the same class of scanners and utilize the same type of lamp. Their similarities in light source and target user group, combined with the expectation that electronics generally get better with subsequent releases, suggest that 10000XL's electronic noise is at the same level as, or lower than, the 1680Pro.

2.6.2 Pre-scanning techniques described in literature and background correction reported by various authors

In EBT film dosimetry, the measured absolute dose is related to net optical density via a calibration curve. The net optical density describes the change in optical density before and after exposure to ionizing radiation, therefore it is necessary to measure the optical density of blank EBT film in order to obtain net optical density measurements. However, it is interesting to note that in the literature, more than one background signal has been defined. Devic *et al* (2005) suggested that the background pixel value should be defined as the measured pixel value of black opaque cardboard. Other authors such as Battum *et al* described the pixel values measured when scanning the scanning bed without anything on the glass, and incorporated a correction factor for it. The following equation was reported by Devic *et al,* and adopted by Martisikova *et al* as their definition of net optical density:

$$netOD = OD_{\text{exp}} - OD_{\text{unexp}} = \log_{10}\left(\frac{PV_{\text{unexp}} - PV_{\text{bckg}}}{PV_{\text{exp}} - PV_{\text{bckg}}}\right)$$

where PV_{unexp} refers to the pixel value of blank EBT film, PV_{exp} refers to pixel value of exposed EBT film, and PV_{bckg} refers to pixel value of opaque black cardboard. In such protocols, it is necessary to pre-scan each EBT film before irradiation, to correct for lack of homogeneity in the protective layer of EBT film. However, there is no consensus on the need for pre-scanning. Saur *et al* (2008), for example, did not perform any pre-scanning or background correction of the glass plate.

2.7 Calibration curve reported in literature

For a non-linear detector such as EBT film that does not have theoretical models describing its expected response, the calibration curve provides a link between delivered dose and measured film response through empirical data. GafChromic EBT films are sold in boxes, with 25 sheets per box. Each box has a batch number, but different boxes can have the same batch number. According to ISP, every batch of EBT film meets or exceeds a minimum sensitivity, but no maximum sensitivity is specified for a particular batch of film. Therefore it is necessary to calibrate each batch. Since the calibration curve is an empirical fit with arbitrary equations, it is desirable to have a large number of data points in order to investigate the goodness of fit. On the other hand, due to the small number of films contained in each box, it would be labor intensive to perform a calibration with many points for each batch in a clinical environment. As a compromise, the most popular clinical protocol involves eight pieces of film, of which seven are irradiated one at a time. This provides seven data points for fitting with a two or three-parameter equation that crosses the origin. Even with this approach, various protocols reported in the literature differ in dose delivery and curve fitting. This section will investigate these two aspects of establishing a calibration curve as reported in literature. Before such comparison, the issue of film orientation will be introduced, even though a consensus has been reached in the literature on this topic.

2.7.1 Film orientation

EBT film response in a flatbed scanner has been shown to depend on the film orientation. This dependence arises from the coating direction of the needle-like polymer used as the active component in EBT film (Saur *et al*, 2008). The film is supplied as 8 x 10 inch rectangular sheets, and the designation of orientation is shown in Figure 2.7. The portrait orientation refers to aligning the long edge of the film against the long edge of the scanner bed, while the landscape orientation refers to aligning the short edge of the film against the long edge of the scanner bed. Extensive literature has been published on this

subject, with the same conclusion that it is important to maintain the same orientation in the calibration and the dose measurement phase. One example of the effect of rotating the film is shown in Figure 2.8. When the film is rotated 180 degrees or flipped from one side to the other, no measurable effects have been reported (Battum *et al*, 2008). Note that Lynch *et al* (2006) reported a very large (up to factor of five) effect on measured optical density when a piece of EBT film is rotated 90 degrees in a Microtek ScanMaker i900 flatbed document scanner, while the Epson 1680Pro only suffered 15 % change in optical density when the film is rotated. This reinforces the notion that a particular type of flatbed scanner needs to be thoroughly investigated before an EBT film dosimetry protocol is established with it.

Note that ISP recommends landscape orientation for EBT film scanning in flatbed scanners, due to its higher signal to noise ratio. In this project we chose the portrait orientation because it reduced the magnitude of the lateral correction needed when a whole sheet of EBT film is scanned. Our investigation revealed that the higher signal to noise ratio does not reduce the dose uncertainty significantly, as the uncertainty is dominated by film sensitivity fluctuations.

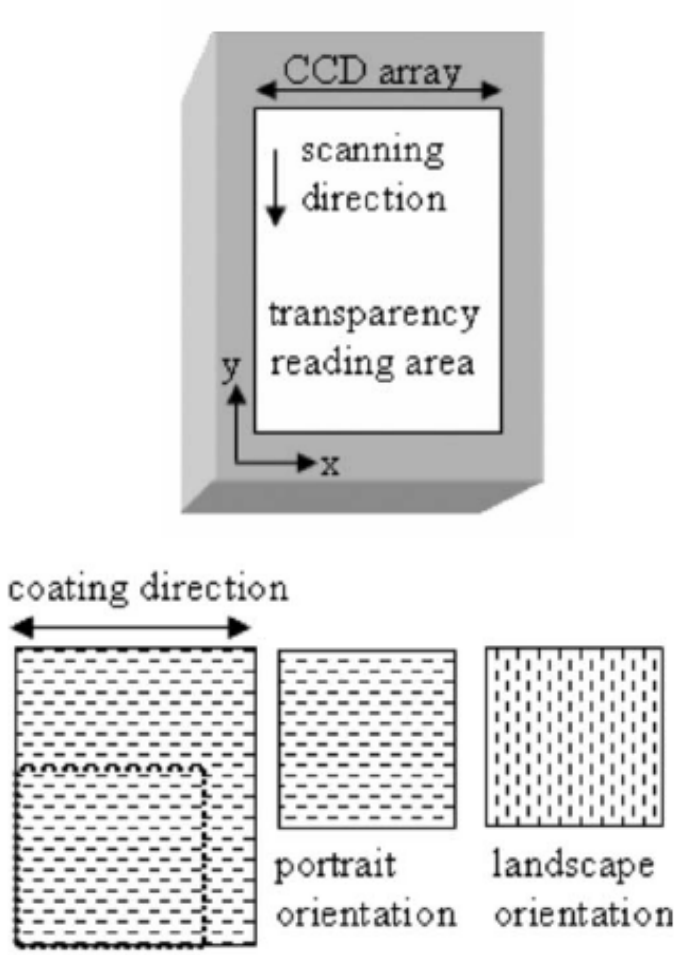

Figure 2.7. Illustration of EBT film coating and the designation of film orientation when scanned in a flatbed scanner (Saur *et al*, 2008). Note that this designation is widely used in literature and will be adopted in this thesis.

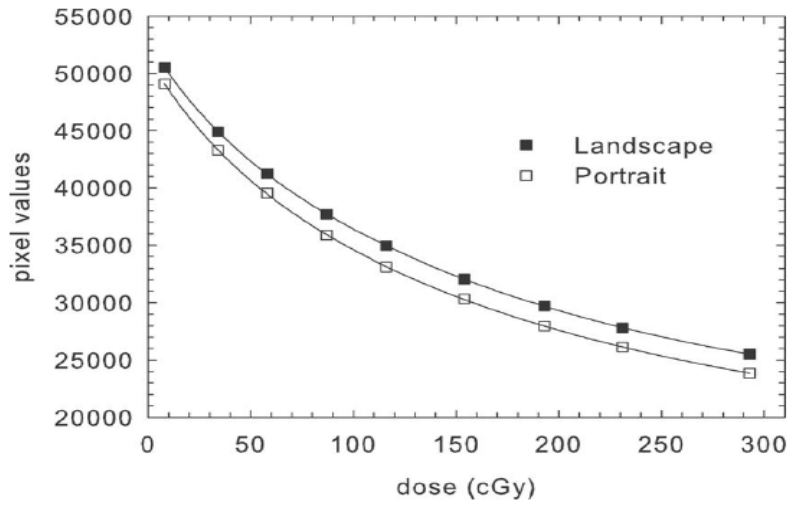

Figure 2.8 Example of film orientation's impact on calibration curve reported (Saur *et al,* 2008).

2.7.2 Dose delivery

EBT film calibration is generally carried out in a plastic phantom, where EBT films are irradiated to a known dose. The most accurate approach involves cutting an 8 x 10 sheet of EBT film into several pieces, and each piece is irradiated in a solid phantom. In this case, the dose to a particular area of film can be accurately measured with an ionization chamber, which is placed in the position of the film and exposed to the same beam as the film. This is done before film irradiation is performed. The drawback of such approach, however, is the relatively long (1 hour or more) experimental time, as each data point corresponds to entering the linear accelerator room and replacing the film. Since each box contains only 25 sheets of film, it is desirable to have a faster calibration procedure in clinical environment. Various authors have reported techniques of delivering different doses to different parts of a sheet of film at once. Battum *et al* employed a dynamic step and shoot dose step-wedge field with 8 dose steps. The experiment was performed in water and the dose step wedge was calibrated with an ionization chamber in water (Battum *et al*, 2008). Menegotti *et al* (2008) irradiated a single film to six levels of dose using asymmetric fields. The dose delivered was verified with a PTW Seven29™ 2D

chamber array and a PTW 31013 ionization chamber. Such techniques significantly shorten the calibration time, but the authors have not demonstrated good dosimetric accuracy of their approach. Currently most reported protocols still irradiate different pieces of EBT film sequentially. Such approach requires entering the linear accelerator room multiple times, but dosimetry accuracy can be better than 1 %, based on the clinical implementation of the TG-51 protocol (Almond *et al*, 1999).

We would like to draw the attention to the difference between dose to EBT film and dose to water in absence of EBT film. For ionization chambers, cavity theory is used to convert dose to air inside the chamber cavity to dose to water in absence of a chamber cavity. For film dosimetry, the EBT film is assumed to be water equivalent, and its effect on absorbed dose is neglected. The relatively low atomic number and relative thinness of EBT film allows this approximation to be made. Therefore dose to water measured by a Farmer-type chamber using TG-51 protocol is assumed to be the dose to film. Note that all authors neglect the difference between dose to water and dose to film, due to the lack of air cavity and the relatively low accuracy of film dosimetry compared to ionization chamber measurements.

2.7.3 Curve fitting

Since no consensus has been reached on the ideal equation of the EBT film calibration curve, various non-linear equations have been attempted. A popular method of searching for the best empirical equation is to input the data points into the software TableCurve[5] 2D™, which attempts to fit the data points with a large number of equations. According to Devic, (private conversation) if the standard eight point data set is used, and constraint is set to two parameters, a good choice is

$$D = a\ net\,OD + b\ net\,OD^{n},$$

[5] Systat Software Inc. www.sigmaplot.com

Where n may be 2 or 2.5. Note that the value of n was not set as a parameter, but several equations with different values of n commonly used in data analysis were used to fit the data set. Since this equation was published shortly after the EBT film became commercially available, it is very popular in the literature. For literatures that report more than 8 points in calibration, the value of n is often set as a parameter. For example, Martisikova *et al* (2008) employed the above equation with a, b, and n as free parameters in a 12 point fit.

Other than the above equation introduced by Devic *et al*, other non-linear, non-polynomial equations have been attempted. For example, Battum *et al* reported a calibration equation based on exponential behavior:

$$OD = OD_{\max}\{1 - \exp(-c_1 D/OD_{\max})\}$$

Where OD_{max} is a global parameter for all batches of EBT film, and c_1 is a parameter that describes each individual film batch. This equation is then inverted to a polynomial function of the fourth degree to obtain an equation that calculates dose based on optical density.

The drawback of non-polynomial equations is the difficulty in predicting the behavior of their uncertainty. Polynomial equations may require more parameters to describe the calibration properly, but Taylor's theorem provides the mathematical support for their application. Crop *et al* (2008) performed extensive analysis on the fitting of EBT film calibration by first obtaining a calibration curve with 38 points, and then repeating the standard 7 dose point calibration 12 times. The authors reported that when care is taken in data weighting during the fitting process, adequate results can be obtained using a three parameter polynomial with 7 dose points.

A recent article by Bouchard *et al* presented a theoretical analysis of different types of equations used in fitting EBT film's calibration curve (Bouchard *et al*, 2009). It could potentially provide the theoretical framework for choosing the best equation for describing the calibration curve. Unfortunately, this thesis project is unable to utilize such framework, as the article is published near the end of my thesis writing.

2.8 Energy and radiation type dependence of EBT film

GafChromic EBT film has been claimed to be insensitive to beam energy and radiation type. Unlike ionization chambers which introduce an air cavity into a phantom, EBT film's density and effective atomic number are similar to water, therefore it does not cause a significant perturbation of the radiation field. At the time of writing, no literature has reported any energy dependence on the sensitivity of the EBT film. However, it is expected that the EBT film is energy dependent below the 75 kV energy level, due to the presence of Chlorine. This change in composition of EBT film was meant to make the film suitable for dosimetry in water, as previous version of EBT film can only be used in solid phantoms. The challenge of verifying this claim lies in the lack of accuracy in low energy dosimetry. In this project, we are primarily interested in energy dependence of EBT film at the megavoltage level and especially on the transfer of the calibration curve obtained in photon beams into electron measurements. In the current literature, there is a lack of accurate film sensitivity measurements in electron beams. This may be due to the lack of EBT use in clinical electron beams, as IMRT does not use electron beams.

2.8.1 Energy dependence at or above Cobalt-60

Various authors have shown that EBT film is energy independent in mega voltage x-ray beams at the level of their respective experimental uncertainty. Butson *et al* (2006) reported that the sensitivity difference between 6 MV and 18 MV photons beams is less than 1 %. Although EBT applications in Cobalt beam have been reported (Martisikova *et al*, 2008), direct comparison of Cobalt and Linac calibrations have not been reported at the time of writing. For electron beams, Su *et al* (2007) reported energy dependence to be within ±4 % for electron energies from 6 to 22 MeV, but the authors were reluctant to report an energy dependence of EBT film. Note that literature about EBT use in electron beams is of special interest in this project, as we intend to use EBT film in electron beams produced by Vickers experimental accelerator. Figure 2.9 shows electron energy dependence of EBT film as reported by Su *et al*. A

glance of the results suggests that the authors may have underestimated their uncertainty, as they used the relative standard deviation of scan values as their error bars. Such approach only addresses uncertainties due to the scanner, and ignores film uniformity effects.

2.8.2 Energy dependence below Cobalt-60

Due to its very high spatial resolution, EBT film dosimetry in brachytherapy is an active research topic. Despite the introduction of Chlorine into the film, energy dependence has not been reported in peer-reviewed literature. Chiu-Tsao *et al* (2008) compared EBT dose response between an ^{125}I seed, which has a mean energy of 28.4 keV, and a 6 MV photon beam, and found the difference in film sensitivities measured in the two radiation modalities to be less than the experimental uncertainty of measuring dose delivered by ^{125}I seeds. Figure 2.10 shows ^{125}I and a 6 MV photon beam calibration comparison reported by Chiu-Tsao *et al*. It is interesting to note that a visual inspection of Figure 2.10 would suggest an energy dependence of EBT film as the ^{125}I calibration curve seemed less sensitive than the 6 MV curve. The authors were reluctant to suggest this, as they reported a 7 % uncertainty for both green and red light dose conversion. This example highlights the difficulty of accurate EBT film dosimetry in radiation modalities other than megavoltage photon beams. Other work on EBT application with low energy photons has generally assumed energy independence of EBT film, due to the difficulty of measuring dose accurately in low energy radiation. For example, Keller *et al* (2008) used EBT film for dosimetry in 100 kVp, 300 kVp x rays, and ^{192}Ir gamma rays by applying the 6 MV Linac beam calibration to the above energies.

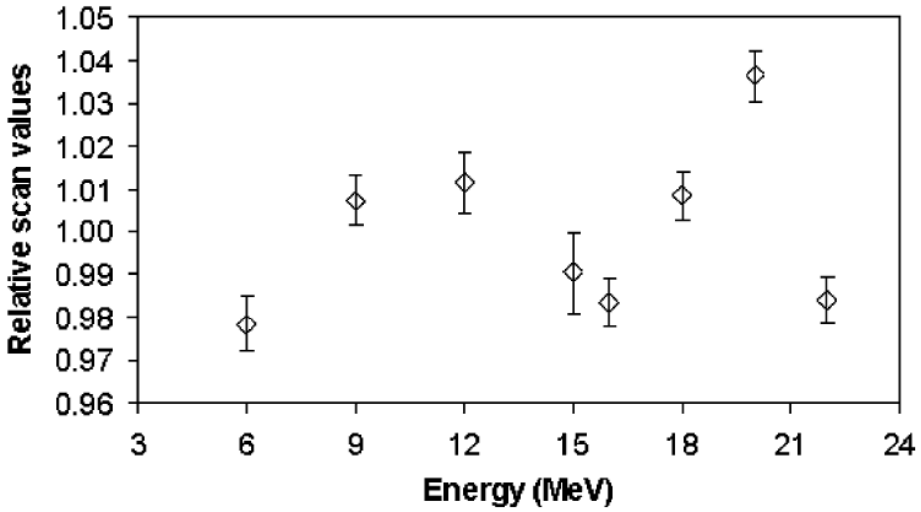

Figure 2.9. Energy dependence of EBT film in electron beam (Su *et al,* 2007).

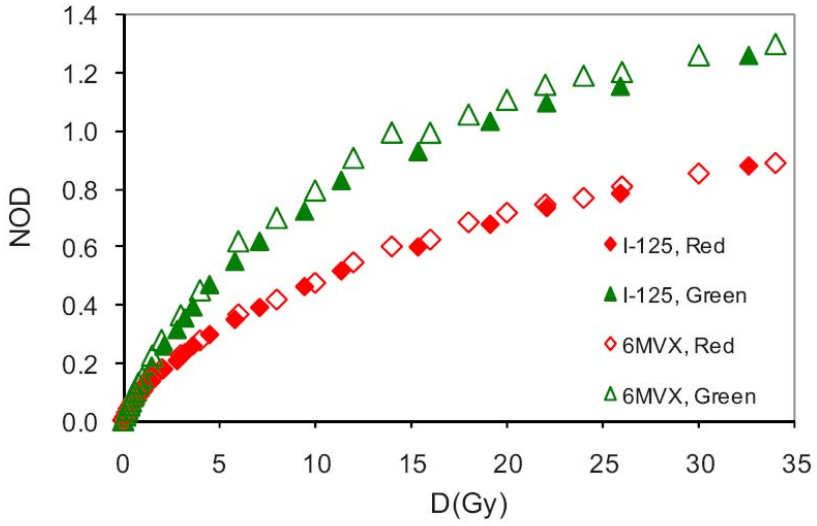

Figure 2.10. Comparison of EBT calibration in ^{125}I and 6MV X-ray, reported by Chiu-Tsao *et al* (2008).

2.9 Scanner uniformity - light scattering effect

2.9.1 Background Theory

Systematic lateral inhomogeneity of flat-bed scanners when scanning EBT films has been reported in the literature. It is believed to rise from the different length of light tube a given detector "sees". A detector at the center receives light from both sides, while a detector near the edge only receives light from one side. Therefore, one would expect a symmetric inhomogeneity in the lateral direction, with the deviation increasing as one moves further away from center. This behaviour has been confirmed by literature, but reports vary on the detailed behaviour. The light output is not assumed to be uniform along the lamp, but a calibration slit was built into the scanner to correct for non-uniform light output along the lamp. All results quoted in the literature review use the 1680pro scanner. Figure 2.11 shows an illustration of film scanning geometry. In this project, we refer to the direction parallel to scanner lamp as lateral direction, and direction perpendicular to scanner lamp as longitudinal direction.

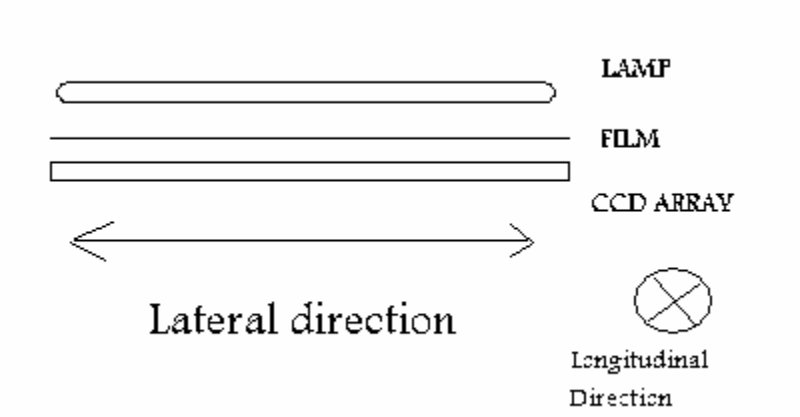

Figure 2.11. Film scanning geometry, not drawn to scale. CCD detectors at the center are expected to receive more scattered light than detectors at the edge. A illustration of lateral and longitudinal directions are included.

2.9.2 Types of corrections presented in literature

Corrections presented in the literature can be divided into two groups. Some authors de-couple the lateral and longitudinal direction, and generally consider the longitudinal direction to be uniform, i.e. no correction is required. Other authors produce two-dimensional correction matrixes by measuring scanner responses at various points of the scanner bed. Note that such an approach is very cumbersome. Because this correction is expected to be optical density dependent, the resulting correction matrix will be three dimensional and difficult to present.

2.9.3 De-coupling approaches presented in literature

Battum *et al* (2008) applied lateral correction curves based on optical density, measuring relative OD at five positions along the scanner width for each optical density. Based on their result, the claim is that a single, averaged correction factor can be used for all optical densities. Figure 2.12 shows the data. Note that only five data points are collected to describe a second order polynomial that have three free parameters. This is a common problem found in literature, where a very small number of data points are collected to describe the lateral uniformity correction of flatbed scanners. Lynch *et al* (2006) created a stepwedge by exposing a sheet of EBT film to sunlight incrementally in 1.5 × 25 cm strips. 16 steps were created over approximately 20 min. Such step wedge was used to evaluate scanner homogeneity. Figure 2.13 shows the figure presented by Lynch *et al*. Menegotti *et al* (2008) used a similar approach to Lynch *et al*, but using a Linac instead of sunlight to produce a dose wedge.

2.9.4 Correction matrix approaches presented in literature

Paelinck *et al* (2007) reported a correction technique using 11 x 7 positions for four different dose levels. Their figures (shown in Figure 2.14) showed a large deviation along the longitudinal direction. In their protocol, an average correction factor was used for all optical densities. Saur and Frengen used a 5x5 matrix for correcting inhomogeneity in their 2008 paper. They measured small, but non-

negligible deviations in the longitudinal direction. They also used a two-dimensional correction matrix for all doses between 8 and 293 cGy.

2.9.5 Drawbacks of both approaches

Upon reviewing the literature, it is found that lateral scattering correction techniques still require improvement. The multiple position approach uses not enough data points, and the uniform dose strip approach shows a lack of uniform source of dose.

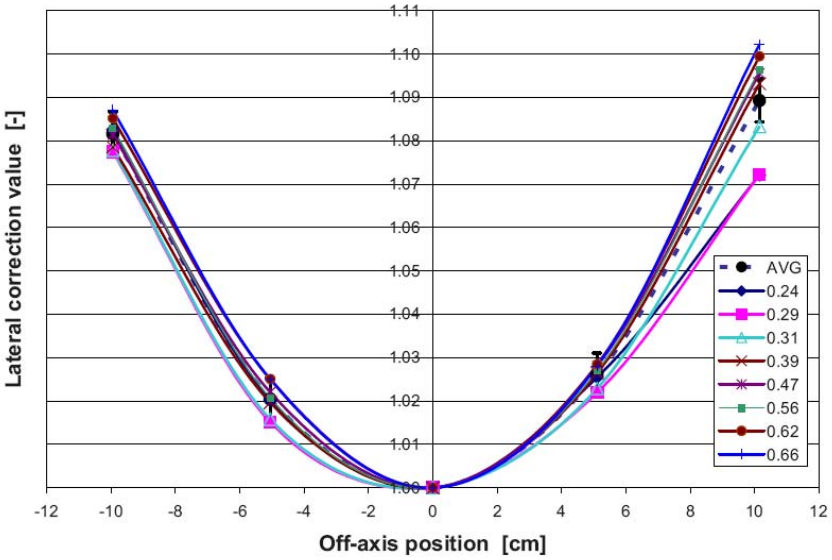

Figure 2.12. One dimensional corrections reported by Battum *et al*.

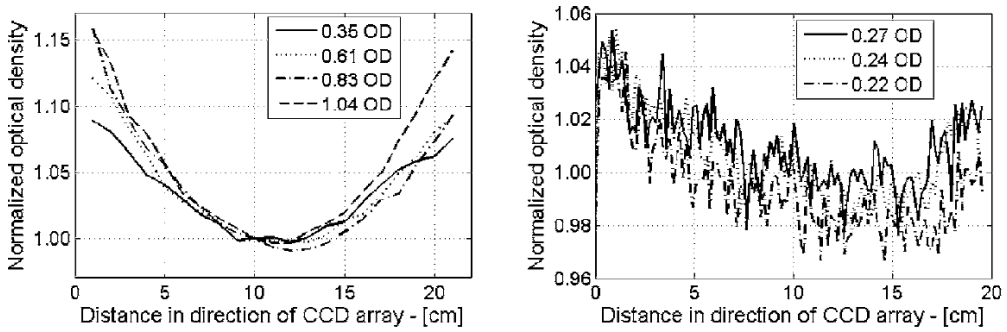

Figure 2.13. A popular approach to scanner uniformity correction (Lynch *et al*, 2006), using a strip of film believed to be uniformly irradiated.

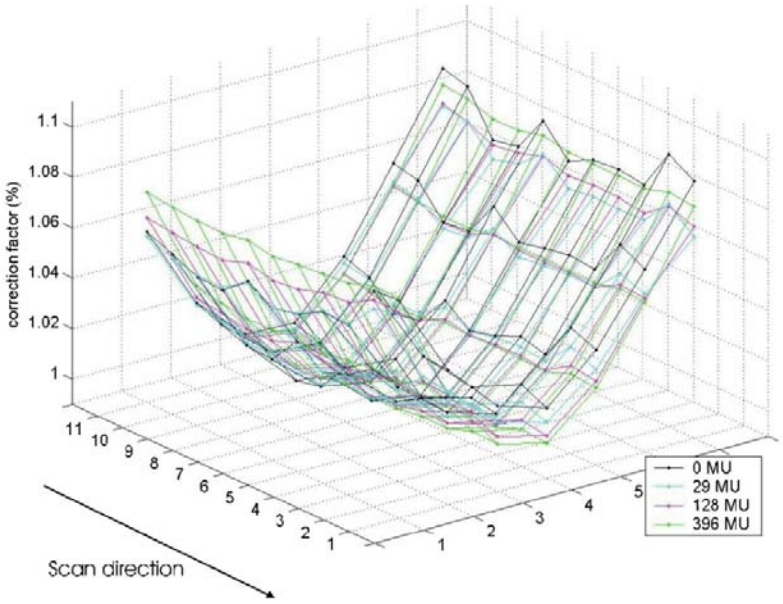

Figure 2.14. Three-dimensional correction matrix approach presented by Paelinck *et al* (2006). Note that despite the presentations of several surface plots, the implemented protocol used an average correction matrix for all doses.

2.10 Film development process

Unlike radiographic films, radiochromic films are self-developing and do not require a dedicated developer. The drawback of the self-developing feature is the relatively long development time. Earlier versions of radiochromic films had a development time on the order of a week, while EBT films' optical density has been shown to stabilize after a few hours. Currently, the consensus in the literature is that the film development effect becomes negligible after 24 hours, and the conservative protocols in the literature wait at least a day after irradiation before scanning is performed (Battum *et al*, 2008). Since most of the development happens within the first few hours after irradiation, some clinical protocols wait only 6 hours (Saur *et al*, 2008). In this chapter, literature regarding film development after irradiation is reviewed, based on the time scale investigated. Most studies in the literature focuses on EBT film development during the first 24 hours after irradiation, but a recent paper (Martisikova 2008) has investigated the darkening of film after the first day.

2.10.1 Film development during the first 24 hours

Early literature showed that the opacity of EBT film stabilizes to the level of scanner reproducibility after about 12 hours, but this observation was limited by the difficulty in reading the same piece of film in a reproducible fashion.

2.10.2 Film development after the first day

Until recently, there is a lack of literature describing the long-term development of irradiated EBT films after the first day. Martisikova *et al* (2008) showed that film development continues for at least seven days, with a total increase in optical density of up to 5 %. This darkening effect was also shown to be temperature and dose dependent. A film development figure taken from this PMB paper is shown in figure 2.15. Note that the authors showed 1 % scanner stability from one day to another, which is better than scanner stability reported for the Epson 1690Pro Scanner .

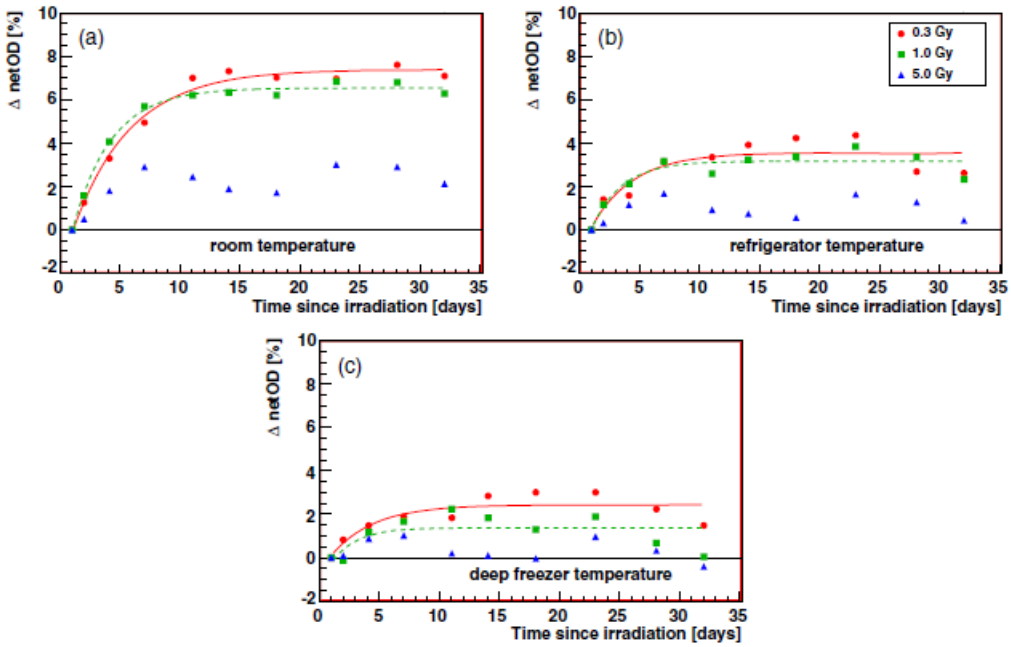

Figure 2.15. EBT film development over the course of a month, presented by Martisikova *et al*. Such results show that film development after the first 24 hours is not negligible.

2.11 Humidity effect

GafChromic EBT film is designed for use in both solid phantom and water, but limited literature is available for the effect of humidity and use of EBT film in water. Battum *et al*'s 2008 paper is so far the only literature where EBT film is immersed in water. Rink *et al* (2008) reported a 20 % drop in EBT film sensitivity after baking the film in a drying oven for 24 hours at 50 ºC. This raises the possibility that EBT film sensitivity is dependent on its storage history in terms of temperature and humidity. Since water is a critical component of both EBT crystals and the gelatine that EBT crystals are suspended in, a change of water content in EBT film is expected to have an effect on film sensitivity.

2.12 Applications in 1D profile measurement

Despite various authors claiming the EBT film as a two-dimensional reference dosimeter, there is limited literature comparing EBT film measurement with established dosimeters at the level of claimed film dosimetry uncertainty. Most literatures focus on comparison between dose profiles corrected for scanner uniformity effect and profiles not corrected for scanner uniformity effect and emphasize that corrected dose profiles agree with known 1D detectors much better than uncorrected profiles (Paelinck *et al* 2006, Menegotti *et al* 2008, Chung *et al* 2008). The strongest comparison between EBT film and ionization chamber-based measurement is by Battum *et al* (2008), where PDD and dose profiles were measured with both EBT films and scanning ionization chamber. The dose profile measurement is shown in figure 2.16. The profiles obtained with both dosimeters were compared and the differences shown in a graph. This result showed that variations in film sensitivity within a sheet of film and between different sheets in the same batch are the dominant contribution to uncertainties in EBT film dosimetry. Such variation is considered to be "not random but unpredictable" (Battum *et al,* 2008). Since the distribution is not Gaussian, reducing the spatial resolution does not reduce the uncertainty due to sensitivity variation, and averaging over several films is the only solution to such a problem.

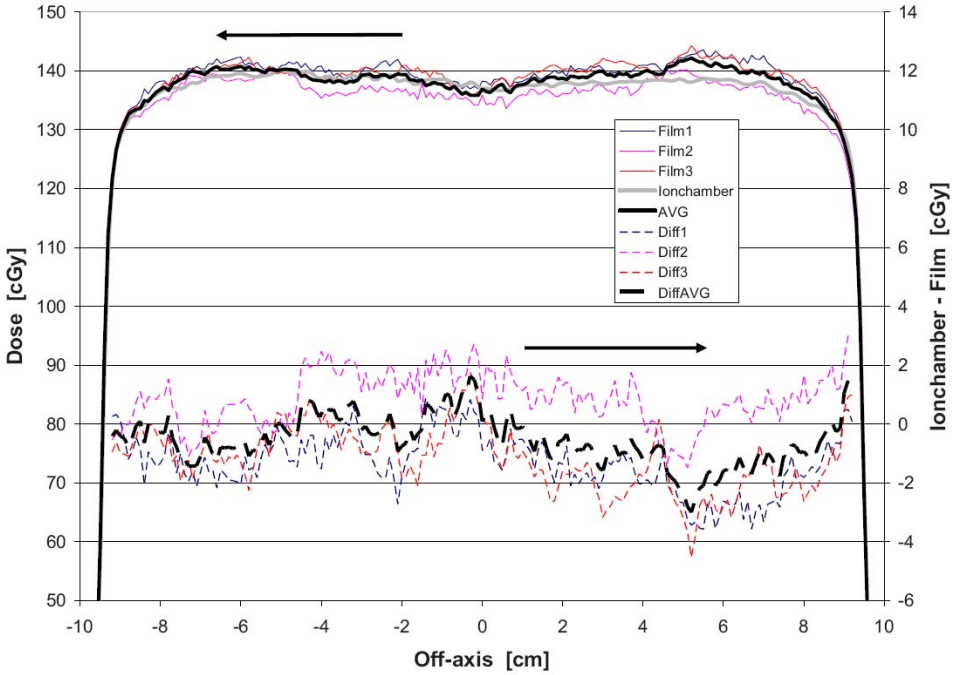

Figure 2.16. Comparison between EBT film and ionization chamber scanning in measuring dose profile of a 18 x 18 cm^2 field at 6MV. Note that the film measurements differ from each other due to non-uniformity of film.

2.13 Applications in 2D profile measurement - IMRT

Current 2D dose measurements of EBT film presented in literature is limited to IMRT plan verification. The results reported are percentage of pixels passing the gamma index at a certain level. The gamma quantity is the minimum distance in the renormalized multidimensional space between the evaluated distribution and the reference point. The algorithm for calculating Gamma Index is usually built into the clinical software, but detailed explanation is available in the literature (Low *et al*, 2003). Although this is the target market of EBT films, it is not relevant to this project. Nevertheless, IMRT verification results can serve as the ultimate test of EBT film dosimetry protocols reported in literature, as it compares dose distributions in an entire field, rather than just a single point or a line.

2.13.1 Literature that compare EBT distributions to treatment simulation distribution

Chung *et al* (2008) compared dose distribution measured by film to dose distribution from the Pinnacle treatment planning system. Passing pixels were in the 92 % to 95 % range. Note that the authors did not perform scanner uniformity correction, as the aim of the project was to establish a protocol that ignores scanner uniformity correction.

2.13.2 Literature that compare EBT distributions to another 2D dose distribution measurement device.

Menegotti *et al* (2008) reported the comparison between dose distributions measured by EBT film and by a PTW Seven 29™ 2D array. At 3 %, 3 mm, with gamma value set to less than 1 %, 91 % of pixels agree for an inverse pyramid pattern, and 98 % of pixels agree for an open field.

2.14 Aim of this thesis project

In this M.Sc. thesis project, we will investigate the various areas of EBT film dosimetry in a rigorous manner and establish an EBT film dosimetry protocol that measures 2D dose distributions accurate to 2 % level. Film measurements will be compared directly to conventional dosimeters, and the protocol will be used on the NRC Vickers linear accelerator experiments. The measurements made using EBT film will be added to measurements made by ion chambers that will verify the accuracy of Monte Carlo simulations. In other words, EBT film will be used as an additional dosimeter in Monte-Carlo benchmarking. Based on the published results, the following effects can cause an error of 5 % or more if not correctly addressed:

1. Film orientation effect due to polarity of film and scanner.
2. Scanner uniformity in the lateral direction, due to scattering of scanner lamp light.

With the goal of 1 % overall standard uncertainty in mind, we plan to investigate the areas that contribute anywhere from 0.5 % to 5 % to the dose uncertainty, but do not yet have a consensus on the optimal approach:

1. Darkening due to scanner lamp
2. Scanner fluctuation
3. Scanner noise and pre-scanning
4. Mathematical description of calibration curve
5. Scanner uniformity in the lateral direction
6. EBT film development after irradiation

As a relatively new but rapidly maturing field, the literature has reached consensus on the following subject:

1. EBT film is superior to earlier versions of radiochromic films.

2. The use of film readers other than flatbed scanners is not recommended.

3. EBT film is expected to be energy and radiation type independent for megavoltage photon and electron beams, due to a lack of literature claiming otherwise. The energy independence claim in literature, however, is often at the 5 % level, which is not acceptable for a standards lab, or even clinical applications. The energy independence of EBT film will be verified in this project.

In this project, films other than the EBT model or film readers other than the Epson 10000XL will not be investigated, but the energy independence of the EBT film will be verified. After addressing individual aspects of EBT film dosimetry, we plan to compare dose distributions measured with EBT film with dose distributions measured with other one or two-dimensional dosimeters. Rather than simply extracting a Gamma Index, we plan to measure the differences between different methods of dose measurement quantitatively and see how EBT film compares with other instruments. Both absolute and relative dose measurement using EBT film will be investigated.

Chapter 3 EBT protocol established at NRC

3.1 Overview of protocol

The GafChromic EBT film dosimetry protocol established at NRC utilizes the Epson 10000XL scanner, as it is the model recommended by ISP. This protocol follows the general EBT dosimetry workflow described in the literature, but each step is customized for the highest accuracy possible rather than high throughput.

3.1.1 Overview of experiment

In the calibration phase, a piece of film is cut into 8 pieces, and each piece is given a dose between 0 and 8 Gy. Approximately 24 hours after irradiation, the film is read with the 10000XL scanner, using a PMMA template to ensure that all films are positioned at the same place. A preview is generally performed to reduce the effect of scanner lamp warm-up effect and ensure accurate positioning of film on the scanner bed. In both calibration and measurement phase, a piece of blank film is retained from the particular sheet of EBT film as a reference piece. This reference piece is placed in the same environment as the irradiated pieces, but never exposed to any ionization radiation. Currently all film experiments are performed in Virtual Water™ phantom[6], where the environment of the film does not have any significant effect on measurement. In the future, EBT film may be used in a water phantom, and the effect of water on EBT film can be accounted for by submerging the reference piece in water for the same length of time as the irradiated piece, without the radiation exposure. In analysis, the reference piece is defined as zero optical density. This approach was inspired by Devic *et al* (2005)'s environmental effect correction technique, but we do not use the opaque cardboard in our protocol (see page 25). The scanned calibration pieces resulted in 8-bit RGB images in TIFF format, which are analyzed to produce a calibration curve.

In the measurement phase, a large piece of film is cut from a blank EBT film of the same batch, and exposed in the radiation field of interest. This film is then scanned approximately 24 hours after irradiation with its reference piece. The

[6] Med-Cal, Verona, WI

scanned image is then converted to an optical density map, as optical density, rather than pixel value, is the parameter used in the calibration curve. This optical density map is then corrected for scanner uniformity effects, and converted to a dose map using the calibration curve. Since the film is scanned at 96 dpi, or 0.265 mm/pixel, the dose map is often re-sampled to reduce individual pixel uncertainty at the expense of spatial resolution. The typical pixel size in the final dose map is 1.3×1.3 mm^2.

3.1.2 Software packages used in this protocol

Matlab®[7] is the software package most commonly reported in the literature (Devic *et al* 2005, Battum *et al* 2008). In this project, Matlab 2008a with the add-on image analysis package was installed on a PC running Windows Vista Ultimate 64 bit edition. The 64 bit edition was chosen to utilize the eight gigabytes of memory available on the PC. Custom-written Matlab scripts were used for both calibration and dose measurement phases. A specific script is written for each task, and no Graphical User Interface (GUI) was designed. This approach was to ensure that all data manipulation is known before a script is executed, to protect the integrity of measurement. The software EpsonScan, shipped with the scanner, was used to operate the scanner and acquire the image. The scanner was also shipped with the SilverScan software, which some authors in the literature have used to automatically repeat a scan multiple times (Battum *et al*, 2008). Unfortunately, such software was not compatible with the 64-bit Vista; therefore repeated scans were performed by hand. In the literature, ImageJ is another popular software package in image analysis, but it was also not compatible with 64 bit Vista, and not used in this project. Microsoft Excel was used to analyze both calibration curve and dose profiles produced by custom-written Matlab scripts.

[7] The Mathworks Inc. Natick, MA

3.2 Investigation of repeated scanning and temperature effects of 10000XL

3.2.1 Measured temperature effect

In the literature, increasing optical density with repeated scanning has been reported, but no consensus has been reached about the cause of this effect. The primary concern is whether this effect is due to a permanent darkening of the film by the scanner lamp or whether it is a temporary effect due to increasing temperature of scanner bed. To verify this, we attached the sensor of a Digi-Sense[8] thermometer to the scanner bed using tape, and repeatedly scanned a piece of film while recording the temperature. The Digi-Sense thermometer is traceable to a primary standard and has temperature accuracy of better than 0.5 ºC. Figure 3.1 shows the temperature effect on EBT film measurement. Compared to effects reported in the literature about the 1680Pro, the temperature effect on the 10000XL is less than 0.6 % when measured in pixel values. The steep drop in the beginning is due to lamp start-up effect, as no preview was performed.

3.2.2 Significance of temperature effect

In the experiment described by Figure 3.1, 100 scans at 300 DPI resolution were required to bring the temperature from room temperature to 30 ºC. At the 96 DPI used in this protocol, the scanner lamp stayed on for a much shorter time, and 100 consecutive scans of the entire scanner bed produced a significantly lower temperature than 30 ºC. Since our scan involves only one scan per film, we expect the temperature effect to be insignificant.

[8] Thermo Fisher Scientific, Waltham, MA

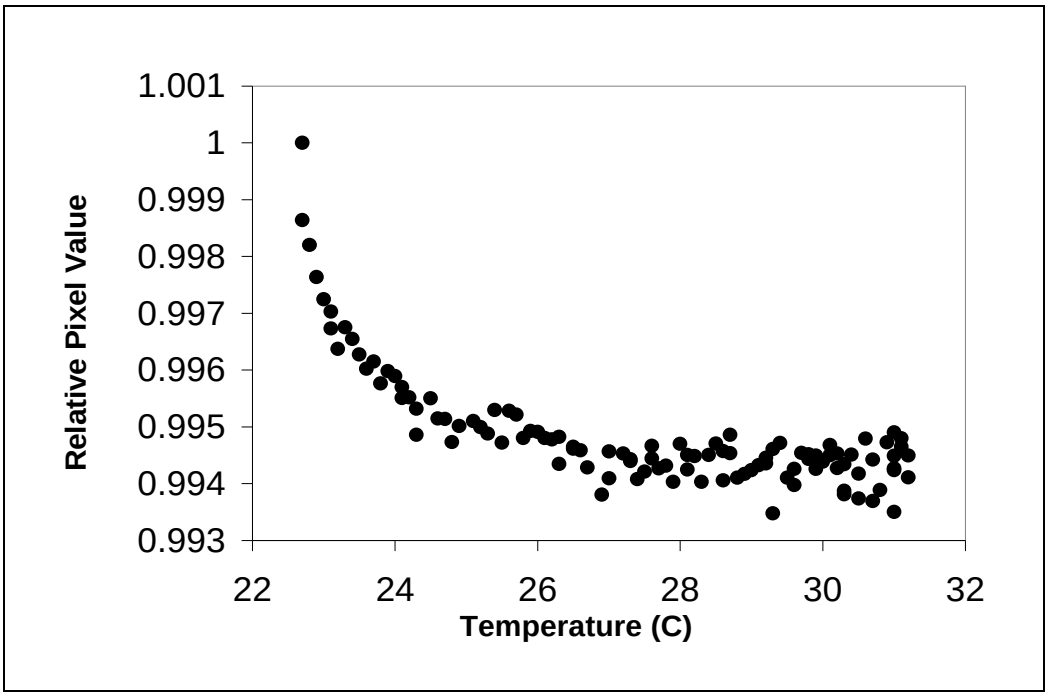

Figure 3.1. Measured pixel value as a function of temperature during repeated scanning of a blank EBT film. The film was scanned 100 times consecutively.

3.3 Two-state fluctuation and reference piece correction

3.3.1 Evidence of scanner response fluctuation

The investigation of repeated scanning in literature only focuses on gradual changes in scanner response, instead of a distribution of responses when there is no systematic trend. We repeatedly scanning a blank film at 96 DPI over all small area, which does not cause any significant scanner warm-up effect due to the short scan duration. Without the scanner warm-up effect, we observed a two-state fluctuation behaviour of the 10000XL scanner, as shown in Figure 3.2. Further investigation showed that this fluctuation is non-random and unpredictable and averaging of multiple scans can not reduce this effect. If this effect is not corrected, it would add up to 1.3 % to the uncertainty in the measured dose. This finding is consistent with "day to day" scanner stability reported in literature, where up to 0.7 % (1 SD) uncertainty was reported. To correct this effect, a reference piece scanning approach was implemented in our protocol.

3.3.2 Reference piece correction implemented in our protocol

Further investigation showed that this fluctuation affects measurements of all doses in the same directions and about the same magnitude, and the fluctuation is uniform across the scanner bed. To correct for it, a reference piece of blank film is placed next to the film of interest. Figure 3.3 shows an example of this approach, where a PMMA template is placed on the scanner bed and aligned to the edge of scanner bed. This template also ensures that the calibration film is always placed at the same position on the scanner bed and does not get accidentally rotated. In calibration phase, because the film pieces are scanned sequentially, a separate piece of EBT film cut from another sheet is placed next to the film of interest to serve as the reference piece. This extra piece of film from another sheet is necessary because the unirradiated film piece cut from the calibration sheet is scanned at the same position as the irradiated pieces. In the measurement phase, the unirradiated piece cut from the same sheet of EBT film as the experimental piece is used as the reference piece and placed next to the experimental piece in scanning. This unirradiated piece serves as both the

reference and the zero-dose piece. Note that the unirradiated piece is not scanned at the same position of scanner bed as the experimental piece in the measurement phase, because we desire a simpler protocol. This difference was found to have negligible effect on measurement accuracy.

Note that although this behaviour is unpredictable, the magnitude of fluctuation is still small compared to uncertainties reported in the literature. We believe that this fluctuation can be attributed to the scanner lamp calibration process, rather than ADC instability of the scanner. Such fluctuations can also be observed in Figure 2.15, which showed day-to-day fluctuations of the scanner at the 0.7 % level.

3.3.3 Reference piece correction's contribution to EBT film dosimetry protocol.

The reference piece correction technique was employed in all EBT film measurements, including the study of temperature effect presented in section 3.2. The results shown in Figure 3.1 were already corrected for scanner fluctuation, allowing the scanner start-up effect and temperature effect to be observed. The long term darkening effect investigation of EBT film presented in section 3.8 was also made possible by the reference piece correction technique. By removing scanner fluctuation effects, we measured the small increases in optical density after the first 24 hours. Without this technique, it would not be possible to measure the optical density of the same piece of film with an accuracy of 0.3 % or better over the course of three months.

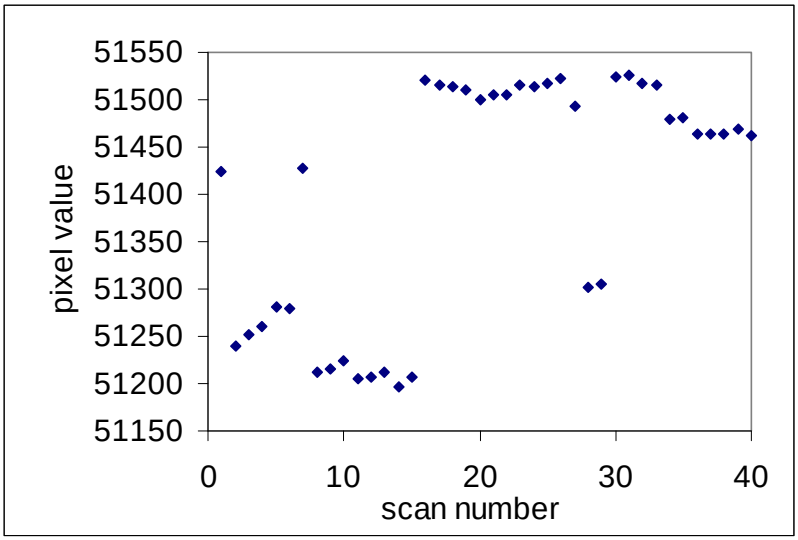

Figure 3.2. Observed two-state fluctuation of 10000XL scanner. Note that this is a non-random, but unpredictable fluctuation, instead of a Gaussian noise.

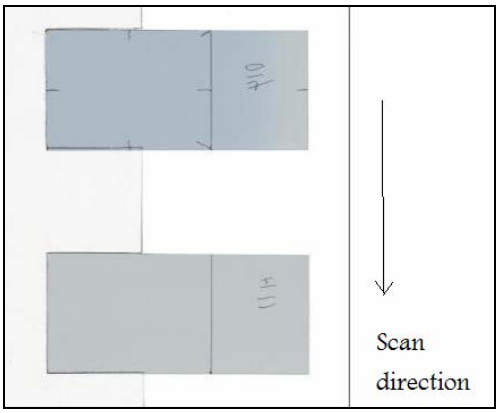

Figure 3.3. Reference piece approach in calibration phase. The top piece is the film of interest from the calibration set. The bottom piece is a reference piece cut from another sheet of EBT film. The optical density of this reference piece is arbitrary, as it only serves to correct scanner fluctuations that occur during the scanning of eight pieces of film.

3.4 Resolution and uncertainties of EBT film

3.4.1 Sources of noise and impact on resolution

Extensive literature has been published on the single-pixel uncertainty of EBT film dosimetry. What the literature lacks is the de-coupling of the three components of noise: noise from scanner, noise in a blank piece of EBT film (e.g. due to the polyester cover), and noise due to the active component of EBT film. In this project, we studied each component separately, and arrived at the conclusion that the dominant effect is the noise due to the active component of EBT film. In other words, the finite size of EBT crystals produce noise that is higher than electronic noise of scanner or the noise exhibited by a blank piece of EBT film. Since this effect only surfaces after a piece of film is irradiated, pre-scanning the film before irradiation does not significantly reduce the single-pixel noise of EBT film measurement. The low electronic noise of the scanner compared to film grain noise also makes repeated scanning unnecessary; therefore we only scan the film once in this protocol. The noise due to film crystal size is the ultimate limiting factor in resolution of our EBT film dosimetry protocol. In the following sections, we will present the levels of scanner electronic noise, blank film noise, and irradiated film noise.

3.4.2 Scanner electronic noise

To isolate noise from the 10000XL scanner, a blank transparency slide was scanned at 96 DPI, which is the scanning resolution used in EBT film scanning. A line profile was taken through the resulting image to provide detailed information on noise levels of a blank media. In this experiment, we consider a worst case scenario where all noise measured in scanning a blank transparency slide is attributed to the scanner electronic noise, rather than any non-uniformity of transparency slide. In other words, we attempt to find the upper limit of scanner electronic noise. As shown in Figure 3.4, the image pixels showed no systematic trends through a 7 cm line, starting at the 7 cm position and ending at the 14 cm position, and the distribution of pixel values appeared to be random. A histogram of the same data, shown in Figure 3.5, demonstrated that the noise is

Gaussian, with a standard deviation of 0.4 %. The lack of systematic trend and the Gaussian distribution of noise indicates that single-pixel noise level due to the scanner can be reduced by reducing the spatial resolution. Since the targeted spatial resolution of this protocol is 1 mm^2, 25 pixels in a 96 DPI image can be averaged to reduce the spatial resolution to 1 mm^2 and noise level to the order of 0.1 %.

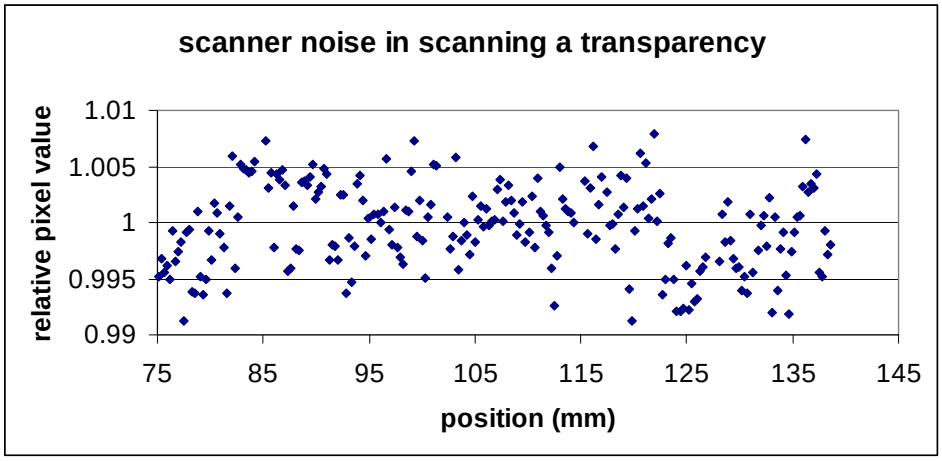

Figure 3.4. Relative pixel value of a line profile through the image of a transparency.

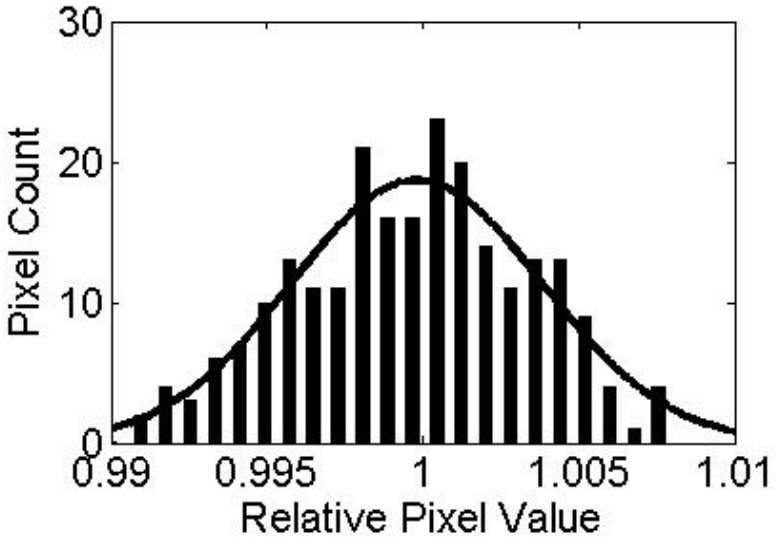

Figure 3.5. Histogram of scanner electronic noise at 96 DPI. A Gaussian fit of the histogram was also shown in the figure.

3.4.3 Noise due to blank EBT film

Various authors have reported pre-scanning techniques to correct for noise and non-homogeneities of blank EBT films, but no investigation of the uniformity of blank EBT film has been reported in the literature (Devic *et al*, 2005). To study the flatness of blank EBT film, we scanned a piece of EBT film at 96 DPI. Since we already established the response uniformity and noise level of the scanner, a comparison of noise levels showed that noise from a blank EBT film is at, or below, the level of noise from a blank transparency. Figure 3.6 and Figure 3.7 shows the noise raw data and the noise histogram, respectively. The histogram also appears to be Gaussian. The standard deviation of a blank image at 96 DPI is 0.3 % when measured in pixel value, and potential long-term trend is estimated to be less than 0.2 %. Given that the line profile was taken over 20 cm, we conclude that EBT blank film can be considered uniform for this project. We would like to again emphasize the Gaussian distribution of noise and the 0.2×0.2 mm^2 resolution employed. Given our overall goal of 1 mm spatial resolution and 1 % standard uncertainty, the reduced spatial resolution through pixel averaging will bring the single-pixel noise down to a negligible level while no systematic trends have been observed. Therefore pre-scanning of blank EBT film or repeated scanning is not implemented in this protocol. The next section will demonstrate the single-pixel noise level of irradiated film and its dominance compared to noise level of a blank film.

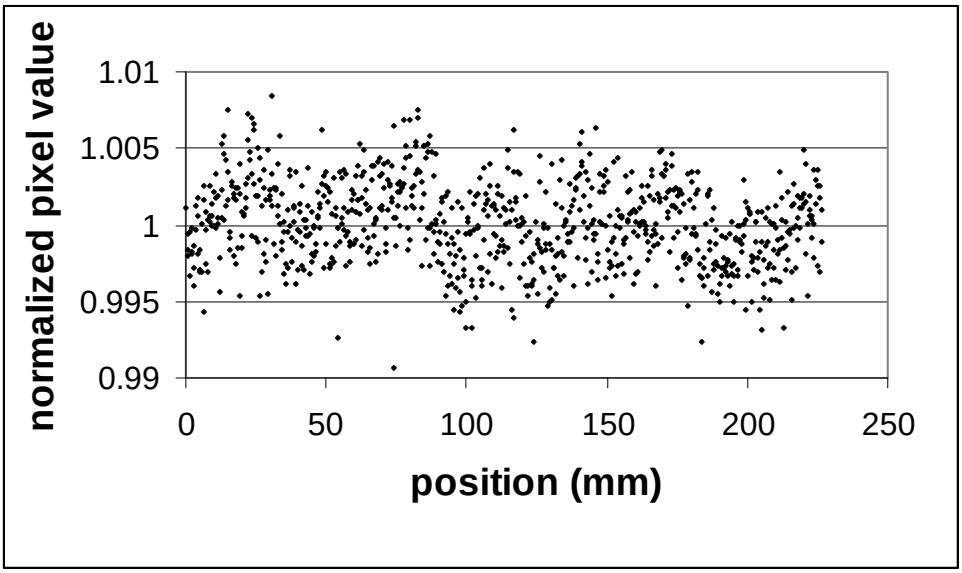

Figure 3.6. Relative pixel value of blank EBT film through a line profile of 20 cm. A comparison of this figure and figure 3.4.2 showed that blank EBT film does not introduce additional noise.

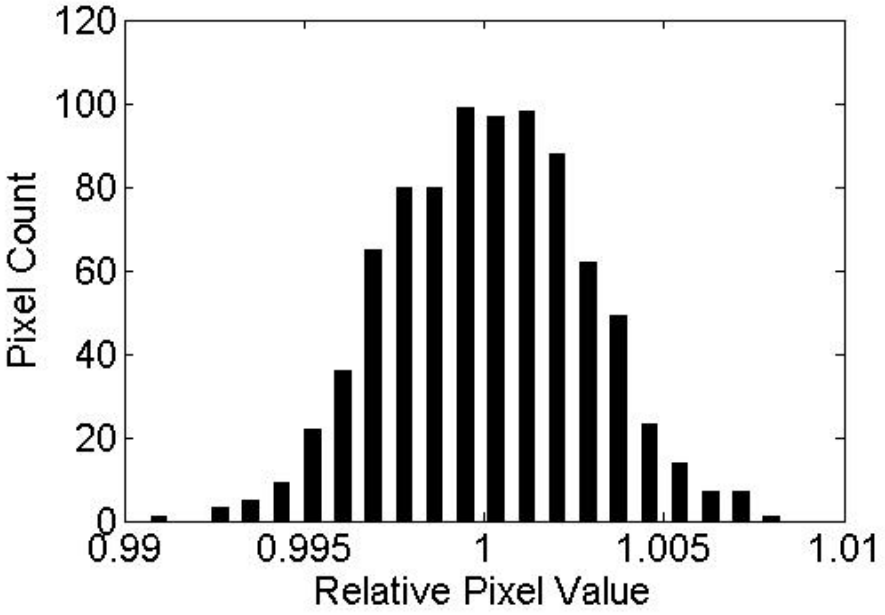

Figure 3.7. Histogram of pixel value distribution of blank EBT film, taken through a line profile at 96 DPI over a distance of 20 cm. The histogram also appears to be Gaussian.

3.4.4 Noise due to irradiated film

Based on existing literature, the grain size of EBT film is expected to be larger than radiographic films and previous versions of radiochromic films, as the crystals used in model EBT are elongated. Such microstructure of EBT crystals leads to a non-uniform distribution of sensitive material at the 0.2 mm level. Since both clinical linear accelerators and Cobalt-60 machines produce radiations that are expected to be smooth at the millimetre level, an inspection of noise level of an EBT film irradiated in an expected flat field can provide information about the noise and spatial resolution of EBT film. To do so, we irradiated a 10x10 cm^2 sheet of EBT film at 5 cm depth in a virtual water phantom in the 6 MV Elekta beam at 1 m. The field size is 10 x 10 cm^2 and dose gradient is expected to be small for a flattened open field. A 1.3 x 1.3 cm^2 square at the centre of field was chosen as area of interest, because the small area reduces the effect of dose gradients. Existing data on field flatness indicate that the dose gradient over 1.3 cm is negligible. When scanned at 96 DPI, the relative pixel values showed Gaussian behaviour, with standard deviation of 0.8 %. The histogram of the normalized pixel value is shown in Figure 3.8. A Gaussian fit of the histogram was also shown in Figure 3.8, demonstrating the Gaussian shape of the noise. Compared to the pixel noise of a blank EBT film, the pixel noise of an irradiated EBT film is the dominant effect. Further investigation of irradiated films scanned at 300 DPI showed much higher noise levels, and confirmed the fact that noise due to EBT film crystals is the limiting factor on the spatial resolution of EBT film dosimetry. Based on this result, all films are scanned at 96 DPI, and 0.2 mm is established as the limiting spatial resolution of EBT films. Note that the approximately Gaussian distribution of the noise would suggest that reducing spatial resolution can improve the accuracy of EBT film dosimetry to better than 0.5 %. Unfortunately, another limiting effect, the sensitivity fluctuations due to manufacturing defects, becomes a dominant factor in dose measurements at the centimetre level. The next section is dedicated to this effect.

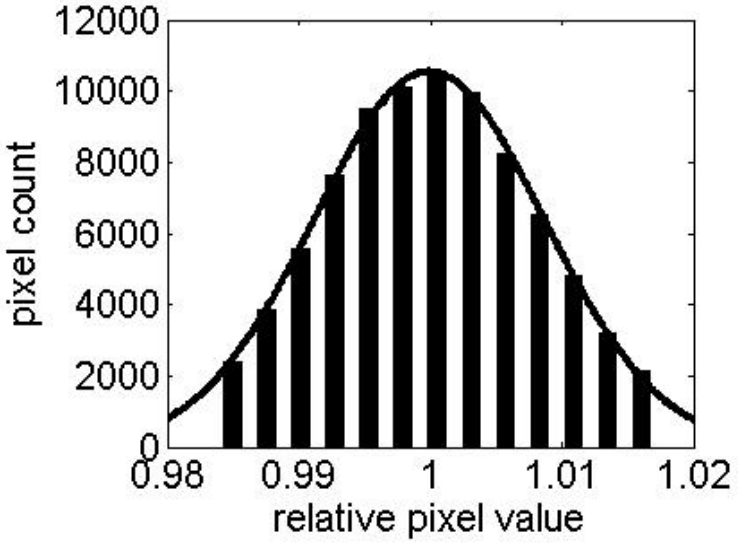

Figure 3.8. Relative pixel value of irradiated EBT film measured over a 1.3 cm by 1.3 cm square, where dose was known to be flat. A Gaussian fit of the histogram is also shown.

3.4.5 EBT film uniformity due to coating process

Various authors have reported that the ultimate limit of any EBT film dosimetry protocol is the uniformity of EBT film (Battum *et al*, 2008). The non-uniformity of EBT film is "non-random and unpredictable", and cannot be known before irradiation was performed. To investigate the behaviour of non-uniformity, we irradiated four 5 cm × 25 cm strips of EBT film cut from the same sheet in a virtual water phantom at 5 cm depth in a 10 × 10 cm^2 wedge field, with the long edge of film strip along the wedge direction. All four strips were given exactly the same dose, with an Exradin[9] A19 Farmer-type chamber positioned at 13 cm depth as a monitor. The measurements from the A19 chamber showed that doses delivered to the four film strips were identical at the 0.2 % level. All films were irradiated within one hour and scanned more than 24 hours after. The films were stored in the same envelope at all times. Therefore film darkening and environmental effects can be assumed to be the same. The measured optical density profiles of the four films showed differences between film strips of up to 2 %, and film uniformity behaved like an unpredictable step function. Figure 3.9 shows the four optical density profiles of the four strips irradiated in the same wedge field. Further analysis of the dose wedge data showed that EBT film sensitivity has a peak-to-peak range of 2.5 %, with a non-Gaussian distribution. In Figure 3.9, pieces A and B showed the largest difference, with consistent sensitivity differences between 2 and 2.5 % through the entire dose wedge, while pieces C and D showed fluctuating sensitivities that lie between pieces A and B. The non-uniformities of film show a patch-like pattern, with each drop or rise of sensitivity lasting 1 cm or more. Such observation shows that film uniformity can not be improved by reducing spatial resolution, as the film sensitivity does not show a Gaussian behaviour. Note that a 2.5 % peak-to-peak sensitivity does not contradict our stated goal of 1 %, 1 SD standard uncertainty, as it translates to 1.3 % peak-to-mean range. Assuming a uniform distribution of uniformity, the standard uncertainty is still less than 1 %. Such behaviour of uniformity is of great concern in relative dose distribution; however, as relative dose profiles are

[9] Standard Imaging, Middleton, WI

generally normalized to an arbitrary point on the film, usually the point of maximum dose. If the film sensitivity at the point of maximum dose differs from sensitivity at the point of interest by 2 % or more, such as pieces A and B in Figure 3.9, an error of 2 % can be introduced in relative dose profiles. In this case, averaging of several pieces of film is the only solution in reducing uncertainties due to film uniformity.

The film strips in the wedge field experiment provide an example of film non-uniformity, but it is still desirable to have a direct demonstration using a known uniform dose. Unfortunately, we do not currently have square fields that are flat to the 0.5 % level, as the Elekta 6MV photon beam is only flat at the 3 % level for a 10 × 10 cm open field, while 10 MV and 25 MV show larger variations. Therefore we chose to use a one-dimensional uniform dose source, a Strontium-90 check source mounted on a Velmex™ linear translational stage. The linear stage was controlled by a computer and the Strontium-90 source moves slowly along a 12 cm long strip of EBT film. Since the output of the Sr-90 source is constant, and the distance between source and film is also constant, a uniform line of dose is expected. As shown in figure 3.10, however, we observed a 2 % sudden drop between the first and second half of the film, when we take a dose profile along the direction of travel. Such fluctuation can only be attributed to the lack of uniformity of EBT film.

Having demonstrated the dominance of a "non-random and unpredictable" non-uniformity due to coating, it is desirable to devise a method of reducing the uncertainty caused by this non-uniformity. Since this non-uniformity only surfaces after irradiation, a potential solution is the double exposure technique, introduced by Klassen *et al* for the MD-55 film. (1997) In this technique, one or more blank EBT films are exposed to a radiation field known to be flat within 0.5%. This exposure is called the pre-irradiation. After pre-irradiation, the films are left in storage for a day, and then scanned. Such scanning reveals the non-uniformity introduced in the film coating process. Here we assume that the non-uniformity correspond to fluctuations in the concentration of EBT crystal across the film surface, therefore the scanned image of the pre-irradiated film provides a

first-order correction that can be applied in the experimental irradiation. Such a technique can be applied to both absolute and relative dose measurements. In the case of absolute dose measurement, it is necessary to accurately measure the absolute dose delivered in the pre-irradiation process. In addition, it is also necessary to account for the darkening effect of EBT film. Section 3.8 will explain the darkening effect in detail, but the conclusion was that environmental conditions caused unpredictable darkening of EBT film even after 24 hours post irradiation. The magnitude of long-term darkening is up to 5 % over the period of 3 months. Such effects make pre-irradiation approach difficult to implement in absolute dose measurements, as the darkening effect of both pre-irradiation and actual field of interest is combined in the final film optical density measurement. For relative dose measurements, darkening of film is less of a concern, as a uniformly irradiated EBT film will darken uniformly. The remaining obstacle for pre-irradiation of EBT film used in relative dose measurement is difficulty in achieving a radiation field flat to the level of 0.5 % or better. The best candidate at this institution is the NRC Co-60 beam, which can potentially achieve such flatness if source-surface distance is increased to 2 meters or more.

Although the pre-irradiation technique has the potential to further reduce uncertainties in dose measurements, we do not have access to the Co-60 beam during this project, and this technique was not implemented. The alternative to this approach is repeating the measurement two or more times using different films and taking the average of measured dose distributions. Battum *et al* (2008) provided detailed analysis of uncertainty reductions achieved in utilizing three sheets of film in dose distribution measurements, and showed that the reduction in uncertainty is consistent with the central limit theorem. Despite the extra cost in film, averaging of multiple films is an attractive alternative to pre-irradiation if the desired measurement is one-dimensional, because film strips, rather than whole sheets of film, can be used.

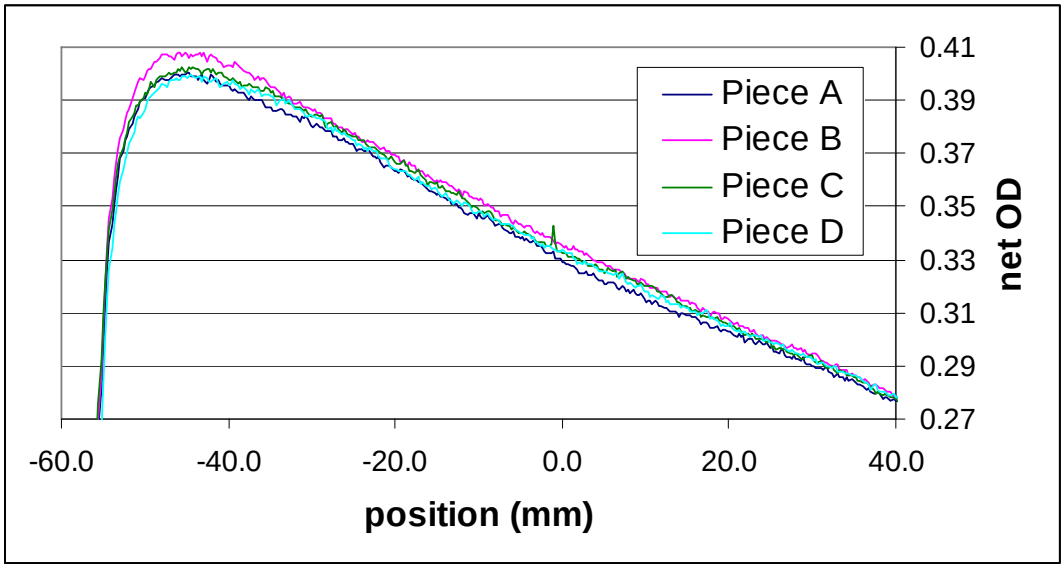

Figure 3.9. Net optical density of four film strips irradiated to identical doses in a wedge field. Note the consistent difference between piece A and B, while piece C and D fluctuate in between the two.

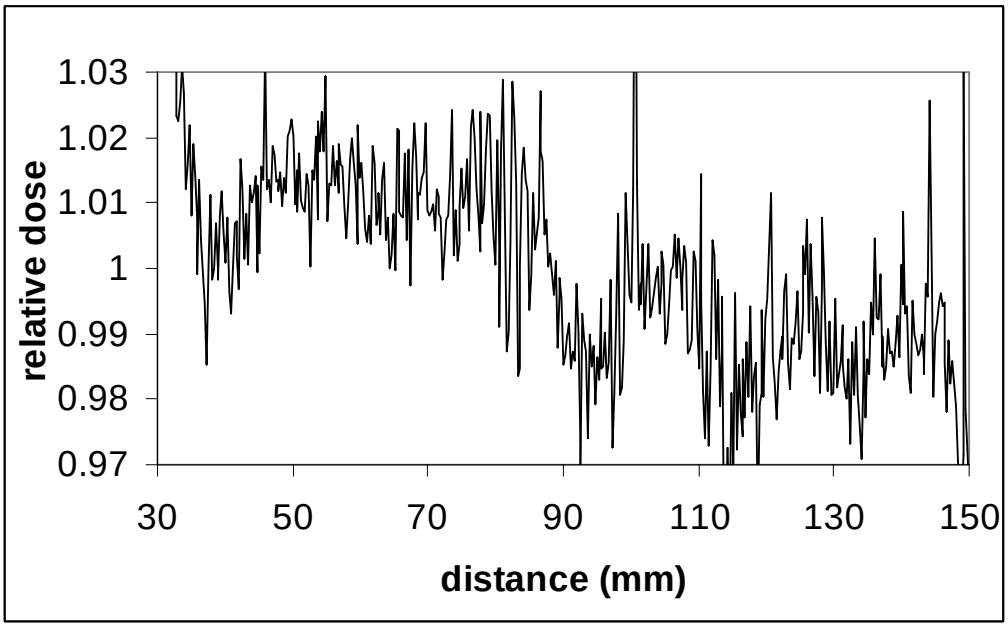

Figure 3.10. Dose profile produced by a Strontium 90 check source mounted on a Velmex linear translational stage.

3.5 Calibration curve of EBT film

3.5.1 32 point calibration for the "true shape" of EBT calibration curve

The GafChromic EBT film, being a non-linear detector, requires calibration through the entire dosimetry range before it is used. Current protocols as reported in literature use eight data point to fit a two parameter equation for each batch. Various authors have reported that a second order polynomial does not accurately describe the calibration curve of EBT film (Devic *et al*, 2005). There are two solutions to this problem: increase the number of parameters in a polynomial equation, or search for a non-linear equation with two parameters that can adequately describe the calibration curve (Devic *et al* 2005, Battum *et al* 2008). Increasing the number of parameters while maintaining the same number of data points reduces the confidence we have on our calibration curve. For example, a fourth order polynomial fit with the constant term set to zero can be applied to a standard 8-piece film calibration, but that would result in 4 free parameters with 7 effective data points, as the zero dose piece is used to set the constant term to zero. Such a fit would result in very small residuals, but with 3 degrees of freedom and 4 parameters, there is little confidence in the data. Any small errors in individual data will be difficult to detect while that small error would have a significant effect in the fit parameters. Another approach is to search for a two-parameter non-linear equation that adequately describes the calibration curve. This approach has its own drawbacks due to difficulties in uncertainty analysis of fitting a non-linear equation.

In this protocol, we decided to use a polynomial to describe the calibration curve of EBT films. The motivation is to ensure predictable behavior of calibration curve for all data measurements. The behavior of polynomials is well understood in theory, and most statistical software packages have robust algorithms for finding the best fit even when multiple fitting parameters are involved. The uncertainty calculation of polynomials is also well developed, making it easier to trust the reported uncertainties reported by data analysis software. For an

unknown function known to cross the origin, such as the calibration curve of EBT films, Taylor's theorem also states that a polynomial can accurately describe a finite portion of the equation. Non-linear equations, on the other hand, do not enjoy such mathematical support.

If we want to accurately describe the calibration curve with a polynomial, one approach would be to have a large number of calibration data points, and apply a higher order polynomial fit. Such an approach would provide robust fitting that sufficiently describes the calibration curve of the film. Figure 3.11 shows an example of such approach, using the 6 MV beam of an Elekta Precise linear accelerator. The 32 pieces of film were cut from a single sheet of 8 inch by 10 inch EBT film, irradiated individually and scanned one day after irradiation. From the graph, we can see that the 4 parameter polynomial adequately describes the shape of the calibration curve. A further inspection of residuals in Figure 3.11 showed no trend in residuals. The residuals are shown in Figure 3.12. Note that the residual shows a non-Gaussian distribution, as demonstrated by the histogram shown in Figure 3.13, because the film uniformity distribution is non-Gaussian. In contrast, the residual of a two-parameter fit using the same data set showed a strong systematic trend, while a three-parameter fit showed local trends and residuals twice as large as that of 4-parameter fit. Given the large degree of freedom and relatively small number of parameters, we conclude that this approach produces an accurate calibration curve with high degree of confidence. The drawback of this approach is that each 32-point calibration requires three hours of experimental time. Given that each batch of EBT film may have different calibration curve, it is not practical to perform routine calibrations using a 32 piece approach. Therefore, a hybrid calibration approach was considered. Such an approach was inspired by Battum *et al*'s EBT calibration protocol, where a two-parameter equation was used to describe each batch of EBT film, but one of the two parameters was a global parameter fixed for all EBT films, and only the second parameter was allowed to change for each batch. In our hybrid calibration approach, individual batch calibration is also limited to one floating parameter.

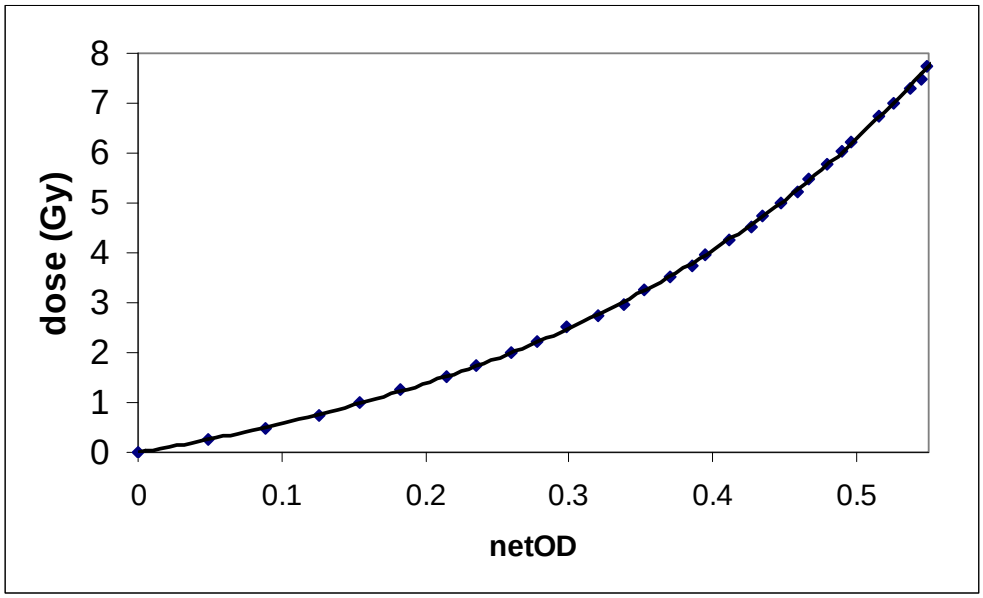

Figure 3.11. 32-piece calibration in 6 MV Elekta beam. Four parameters were used in this calibration curve.

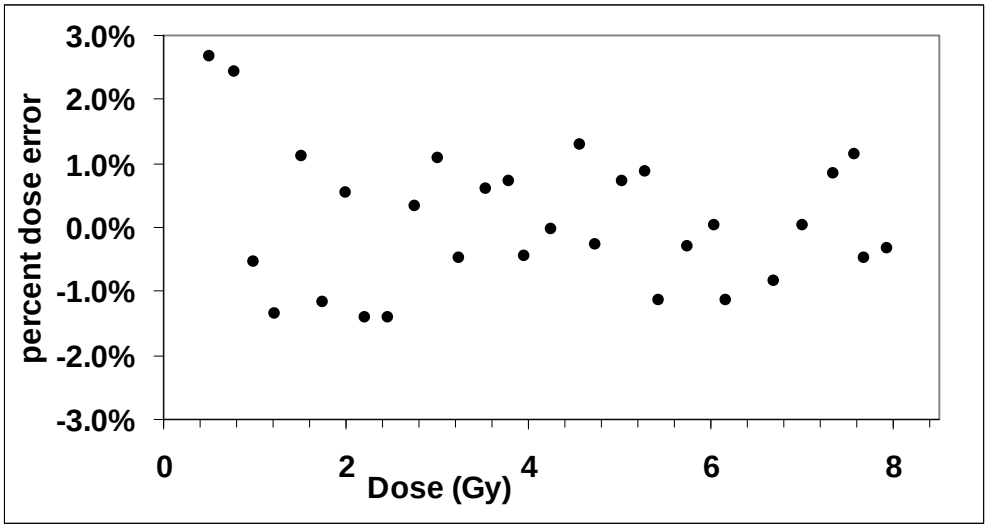

Figure 3.12. Residual of 4-parameter fitting. The residual shows a random behavior, indicating that the film calibration curve can be completely described by a 4th order polynomial.

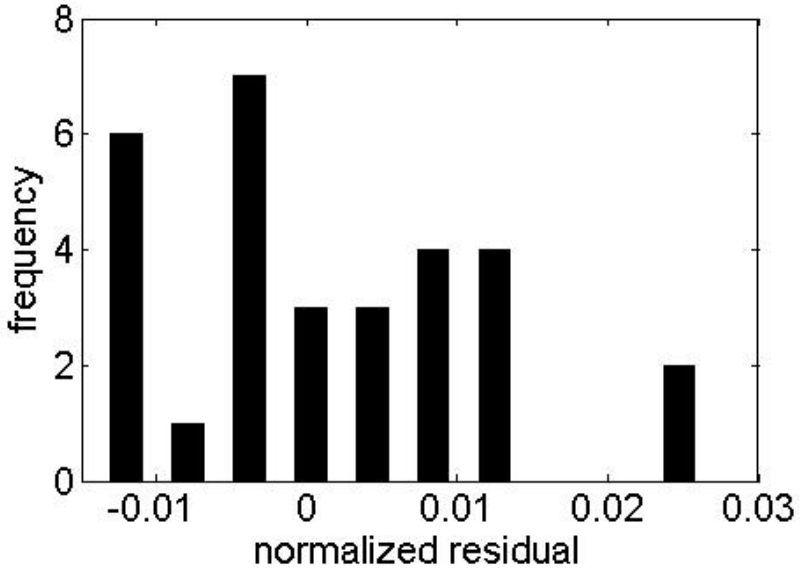

Figure 3.13. Histogram of the residual shown in Figure 3.12. It is not a Gaussian distribution.

3.5.2 Hybrid calibration method and energy & modality dependence of EBT film

The principle behind the hybrid calibration is the assumption that variations in batch-to-batch film sensitivity arises from the different film sensitive layer thickness and concentration of EBT crystal within the sensitive gelatin layer. Since the chemical composition of EBT crystal is fixed, the absorption spectrum of EBT sensitive layer before and after exposure to radiation should also be the same across different batches of films. The only difference should be the amount of light absorbed by the EBT crystal. Therefore the curvature of the EBT calibration curve with dose, which can be considered as an expression of EBT crystal absorption spectrum, should remain the same across different batches. In other words, a linear scaling factor should be adequate in describing the sensitivity variations of different batches of EBT films. This approach was inspired by Battum *et al* (2008)*'s* approach of employing a "global parameter" for all EBT films and leaving a single parameter in individual film batch fitting. Note that Battum *et al* used a two-parameter exponential equation in fitting their calibration curve, performing an eight point calibration for each batch. In our approach, we also have only one parameter for each batch of EBT film, but instead of a "global parameter", we assumed a "global curvature" of EBT film. The following is the EBT scaling equation:

$$y = (1+s)\times(a*x^4 + b*x^3 + c*x^2 + d*x)$$

Where a, b, c, and d are fitted parameter from the 32-point calibration, and s is the scaling factor. Figure 3.14 provides a graphical illustration of this hybrid calibration technique. Batch 1 is calibrated with 32 points, while batch 2 is calibrated with only 8 points. Assuming that the shapes of the two curves are the same, a scaling factor can be used to match the calibration curve of batch 2 to that of batch 1. In this experiment, the value of s is obtained by manually entering various values of s until the residuals for all 7 points are evenly distributed in positive and negative territory.

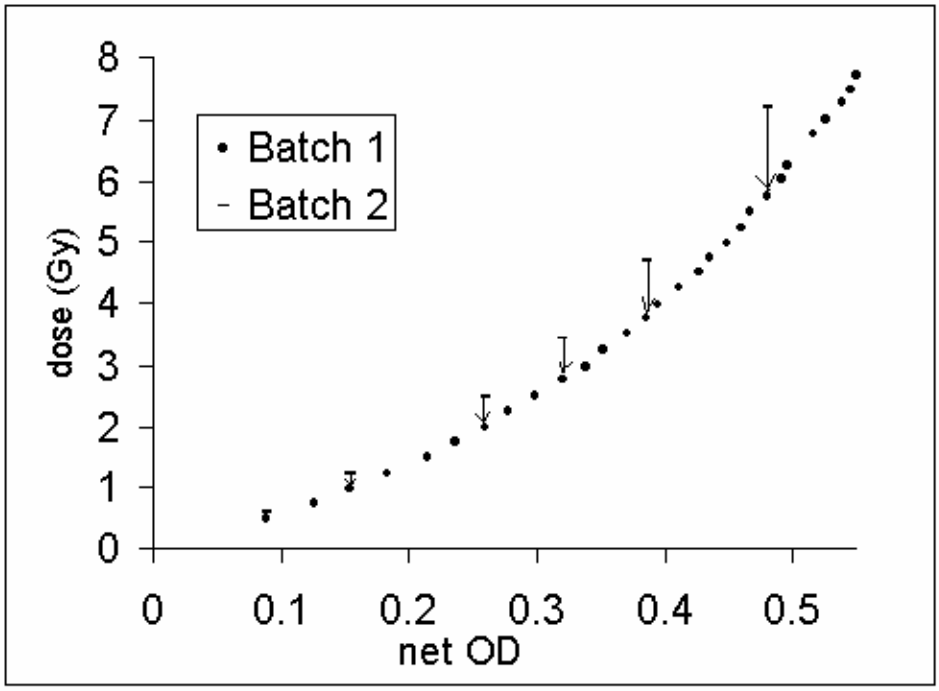

Figure 3.14. A graphical illustration of the principle behind hybrid calibration technique. The dose measured by batch 2 is scaled to the curve of batch 1 through the scaling factor s introduced above.

The results of scaling are shown in figure 3.15 where the residuals of scaling the eight-point calibrations of three batches were plotted against the dose given. Batch one is from the same batch as the 32 point calibration, while batch three contains two boxes. Table 1 shows the magnitude of scaling applied for each batch. Batch one and two show film sensitivity differences below the film uniformity variation level. The two calibration curves of batch three showed strong trends in residuals when scaled to the equation derived from 32 point calibration, and their film sensitivity different from batch one and two by more than two percent. To make a comparison, we deliberated scaled the calibration curves of the two boxes of batch three so that their 8 Gy point match. The rest of their fitting residuals differ by up to 2 %. This large difference suggests that the difficulty in scaling calibration curve of batch three may be attributed to poor film uniformity of the third batch. An email inquiry with EBT film supplier indicated that there has been no change to film production process. Results from more

batches of films will be needed before this hybrid calibration method can be used to obtain uncertainties below 1 %.

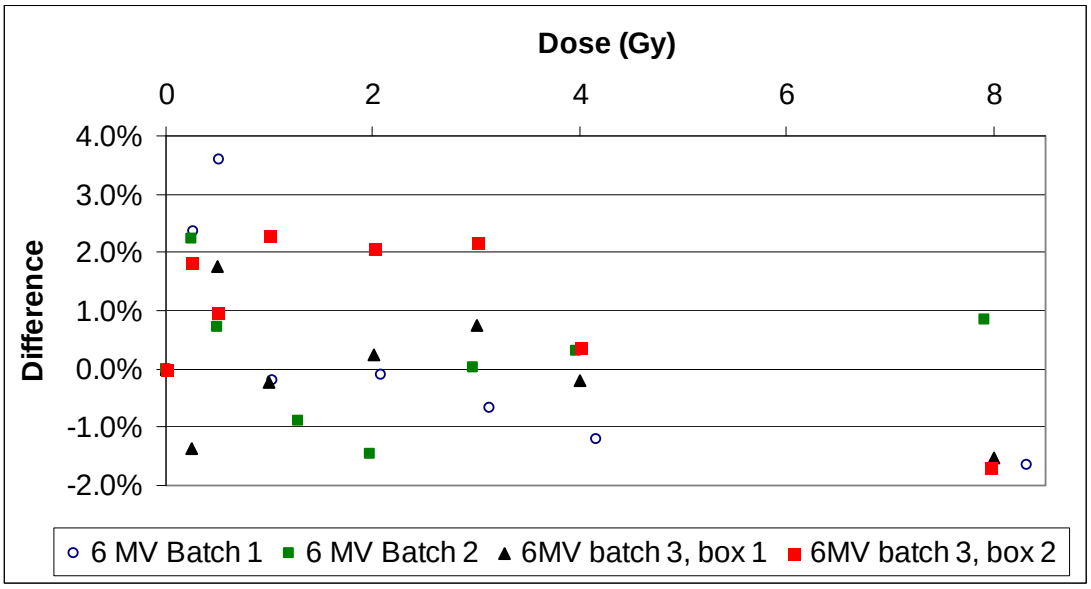

Figure 3.15. Residual of various batch's calibration when scaled to 32-point calibration curve.

Beam and film batch	s (%)
6 MV photon batch 1	0.63
6 MV photon batch 2	-0.2
6 MV photon batch 3, Box 1	-3.0
6 MV photon batch 3, Box 2	-2.3

Table 1. Scaling percentage factors for various 8-point calibrations. S is the parameter introduced in section 3.5.2. Note that batch 1 and 2 have sensitivity differences below the level of film uniformity. The two boxes of batch 3 show similar sensitivity, which is expected as they have the same batch number.

3.6 Energy and beam modality dependence of EBT film

Although the hybrid calibration technique still needs improvement, this idea can still be applied to the investigation of energy and beam modality dependence of EBT film, as energy and beam modality dependences are expected to be present for all dose levels. Since the initial application of this EBT film dosimetry protocol at NRC is for use with the Vickers experimental linear accelerator's megavoltage electron and photon beams, the energy and beam modality dependence investigation is limited to high energy photon and electron beams. The same batch of EBT film was calibrated in Co-60, 6 MV, 10 MV, and 25 MV photon beams, as well as an 18 MeV electron beam. For x-ray calibrations, 10 x 10 cm^2 field, 100 cm SSD and 5 cm depth were used to ensure the same experimental setup as chamber calibration. An Exradin A19 Farmer-type chamber was used to measure the dose delivered to the film. For Co-60 calibration, a calibrated NE2571 Farmer type chamber was used to measured dose. For electron calibration, a calibrated NACP-02[10] and PTW Roos parallel plate chamber was used. As a result, EBT film calibrations were performed in three beam modalities. No direct comparisons between any two of these three beam modalities have been published in the literature, but it is generally assumed that EBT film sensitivity is identical across these three modalities. Our experimental results confirmed this assumption at the 2 % level, which is consistent with the range of sheet-to-sheet sensitivity variation within a single batch. The calibration curves of 6 MV, 10 MV, and 25 MV x-ray, 18 MeV electrons and Co-60 are shown in figure 3.16. The magnitude of scaling applied for each energy and beam modality is shown in Table 2. A further inspection of scaling residuals showed that calibrations performed on the Elekta linear accelerator showed residuals consistent with film uniformity, but the Co-60 calibration showed a strongly "trendy" behavior. Since other solid state detectors such as alanine also showed different response in continuous and pulsed beam (Anton *et al*, 2008), more investigation is needed for the behavior of EBT films in Cobalt beam, if 2 % or

[10] IBA, Germany

better accuracy is required. Figure 3.17 illustrates the residuals of the various energies' calibration curve after scaling to the 32 point curve.

Based on this finding and the consensus in the literature on the energy and beam modality independence of EBT film, we conclude that the calibration curves established using the Elekta 6 MV photon beam can be used on the Vickers photon and electron beams. Note that the EBT film's insensitivity to photon beam quality is very attractive, as the Vickers accelerator can produce X-rays using various target material such as Al, Cu, and Pb, where beam quality may not be known.

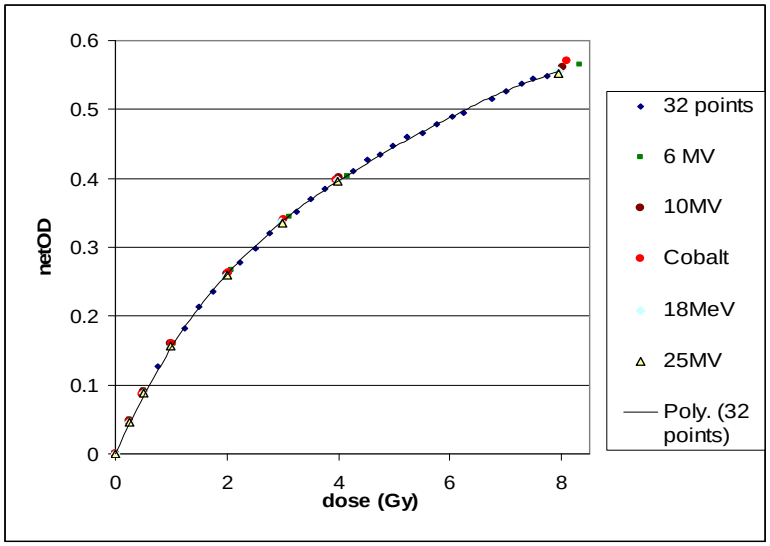

Figure 3.16. EBT film calibration in three X-ray energies and Cobalt. The 8 point measurements fall on the 32 point curve. The line drawn is a fourth-order fit of 32 point data set. The data presented here is not scaled (e.g. original data).

Energy	s (%)
25MV	-1.3
6MV	0.6
6MV	-0.2
18MeV	0.2
10MV	0.2
Cobalt	-2.0

Table 2, Energy and beam modality dependence of EBT film, measured by scaling factors required to match the corresponding 8-point calibration to established 32-point calibration.

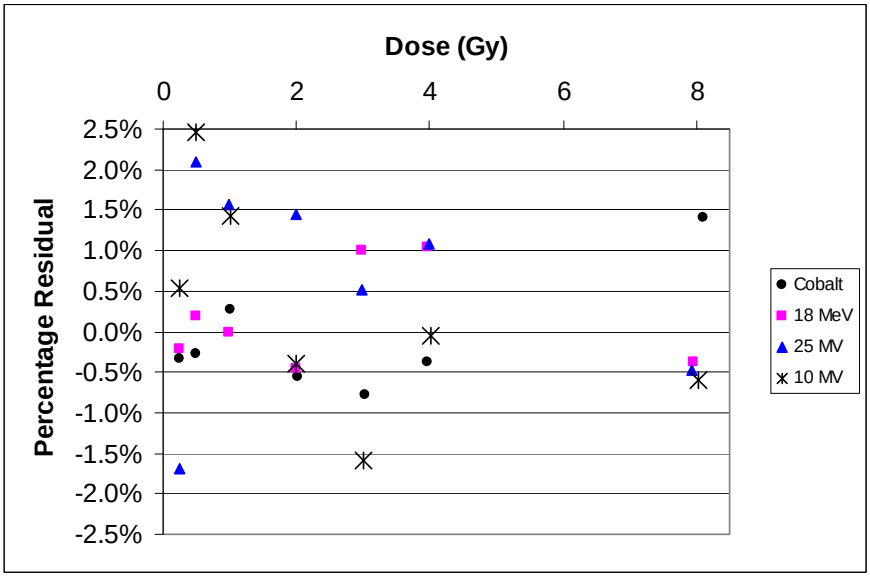

Figure 3.17. Percent residual of various energies after scaling to 32-point fit. Note that the scaling of Co-60 calibration was performed manually to reduce the impact of the 8 Gy data point. In future Co-60 calibrations, the 8 Gy point should be repeated at least twice to ensure it is accurate.

3.7 Scanner uniformity investigation

The scanner uniformity is a well-known artifact of flat-bed color scanners when used in EBT film dosimetry, but no consensus has been reached on this subject. This section will present our investigation of this subject.

3.7.1 Lateral uniformity correction

Eight film pieces irradiated to between 0 and 8 Gy were scanned at various lateral positions of the scanner, one piece at a time, while maintaining the same longitudinal position. Another unirradiated film was placed on the lower center part of the scanner bed, to account for the two-state fluctuation behavior of the scanner, as documented in section 3.3. The position of the film of interest was obtained from the image file, using the resolution reported by the manufacturer. The geometric accuracy of the scanner was verified in a separate experiment and confirmed to be better than 1 %. The average pixel value in the ROI was converted to net optical density and plotted against the x-position on the scanner bed. Between 15 and 20 points were obtained for each dose level. Note that unlike existing literature, this approach does not assume the middle of scanner bed to be the minimum OD position. Instead, the position of minimum OD was experimentally determined, and found to be close to, but not exactly at, the geometric mid-point of the scanner bed. The results of this measurement showed a strong lateral non-uniformity as expected. In the literature, various authors have assumed the lateral correction to be symmetric and could be described by a second order polynomial equation (Battum *et al* 2008, Saur *et al* 2008). Further inspection of data showed that the lateral uniformity correction is not symmetric and can not be adequately described by a second order polynomial. Figure 3.18 showed the symmetry of 2 Gy lateral uniformity measurement by plotting the relative OD values against distance from the minimum point. The left and right sides of the curve does not exhibit the same curvature. Therefore a third order polynomial was used as the correction equation in this protocol. Figure 3.19 shows the same 2 Gy uniformity measurement fitted with a third order polynomial. The fit adequately describes the data points at the 0.5 % level.

Having found the correction equation for one particular dose level, we proceeded to search for a universal correction equation for all dose levels. If the lateral correction was expressed as the difference between the OD at a given position and the minimum OD in the line, the correction was strongly OD-dependent, requiring multiple correction equations and interpolation in-between. Based on this result, we expressed the lateral uniformity correction as relative optical density. When expressed as relative optical density, lateral correction curves for doses from 1 Gy to 8 Gy agree within 1 %, as shown in Figure 3.20. The differences in lateral correction factors for different doses decrease as we get closer to the middle of scanner bed. Based on the desire for a simple scanner correction, we used the lateral correction equation of 2 Gy for all doses between 1 Gy and 8 Gy. Note that this approach is based on the current limited film uniformity, where up to 2 % fluctuation in film sensitivity can occur within a sheet. If a more accurate correction is desired, different correction equations can be employed for different optical densities, and interpolation techniques can be implemented for doses not measured in this experiment. Currently no correction is applied for doses below 1 Gy, because the relative lateral correction for doses below 1 Gy is dose dependent and large, even though the absolute value of the correction is small. Therefore current dose measurements for the Vickers experiment are limited to between 1 and 8 Gy.

After confirming that the lateral correction can be described by a single equation for optical densities of 1 Gy or above, we investigated the lateral inhomogeneity at different longitudinal positions. Figure 3.21 showed the two lateral correction curves obtained at two positions, one is 605 pixels from the top of scanning area, and the second is 1088 pixels from the top of the scanning area. Therefore the lateral correction for the entire scanning bed can be described by an equation for each optical density. In other words, the lateral and longitudinal corrections are de-coupled.

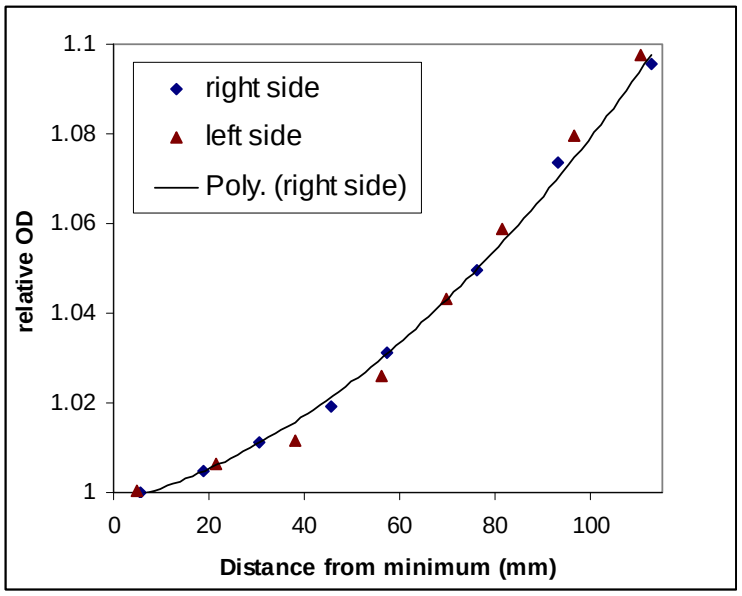

Figure 3.18. Symmetry test of lateral homogeneity correction, measured with a 2 Gy film piece. A second order polynomial fit of the right side indicates that the correction is not symmetric and can not be adequately described by a second order polynomial.

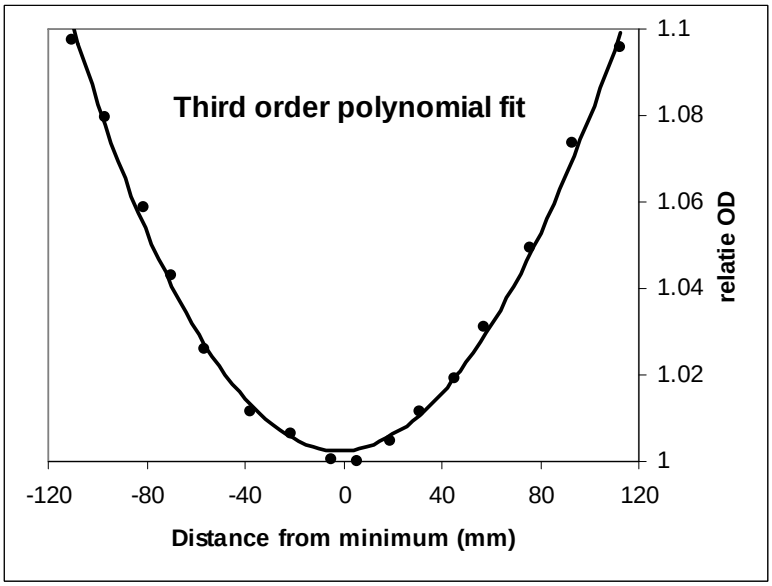

Figure 3.19. Third order polynomial fit of 2 Gy film lateral uniformity correction. Due to the lack of symmetry, a third order polynomial correction was implemented in our protocol.

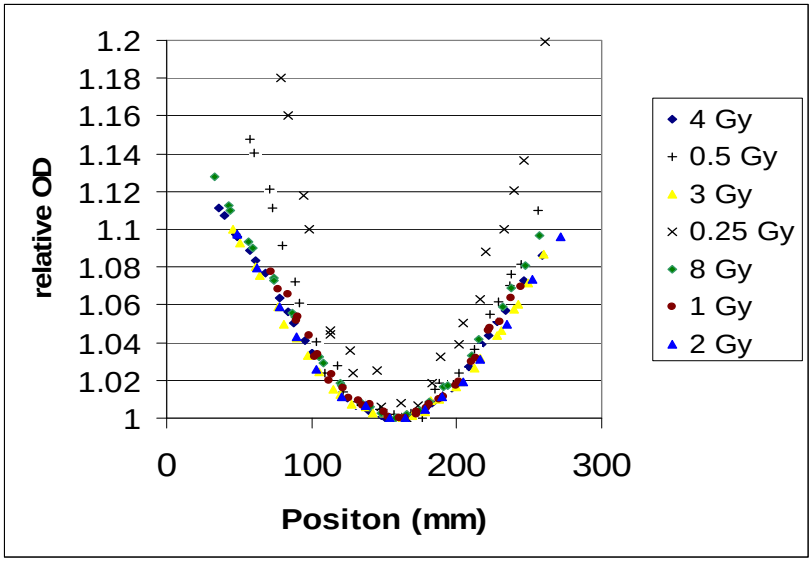

Figure 3.20. Lateral non-homogeneity as expressed in relative OD.

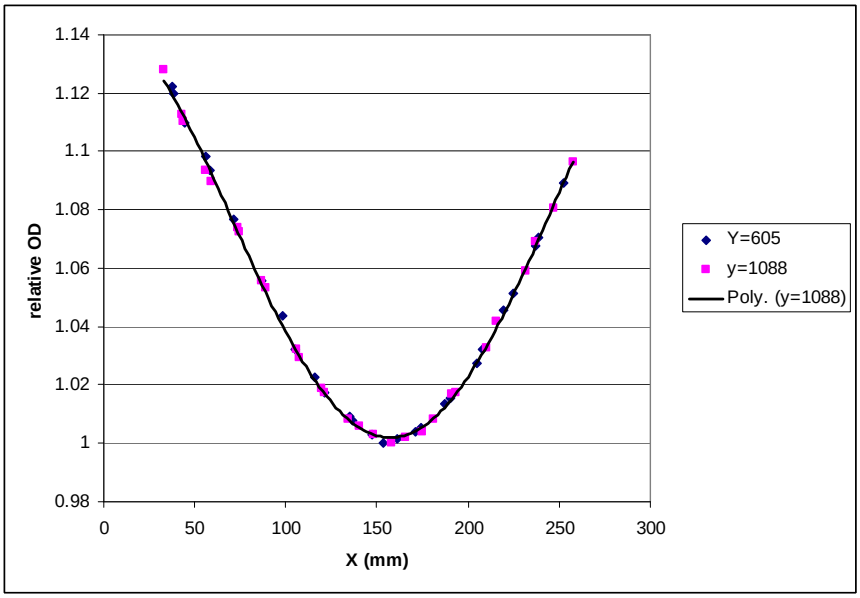

Figure 3.21. Lateral non-uniformity for film irradiated to 8 Gy. The shape and position of minimum of the two curves agree within noise level. A fourth order polynomial fit was added to demonstrate the level of agreement compared to noise.

3.7.2 Longitudinal correction

Only a handful of papers in the literature report a significant longitudinal non-homogeneity (Paelinck *et al*, 2006), but those papers that ignore such inhomogeneity do not provide evidence of homogeneity satisfactorily (Battum *et al*, 2008). By measuring the OD of a single piece of film along the central axis of the scanner, we confirmed that any longitudinal inhomogeneity would be comparable to experimental error introduced by scanning and replacing a film multiple times. Figure 3.22 shows the longitudinal dependence of optical density for a film irradiated to 2 Gy. The points are normalized to their mean. A linear fit revealed a trend in observed data, but total deviation over a distance of 20 cm will be less than 0.2 %. Given the 20 x 20 cm^2 maximum size of EBT film used in this protocol, any longitudinal correction is ignored. Note that the longitudinal correction measurements also showcase the results of scanner fluctuation correction technique and the reproducibility of our protocol in reading the same piece of film after mechanically disturbing it.

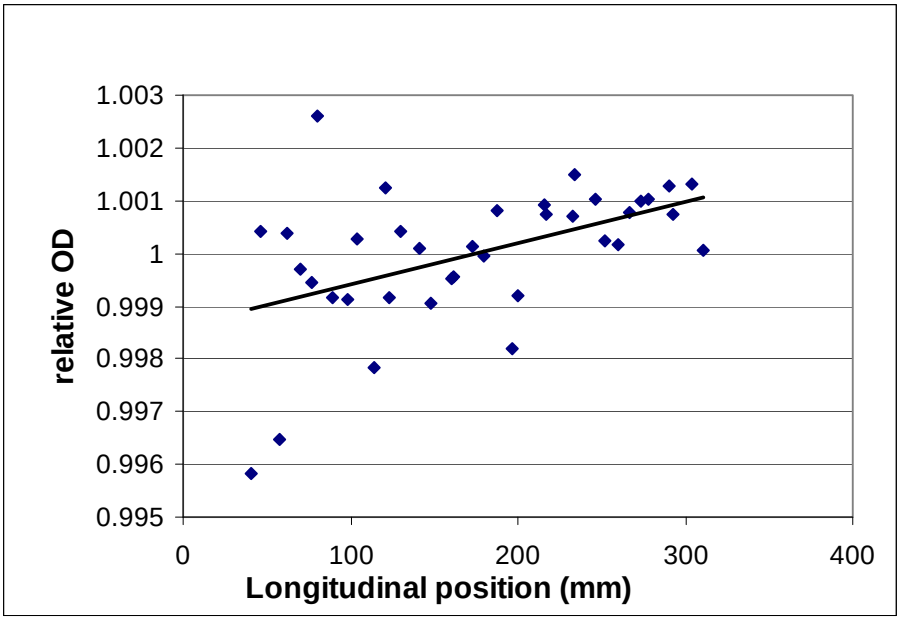

Figure 3.22. Longitudinal uniformity measured with a 2 Gy film piece.

3.8 Long and short term darkening of EBT film

3.8.1 Summary of literature review and techniques employed for this work.

GafChromic EBT film is known to require curing time in order to reach a stable optical density. The reason behind the need of film development time is poorly documented in the literature, but Dr. David Lewis of ISP Corp provided some basic explanation in a recent presentation. Put in a simplified manner, EBT film's change of color is a result of the connection of many monomers into a polymer. As monomers are added to the polymer chain, the polymer "shrinks". As the polymer gets longer, the additional monomers are further away from it, making subsequent reaction less likely. Therefore, although the polymerization process never completely stops, its speed approaches zero exponentially as time goes on. Such a theoretical explanation suggests that EBT's post-irradiation development may be best viewed on a log-linear scale.

Current literature generally covers the first 24 hours of darkening, and various authors have shown that darkening effects are sufficiently small for clinical purposes after 24 hours. Therefore most protocols recommend 24 hour or longer development time, with the stipulation that scanning is performed at fixed time after irradiation. There is very limited data on long-term darkening, even though it has been acknowledged that a long-term darkening effect is present. The only literature so far is by Martisikova *et al* (2008), which suggests that film darkening stops after 10 days. The newest model of scanner recommended by ISP, the Epson Expression 10000 XL, has been shown to have optical density reproducibility of better than 0.2 %, if a reference piece is used to correct for scanner fluctuation. Such improvement has made darkening effect study beyond the first 24 hours feasible.

3.8.2 Darkening within 24 hours

Various authors have reported on the darkening of EBT film for the first 24 hours after irradiation. The typical curve showed dramatic OD increases for the first 2 to 4 hours post irradiation, and much slower increases between 4 and 24 hours. We have also reproduced such data, and plotted it in log-linear scale. The results

are shown in Figure 3.23. Note that the first measurement of optical density was not taken immediately after irradiation, due to the different pieces irradiated at different time. The log-linear behavior of darkening within the first 24 hours is evident in this figure.

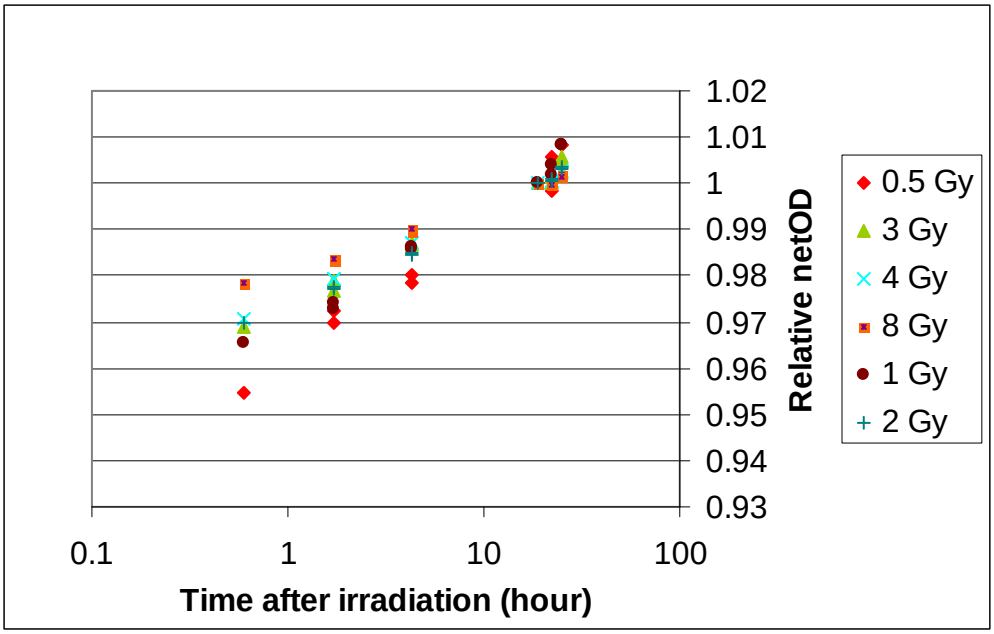

Figure 3.23. Short term darkening of EBT film. Note that as the irradiation of all 7 pieces of film takes in excess of one hour, we do not have data for the first few minute post-irradiation.

3.8.2 Darkening beyond first day and up to 3 months

The approach of scanning after 24 hours is a sensible approach, as a few hours of error will not cause any systematic error of more than one percent, which is satisfactory for clinical purposes. The lack of information on long-term darkening, however, means that the image file is the only archive available for the dose distribution. As the film darkens over time, it would be desirable to read the film several days or weeks after, and re-construct the dose. Doing such would require detailed knowledge of the film darkening process beyond the first day and this section documents our investigation of such behavior.

The strongest evidence of long-term darkening comes from our 32 point calibration, which is the calibration with the most data points in this project. The calibration film set was kept in a metal cabinet at room temperature, in a basement, to avoid sunlight exposure. Up to 5 % darkening was observed over the course of three months, and the darkening is approximately linear. Figure 3.24 demonstrates such behavior. Measurements at two weeks and one month, however, showed that darkening is not always linear. Note that unlike the experiment of 24 hour darkening, the films were removed from scanner bed between each scan in order to avoid prolonged exposure to ambient light. This measurement is therefore made possible by our Lucite template designed for scanning calibration film pieces, and our scanner fluctuation correction technique. The 0.2 % reproducibility in scanning the same piece of film in different days allowed us to detect the small changes in optical density as the film darkens.

After demonstrating the long-term darkening of EBT film, we investigated the reproducibility of EBT film's long term darkening. The long-term darkening study of 32 point calibration set showed that the darkening effect is an increasing function of net optical density, and that the net optical density increase is not always a linear function. Use of EBT film itself as dose information archive requires knowledge about both the rate of darkening and the shape of the darkening curve. For this purpose, a 6 MV X-Ray calibration film set and an 18 MeV electron calibration film set were irradiated at the same day, and both were scanned one day after. They were then scanned again 30 days after to obtain

the darkening curve over 30 days. A 25 MV x-ray calibration film set were irradiated at a different day. This film set was scanned at one day and after 40 days to obtain its darkening curve. The result is shown in Figure 3.25. The 6 MV x-ray and 18 MeV electron calibration sets showed a very similar darkening curve after 30 days, while the 25 MV x-ray data showed much lower level of darkening after 40 days. Such results indicate that long-term darkening of EBT film may be dependent on the environmental history of the film after the irradiation, while the energy and beam modality of the film does not play any significant role. Such behaviors make using EBT film itself as a dose archive in a clinical environment unfeasible, as strict environmental control will likely be required if accurate long-term darkening is to be predicted. If storage in an environmental chamber was to be implemented in the future, however, film-to-film variations of long-term darkening would still need to be investigated.

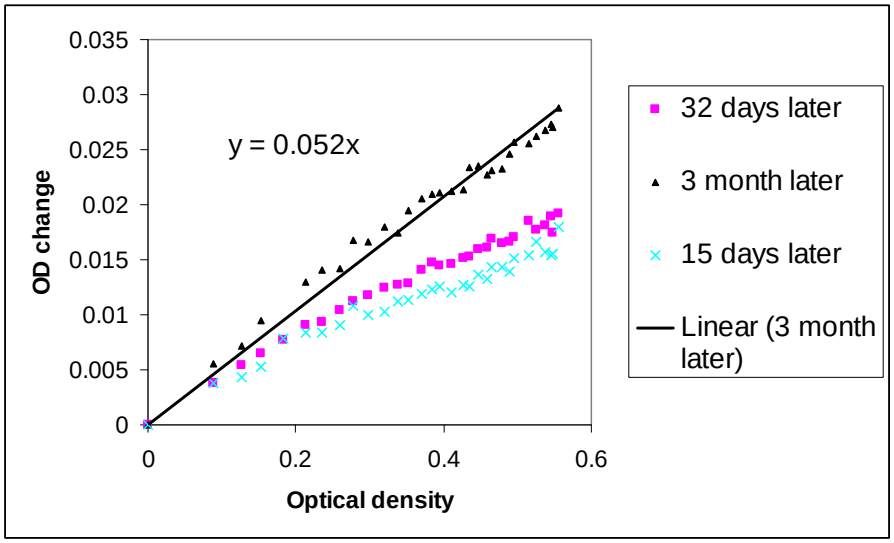

Figure 3.24. The 32 piece set's optical density change over the course of 3 months.

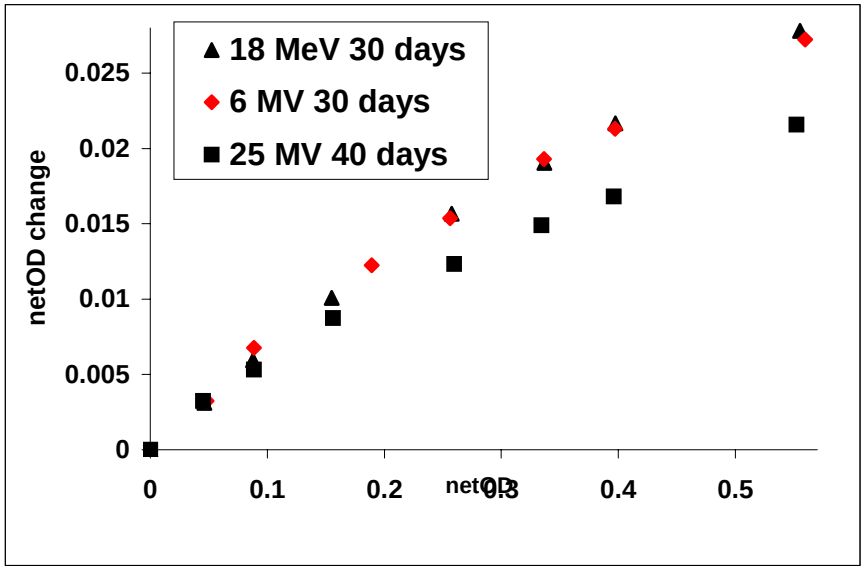

Figure 3.25. Darkening measurement of 6 MV X-ray, 25 MV X-ray, and 18 MeV electron calibration set.

3.9 Humidity effect and TinyTag humidity logger

3.9.1 Background

Rink *et al* (2008)'s paper on the humidity effect of EBT films reported that drying a film in a drying oven at 50 ºC for 24 hours can cause a 20 % reduction in sensitivity. Such a result raises the concern of a dry storage environment's impact on film sensitivity, given the low indoor humidity caused by low outside temperature at NRC during winter.

3.9.2 Measurement

A batch of EBT film was stored in its standard cabinet during the NRC winter shutdown, and a TinyTag™ humidity logger [11] was used to record the environmental history. During this three week period, humidity levels between 5 % and 8 % were observed during most evenings, while the temperature remained between 20 ºC and 25 ºC. After the winter break, one sheet of film from this batch was used in a 8-piece calibration, and the results showed that no change in sensitivity can be detected. As seen in Figure 3.26, the change in sensitivity was less than 1.5 %, below the film uniformity level. This preliminary result indicates that the humidity effect is likely not a concern for normal clinical applications.

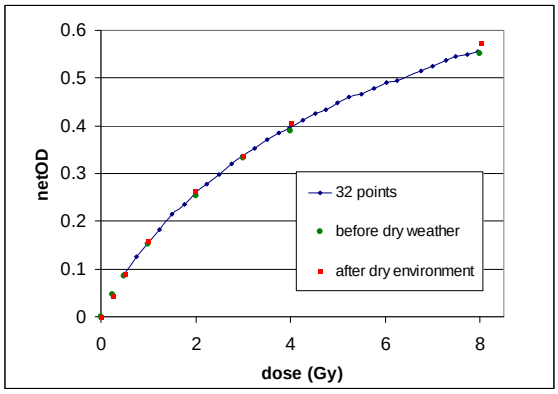

Figure 3.26. Film sensitivity comparison before and after three weeks of relatively dry weather.

[11] Gemini Data Loggers Ltd, West Sussex, UK

Chapter 4 Applications

Having established our own EBT protocol for two-dimensional reference and relative dose distribution measurements, it is necessary to verify its accuracy in measuring such one and two dimensional dose distributions. In the previous section, measurements were focused on small pieces of film. For practical applications, long strips or large sheets of EBT films up to 20 x 20 cm are typically used. Before we can measure an unknown dose using a long strip or a large sheet of EBT film, we need to test the accuracy of our EBT film dosimetry protocol in measuring one and two dimensional dose profiles. In such tests, profiles measured by EBT films will be compared to profiles measured by ionization chamber scans in a water tank and a PTW[12] Starcheck™ 2D ionization chamber array. The results will provide a measure of actual accuracy of EBT protocol when used in measuring unknown dose profiles.

After establishing the precision of our EBT film dosimetry protocol, we will apply it to the measurement of dose distributions from the NRC Vickers accelerator. This application will demonstrate EBT film's capability as a high resolution dosimeter that provides complete two-dimensional dose information.

We would like to emphasize that the experiments in this section are initial investigations on the feasibility of using EBT film in such scientific experiments. The results presented here are meant to demonstrate the capability of our EBT film dosimetry protocol, rather than to provide conclusive results for each particular investigation. For all experiments in the following sections, future work is required before any definite conclusions can be derived.

[12] PTW Freiburg GmbH, Germany

4.1 Comparison with 1D detectors

Before EBT film can be used as a dosimeter in dose profile measurements, it is necessary to verify the accuracy of our film dosimetry protocol using established detectors. Among conventional detectors, ionization chamber scanning using a water tank is considered to be the most accurate, as the same chamber is used in all positions. A Multidata Multiscan™ water tank[13] with a scanning ionization chamber was used to measure dose profiles in the left-right direction of an Elekta 6 MV X-ray open field, at 5 cm depth in water. The left-right direction is also called the A-B direction, which is perpendicular to the gun-target directions in vertical beam setup of clinical Linac experiment. Figure 4.1 shows the directions with regard to the Elekta control system. A 20 x 20 cm square sheet of EBT film was irradiated in the same field at 5 cm depth in a Virtual Water phantom. The results are shown in Figure 4.2, where relative dose profiles were compared. Note that the net optical density of the film was extracted from the scanned image, and the net optical density was converted to absolute dose profile using the calibration curve. This absolute dose profile is then normalized to the beam axis, and the resulting relative dose profile is compared with relative profiles obtained from chamber scanning. Film and water tank measurements agreed within the film uniformity level, with the film showing a 2 % drop in measured dose at the positive edge of the field. This result is consistent with our Strontium-90 experiment, where a 2 % fluctuation in film response was observed. The 20 x 20 square sheet of EBT film allowed us to measure dose profiles in two orthogonal directions, and profiles measured by EBT film agree with scanning chamber measurements in both directions. This provides one evidence that our scanner uniformity correction technique is accurate to the level of film uniformity.

[13] Multidata St Louis, Missouri

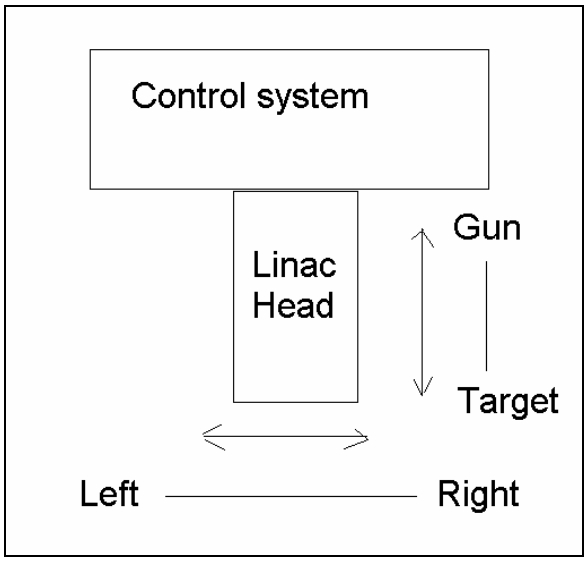

Figure 4.1. The Gun-target and Left-right directions referred to in this section.

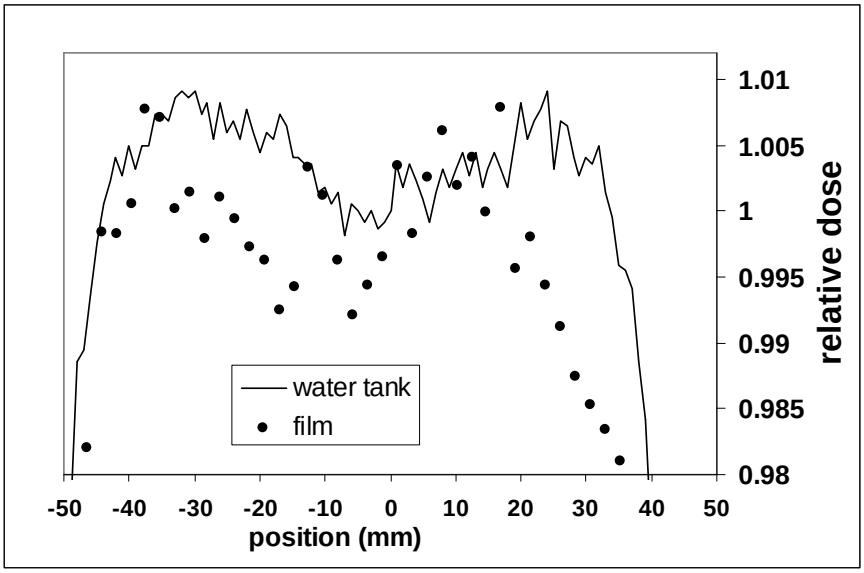

Figure 4.2. Comparison of 6 MV X-Ray open field profiles measured by EBT film and scanning water tank. Note that both profiles are normalized to the beam axis, where the value of position is zero.

After comparing film measurements with water tank measurements, we also want to compare dose profiles measured by EBT film with profiles measured by ionization chamber arrays commonly seen in a clinic. Compared to ionization chamber scanning in water tank, ionization chamber arrays can be used in a solid phantom, making the experimental setup easier. In this experiment, both EBT film and the PTW Starcheck were used in relative dose profile measurements in an Elekta 25 MV x-ray open field at 5 cm depth in virtual water. Unlike the 6 MV beam, the 25 MV beam was not flat and showed significant structure. For further comparison, the relative dose profile was also measured by ionization chamber scanning in water tank. The comparison between Starcheck and EBT film in Virtual Water, and ionization chamber scan in water tank are shown in Figure 4.3. In this figure, relative dose profiles measured by Starcheck and water tank agreed within 1 %. Dose profile measured by EBT film agreed with the other two detectors for part of the profile, but a 2 % jump in film measurement was observed and this can be attributed to the poor uniformity of film. Taking film uniformity into account, EBT film accurately measures dose profile at the 2 % level.

In relative dose profile comparisons, attention needs to be drawn to the process of normalizing the dose profile. For figures presented in this section, EBT dose profiles are normalized to the average of the two data points closest to zero. Since the same area of EBT film is never irradiated twice, the fluctuation in EBT film sensitivity can cause systematic shifts in the normalized dose profile if the area of film used for normalizing the dose profile suffers large sensitivity fluctuations. Better agreement with chamber profile measurements can be obtained if dose points over a larger area is used for normalizing the dose profile, but such approach can not be extended to applications where the dose distribution of interest in unknown. Therefore we chose to normalize the EBT absolute dose profile to the beam axis, and accept the worse agreements with conventional detectors as the result of poor uniformity.

Note that the Starcheck ionization chamber array is marketed as a two-dimensional array, but it does not provide complete two-dimensional dose

information, but rather four one-dimensional profiles arranged in a star-like pattern. Such chamber arrangement provided higher one-dimensional spatial resolution, but does not allow direct comparison of complete two-dimensional dose profiles between Starcheck and EBT film. For complete two-dimensional profiles, a uniformly distributed two-dimensional ionization chamber array such as PTW Seven29™ would be required.

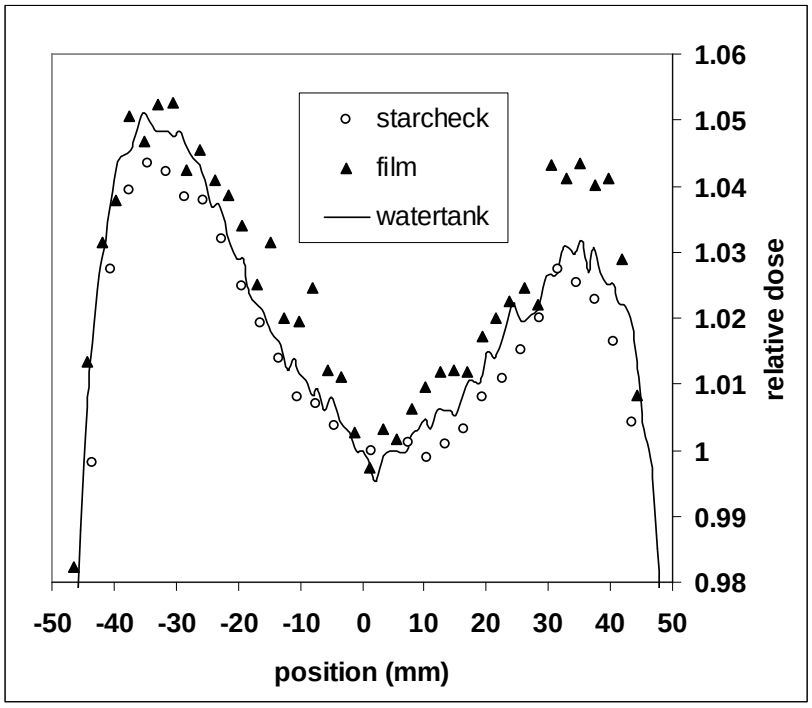

Figure 4.3. Comparison of 25 MV x-ray open field dose profile measured by EBT film, Starcheck, and ionization chamber scan in water tank, all at 5 cm water equivalent depth. Note that Starcheck appeared to underestimate the dose near the edge, but the difference between Starcheck and water tank profiles are within the calibration uncertainty of Starcheck.

4.2 Measurement of Theratron Junior Co-60 field and benefits of a 2D dosimeter

The previous section had shown that for 1D profile measurements, EBT film does not yet provide the same level of accuracy as ionization chamber scans in water tank or ionization chamber arrays such as Starcheck. EBT film's shortcoming in measurement accuracy arises from the fact that an area of film is never irradiated twice; therefore it is not possible to calibrate a piece of film before using it. On the other hand, film does provide complete two-dimensional information with 1-mm or better spatial resolution. Such an advantage was demonstrated in the Theratron Junior Co-60 beam's open field measurement.

The Theratron Junior Radiotherapy Unit[14] (serial #15) at NRC has been used for measurements related to radiation protection purposes, as its dose rate is low. As part of QA process, it was desirable to obtain a complete dose profile of the beam. Due to its low dose rate, scanning the beam with a 3D water tank would be a cumbersome and time-consuming process, as a long dwell time at each position will be required to obtain enough signal for an accurate measurement. In this case, EBT film is a better choice. A piece of EBT film was positioned at 5 cm depth in a Virtual Water phantom, which was placed 1 m from the source. In the first experiment, 2 hours of irradiation produced approximately 1 Gy of dose at the film. Surprisingly, a strip of higher dose was observed on the film. Further investigation revealed that a plate of Virtual Water with a hole designed for ionization chamber has been used in the experiment by mistake. Figure 4.4 shows an optical density map of the EBT film irradiated in this experiment. By adjusting the window level of the graph, we were able to confirm that the shape of the dose artifact matches the shape of the hole in Virtual Water plate. In a subsequent measurement, this mistake was corrected, and EBT film was used to verify that no visible structure was present in the Theratron Junior beam. Such an incident showed the advantage of a complete 2D detector compared to 1D detectors. The dose difference between the area covered by the hole and the rest of the field is 3 %, and the width of the artifact is 6 mm. If a one-dimensional

[14] AECL, Ottawa, Canada

dose profile was measured with ionization chamber scanning, such a mistake may go unnoticed. With complete two-dimensional dose information and the ability to display dose in false color, the shape of the artifact can easily be distinguished by eye. Therefore despite the lower accuracy provided by EBT film, its ability to provide complete two-dimensional dose information is valuable in many situations.

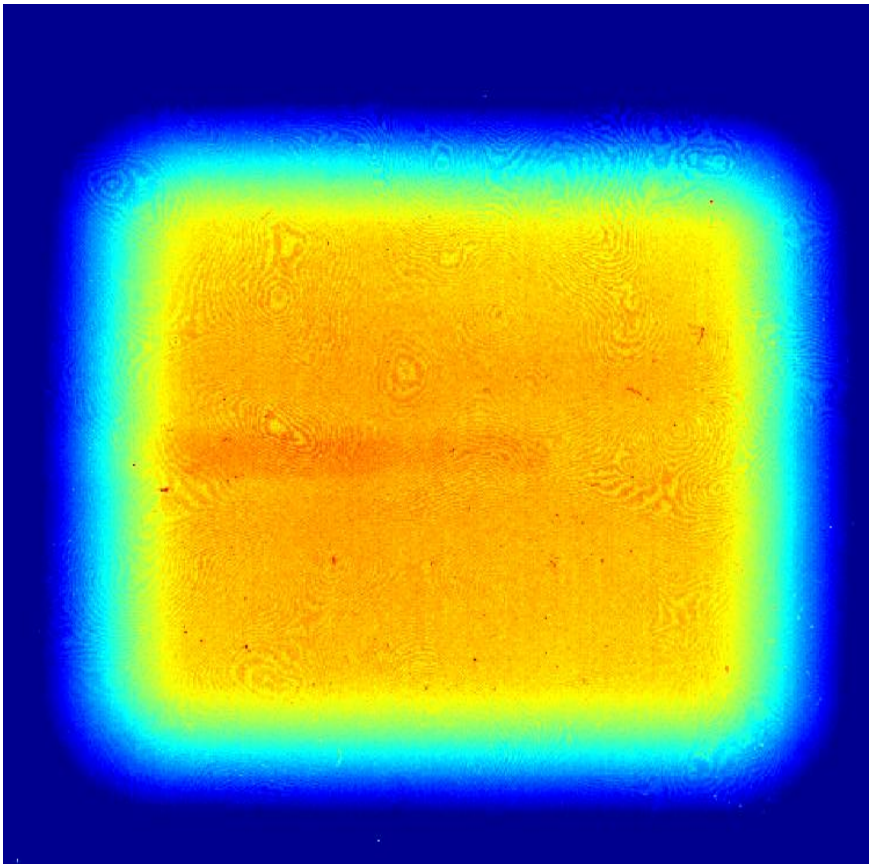

Figure 4.4. Optical density map of EBT film irradiated in Cobalt Junior beam. A strip of higher dose was visible at the center, which was eventually traced to the mistake of using a plate of Virtual water with a hole drilled in it.

4.3 Vickers electron experiment

4.3.1 Introduction to Vickers experimental accelerator

Having established and verified our EBT film dosimetry protocol, we applied this technique to the Vickers dose profile measurement. The Vickers experimental linear accelerator at NRC was commissioned in 1968 for research, rather than clinical, purposes. Figure 4.5 shows a sample picture of a Vickers experiment. We present this photo to emphasize that the Vickers accelerator is significantly different from a clinical Linac. Based on a modular design, custom-made scattering foils and targets of different materials can be mounted on the beam exit window, where an electron pencil beam of up to 40 MeV comes out. As an experimental accelerator, the Vickers has well known geometry and does not have clinical components such as flattening filter or mirror in the path of the beam. Its simple and well known geometry allows accurate description of the accelerator in Monte Carlo simulations. These features of the Vickers makes it an ideal tool for benchmarking Monte Carlo software, because few free parameters are needed in simulating the Vickers beam. Therefore the Vickers accelerator has been used for the purpose of Monte Carlo benchmarking (Ross *et al*, 2008). The Vickers accelerator also has the unique capability of measuring beam current. In other words, the total number of electrons leaving the exit window can be measured. This feature enables the measurement of dose per electron, which is the quantity calculated by Monte Carlo simulations.

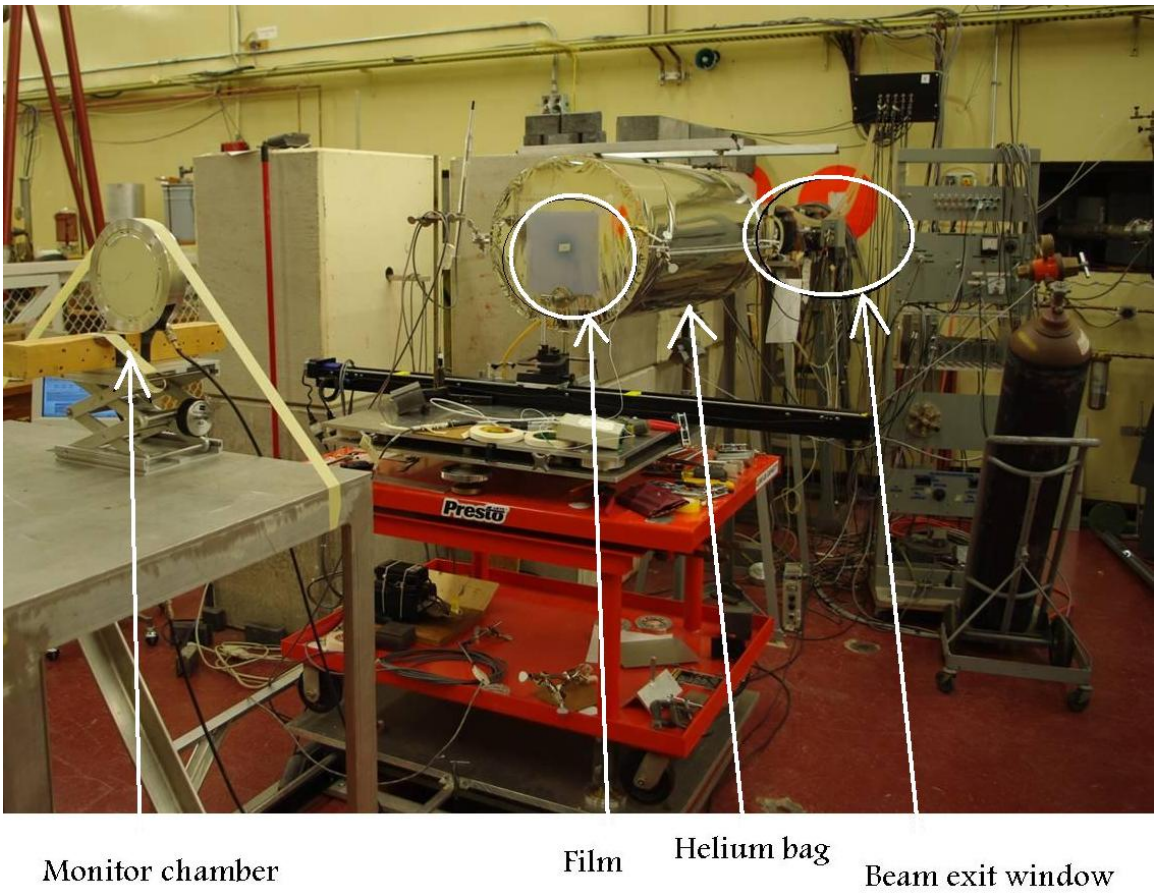

Figure 4.5. Vickers electron experimental setup. The Vickers accelerator is significantly different from a clinical Linac. The monitor chamber provides feedback to the accelerator control system to maintain beam current at a desired level. The helium bag reduces electron scatter in air. The film is mounted on a PMMA plate to provide mechanical support.

4.3.2 Vickers electron beam experimental setup and the motivation for film measurement.

In Vickers electron profile measurements, electron scattering foils made of Al, Cu, Ti, and Au were mounted in front of the exit window one at a time to produce a scattered electron field at the detector plane. For EBT film measurements, 20 MeV electron beam was used, as both ionization chamber measurements and Monte-Carlo simulation results were available for the energy of 20 MeV. The experimental setup is shown in Figure 4.6, where a helium bag is positioned between scattering foil and detector plane to reduce the scattering in air, and a monitor chamber was placed in the beam axis to provide beam control feedback. Compared to a clinical Linac, the elements in the beam path are kept to a minimum to allow accurate description of every element in a Monte Carlo simulation using EGSnrc (Kawrakow, 2000). In previous work, one-dimensional dose profiles were measured with an Exradin A16 ionization chamber mounted on a Velmex linear translation stage. Relative dose profiles were recorded and compared to dose to water profiles calculated in the Monte Carlo simulation. Both ionization chamber measurements and Monte Carlo simulations were normalized to the peak, as the beam was assumed to be circular. The drawback of ionization chamber scanning is the difficulty in measuring two-dimensional dose profiles. Mounting the Velmex translational stage vertically is inconvenient and is not performed for every scattering foil. Even when the vertical dose profile is measured, the collection of only two orthogonal profiles can still miss unexpected structures in the beam. Therefore, complete two-dimensional dose matrixes were desired for verifying the circular symmetry assumed in the Monte Carlo simulations.

Another motivation for EBT film dosimetry is the reported disagreement between Monte Carlo simulations and ionization chamber scan measurements. As reported by Ross *et al*, relative dose profiles predicted by EGSnrc were on average 1.5 % narrower than profiles measured by ionization chamber scan. It is therefore desirable to measure dose profile with another detector to provide further insight on this disagreement.

With the goals of verifying circular symmetry and shedding light on the discrepancy, we applied our radiochromic film dosimetry protocol to the Vickers electron beam dose profile measurement.

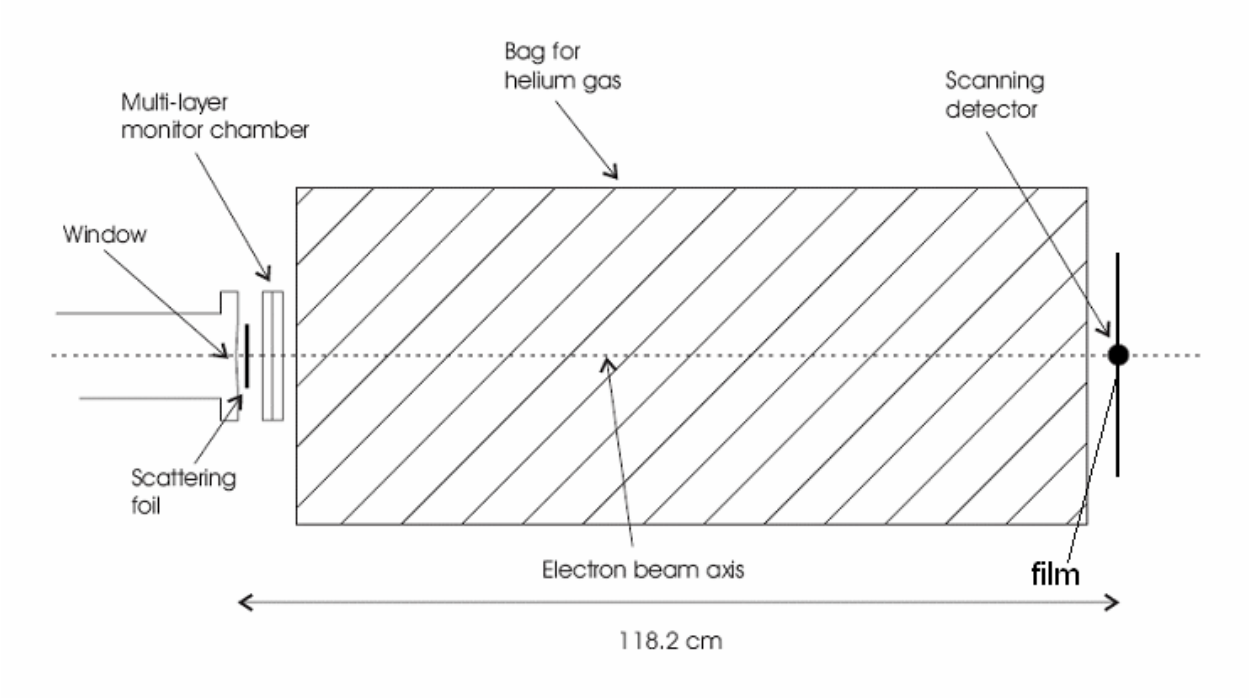

Figure 4.6. Experimental setup of Vickers electron profile measurement, published by Ross *et al* and modified to add the illustration of film position. Note that scanning chamber is mounted during in-air chamber measurements, and EBT film is mounted during film measurements. The two types of detectors are never mounted at the same time.

4.3.3 Vickers electron beam dose profile measurement using EBT films

As seen in Figure 4.6, a 20 x 20 cm sheet of EBT film was mounted perpendicular to the beam axis at the same distance from the beam exit window as the center of the A16 ionization chamber in previous experiments. To provide mechanical support, EBT films were taped to a 1 mm thick sheet of PMMA. The PMMA backing is expected to have an effect on the backscatter conditions of the beam, but this effect should be negligible for relative dose profile measurements. To confirm our assumption, the effect of this PMMA sheet was investigated by comparing a relative dose profile measured with a PMMA backing against a relative dose profile measured without a PMMA backing. In the measurement without a PMMA backing, a rectangular PMMA sheet with the center portion removed was used to provide support for the EBT film. A dose profile of the beam without any scattering foil (i.e. accelerator exit window only) was measured with both setups, and the results are shown in Figure 4.7a and 4.7b, where both profiles were normalized to the center of beam and folded around the origin to magnify any differences observed. The differences between the two profiles were on the level of film uniformity. Based on this result, we concluded that the PMMA has no significant effect on the measured dose profile. Due to the better mechanical support provided by a PMMA backing, it was used in all subsequent measurements.

Before quantitative analysis was performed, we visually inspected two-dimensional dose profiles produced by each scattering foil, looking for unexpected structures in the beam. Each 20 x 20 cm sheet of EBT film was scanned 24 hours after irradiation, and the image was first converted into a net optical density matrix. A two-dimensional dose matrix with 1.3 x 1.3 mm^2 spatial resolution was then derived from the optical density matrix. The level of spatial resolution was chosen to minimize the single-pixel noise caused by microstructures of EBT crystal. Using the value of dose as the z-axis, three-dimensional plots were produced in Matlab. Visual inspection of all dose profiles produced by various scattering foils showed no detectable structures in the beam, and the dose profile appeared circular for all measurements. To help locate the

center of the beam, a contour of the dose matrix at a level equal to 50 % of peak dose was obtained using Matlab's contour feature. The contours obtained in all dose matrixes were highly circular, which allowed us to fit the contour line to a circle and locate the exact center of the beam. An example of contour provided by Matlab is shown in Figure 4.8. Using the beam center located by the contour and circle fit method, the horizontal and vertical dose profiles were extracted from the dose matrix. The extracted profiles were compared to each other to verify the circular symmetry of the beam in a quantitative manner. Figure 4.9a and 4.9b showed the typical extracted profiles and the result of their subtraction. After examining dose profiles produced by all scattering foils, we concluded that all scattered electron profiles are circular to the level of film uniformity and the circular symmetry assumed in Monte Carlo was valid. Note that the complete two-dimensional dose profile obtained in EBT measurements helped us locate the center of the beam after the experiment, rather than relying on laser alignment techniques during the experiment, as it was done for the ionization chamber scans. Therefore EBT measurements provide higher levels of confidence on spatial accuracy, as it does not rely on accurate positioning of detector during the experiment.

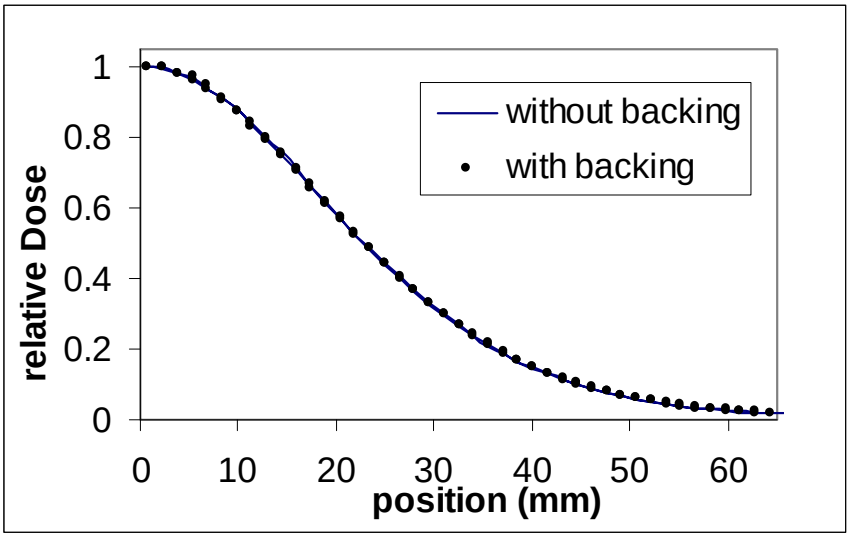

Figure 4.7a. Effect of PMMA backing.

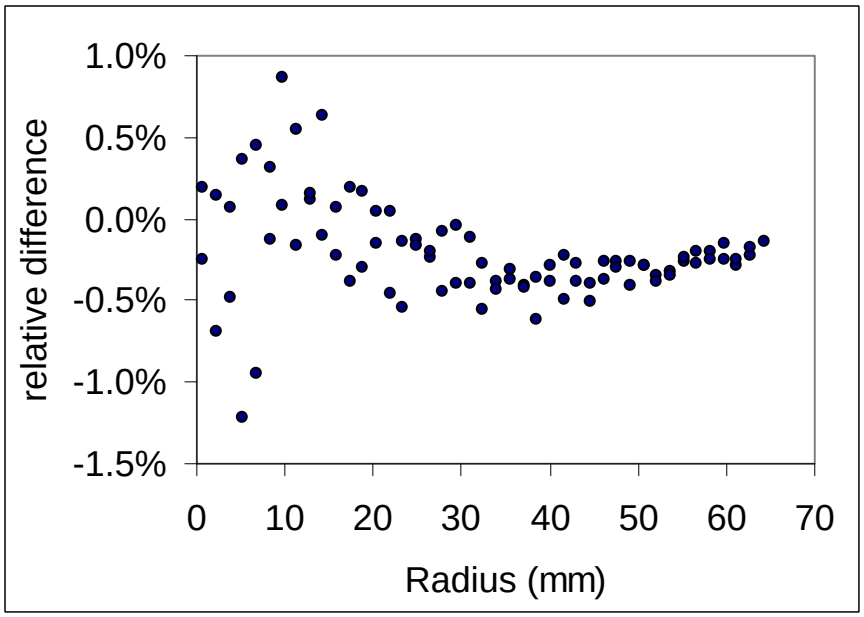

Figure 4.7b. Difference of the two relative profiles shown in 4.7a.

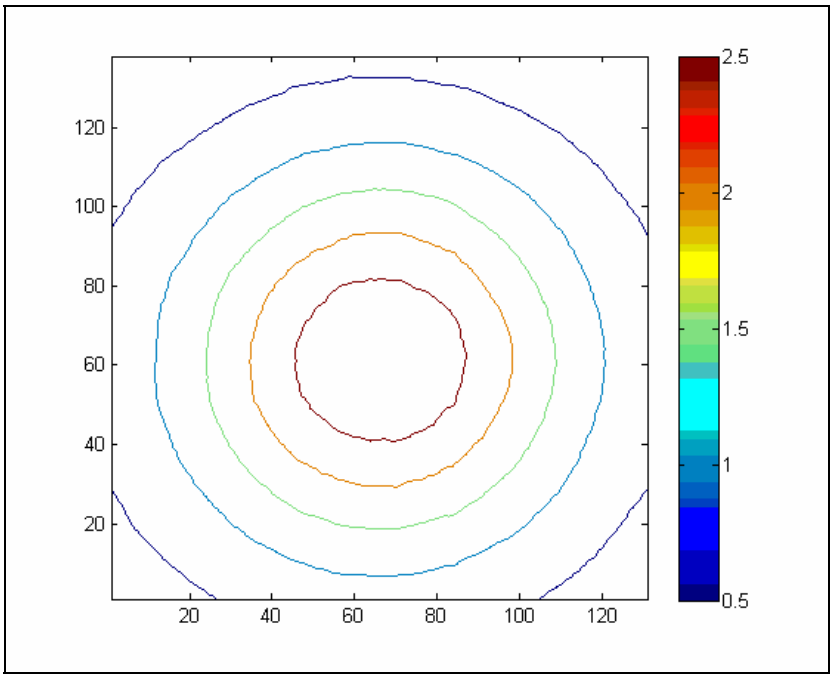

Figure 4.8. Typical contour produced by Matlab's contouring algorithm. The x-y scale shown corresponds to pixels and is arbitrary. The false color scale has unit of Gray.

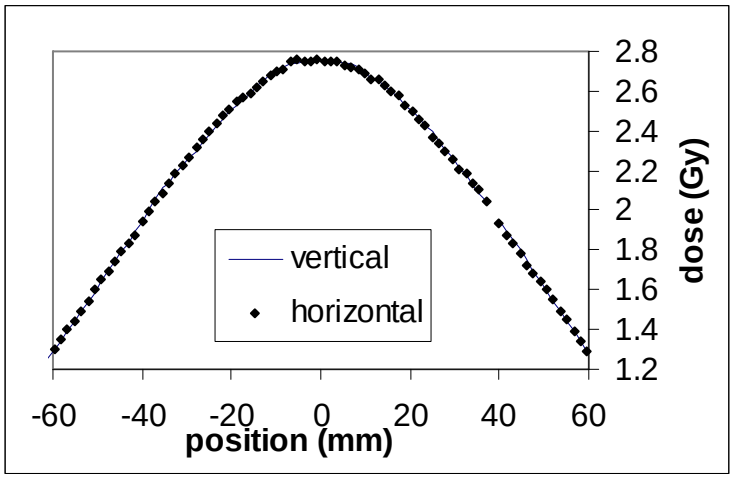

Figure 4.9a. Comparison of vertical and horizontal dose profiles from Al scattering foil experiment. The gap on the graph was due to a scratch on the EBT film

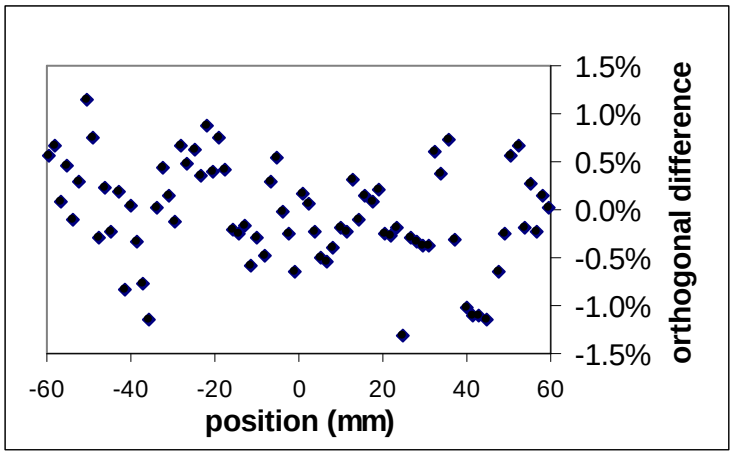

Figure 4.9b. Difference of vertical and horizontal dose profiles shown in above figure. The beam is circular to the level of film uniformity.

4.3.4 Comparison of EBT profile measurements with ionization chamber measurements & Monte-Carlo simulation

Having confirmed the circular symmetry assumed in Monte Carlo simulations, we proceeded to compare dose profiles measured with EBT film with ionization chamber measurements & Monte Carlo simulation. Electron dose profiles extracted from the 2D dose matrix measured by EBT films were normalized to the peak and compared to relative dose profiles measured by ionization chamber scans and Monte-Carlo simulations. In Ross *et al*'s paper (2008), the difference between ionization chamber and Monte-Carlo profiles were quantified by comparing the distances required for the relative dose to fall to 1/e. The EBT film's 20 x 20 cm form factor means that profiles don't extend to relative dose levels as low as 1/e for many of the scattering foils used. Due to this dimensional limit, the section of relative dose profiles between 0.4 and 0.7 is used for matching EBT film profiles and Monte-Carlo simulations, because the broadest electron dose distribution extends to 40 % of peak dose at the edge of the EBT film. A scaling factor was applied to the spatial dimension of the EBT film's relative dose profile so that this region of the film dose profile achieves the best agreement with Monte Carlo simulation. Figure 4.10a and Figure 4.10b showed the relative dose profiles from EBT film measurement, scanning ionization chamber measurement, and Monte Carlo simulation. On average, dose profiles measured by EBT films appear narrower than that predicted by Monte Carlo simulations, while profiles measured by ionization chamber scans are broader than Monte Carlo simulations. Note that due to the limited uniformity of the EBT film, the difference between EBT measurements and Monte Carlo simulations are not statistically significant. The difference between EBT film and ionization chamber measurements, however, is statistically significant. Table 4.3 provides a summary of scaling factors needed to match ionization chamber scans to Monte Carlo simulations. The positive values of scaling indicate that film profiles are narrower than Monte Carlo simulation results. Based on the four materials investigated, no obvious trend with atomic number of foil was observed. The

reason behind the discrepancies between film and ionization chamber measurements remains to be resolved.

Note that the Monte Carlo simulation does not include the presence of film or the composition of the film. Instead, the EBT film is assumed to be a particle fluence detector. Further work is required to further investigate the effect of film thickness and composition on the dosimetry.

We would like to raise the issue of the cost of film for this experiment. For each scattering foil, at least one sheet of EBT film is required for measurement. If uncertainties lower than the uniformity of the film is desired, three or four sheets of film will be required for each foil. Ross *et al* (2008) reported electron scattering measurements with more than 20 foils of different atomic numbers and thicknesses, using ionization chamber scans in air. Repeating the experiments for all foils with EBT film is a costly proposal, as each sheet of film costs $20 CDN at time of writing. Therefore only four foils of different atomic numbers are investigated in this experiment.

In future work, strips of EBT film can be used instead of whole sheets of film. By irradiating several strips of EBT film at the same time and taking the average of dose profiles measured, we can reduce the uncertainty due to film uniformity fluctuations without using too many sheets of films.

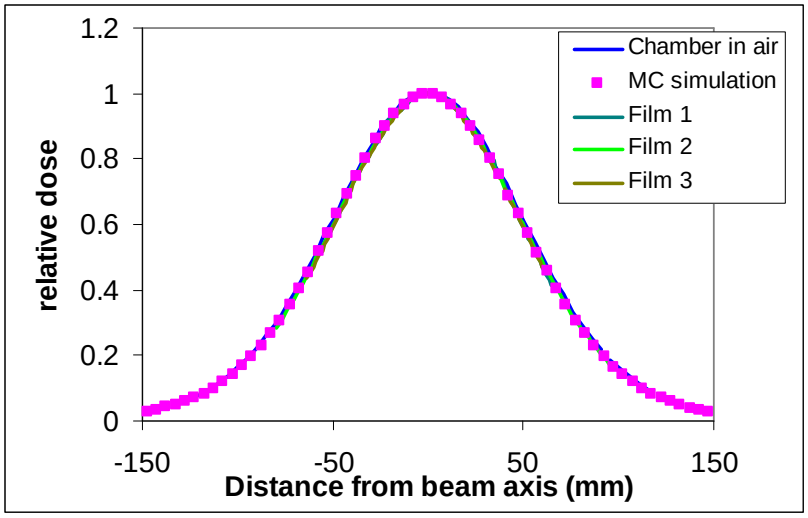

Figure 4.10a. Comparison of Aluminum foil's relative dose profile obtained from film, ionization chamber, and Monte Carlo simulation. All profiles are normalized to the center of the beam.

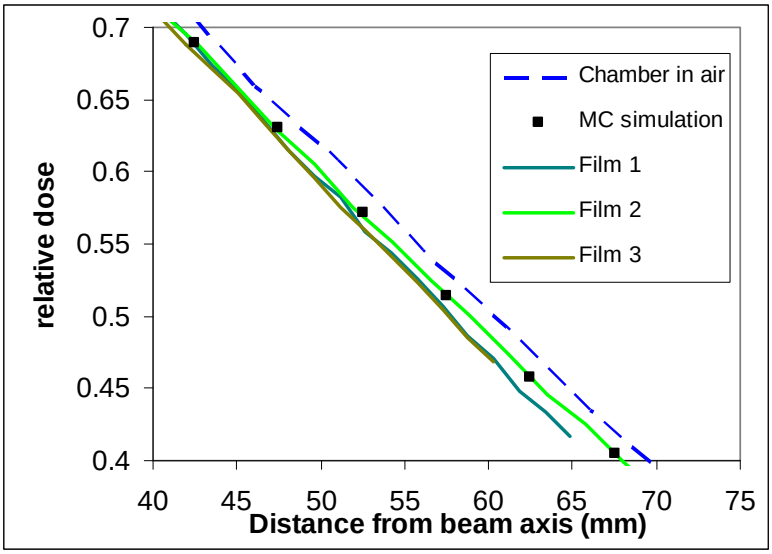

Figure 4.10b. A zoom-in view of the Figure 4.10 a.

Foil	Scaling Factor
Al	1.013
Ti	1.020
Cu	1.015
Au	0.997

Table 4.3 Scaling factor required to match the EBT film measurement with the Monte Carlo simulations. The scaling factor refers to the number multiplied to the X-axis of the film profile in order to match Monte-Carlo simulation.

4.4 Vickers X-ray measurements

4.4.1 Vickers X-ray relative dose profile measurements using EBT film

Besides electron profile measurements, the Vickers linear accelerator has been used to produce x-ray beams for Monte-Carlo benchmarking. In x-ray experiments, the electron scattering foils were replaced by thick, full-stopping x-ray targets of various materials. In this experiment, dose profiles of x-ray beams produced by Be, Al, Cu, Ta, and Pb targets were measured. The Helium bag shown in Figure 4.6 was removed, as in-air scattering was not a concern for x-ray beams.

A Farmer-type ionization chamber was used to measure the relative dose profile in-air. Unlike electron measurements, however, the ionization chamber was equipped with a 4 cm radius cylindrical PMMA build-up cap to provide sufficient build-up. To mimic this experimental geometry, a 20 x 20 cm sheet of EBT film was placed inside a Virtual Water phantom with 5 cm buildup and more than 5 cm of Virtual Water backscatter. Although the geometries are not identical in ionization chamber scans and EBT film measurements, the condition of full build-up allows us to assume that, to first approximation, both detectors are measuring the relative photon fluence of the beam. At the very least, EBT film can provide validations of circular symmetry assumed in Monte-Carlo simulations. Due to the weight of the build-up cap, no vertical profiles have been measured in the x-ray ionization chamber scan experiments.

4.4.2 Circular symmetry validation with EBT films

Similar to EBT film measurements in electron beams, the complete 2D dose profiles obtained by EBT films can be used to verify the circular symmetry assumed in Monte-Carlo simulations. A typical two-dimensional x-ray dose profile is shown in Figure 4.11. The two-dimensional dose profiles were visually inspected to check for unexpected structures in the beam. Overall, the x-ray profiles are broader than electron scatter profiles, and the profiles do not resemble a Gaussian distribution. A comparison of electron and x-ray dose profiles is shown in Figure 4.12. The reduced gradient in the profile means that fluctuations

due to film uniformity have a larger effect in contouring algorithms. After failing to obtain a circular contour of the beam, we resorted to recording the beam center provided by a laser positioning system with ink marks during the experiment. Vertical and horizontal dose profiles were extracted from the two-dimensional dose profiles based on the ink markers and compared against each other. The x-ray beams were confirmed to be circularly symmetric at the level of film uniformity.

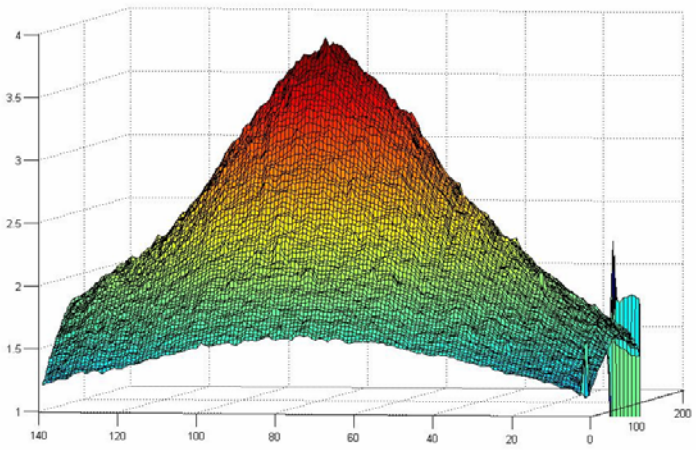

Figure 4.11. Typical example of two-dimensional dose profile measured by EBT film. Note that such "eye candies" only provide qualitative information about circular symmetry of beam.

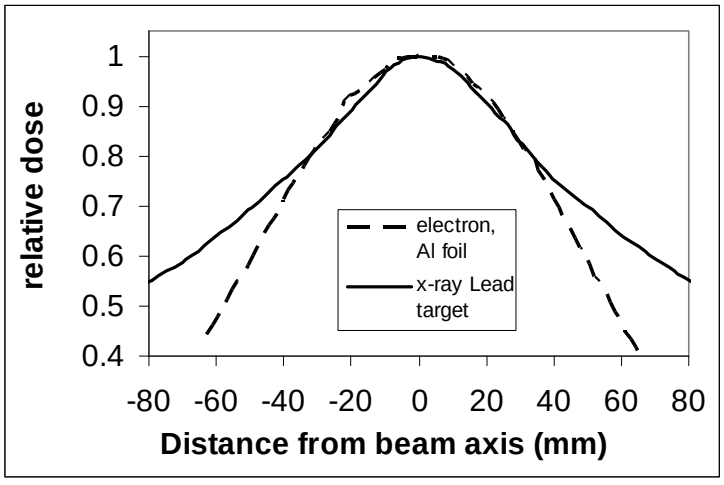

Figure 4.12. Comparison of electron and x-ray relative dose profiles. Aluminum foil and Lead target profiles are shown here.

4.4.3 Introduction of PTW Starcheck™

To provide another method of dose profile measurement, an ionization chamber based detector array, the PTW Starcheck, was also used for dose profile measurements in the Vickers x-ray beams. The Starcheck consists of four arrays of parallel plate chambers arranged in a star-like pattern. Each detector is 2 mm by 8 mm in length and width, and 5 mm in height. Detector spacing is 3 mm for all detector arrays. The Starcheck is pre-calibrated by the vendor with quoted relative response uncertainty of 0.5 %. In this experiment, the Starcheck was used to measure relative dose profiles of the Vickers x-ray beam at 5 cm depth in a Virtual Water phantom. The profiles measured by Starcheck provided additional comparison with ionization chamber scans and Monte-Carlo simulations. For absolute dose measurements, the Starcheck was supplied with a calibration in Co-60 beam, with uncertainty of 1.1 %. In order to use Starcheck for absolute dose measurements on the Vickers accelerator, we calibrated it in the Elekta 25 MV beam using a calibrated Exradin A19 Farmer type chamber, as it has beam quality closest to x-ray beam produced by various targets in Vickers x-ray experiment.

4.4.4 Dose profile measurements using EBT film strips

Due to the broader dose profiles produced by the Vickers x-ray beam, film sensitivity fluctuations had a greater impact on relative dose profiles in X-ray measurements than in electron measurements. To offset this effect, averaging of four film strips were used in the quantitative X-ray profile measurement. Four pieces of film, 5 cm by 20 cm each, were stacked one on top of another and irradiated at once. These films were then scanned sequentially at the same position on the scanner 24 hours after the irradiation. A dose profile is extracted over an 8 mm strip to match the detector width of Starcheck. EBT film profiles were compared to Starcheck measurements, ionization chamber scans, and Monte Carlo simulations. Compared to other detectors, EBT films provided the best agreement with Monte-Carlo simulations for all five targets investigated. However, the different geometries employed in EBT film measurements and Monte-Carlo simulations meant that Monte Carlo simulations based on

geometries employed in film experiments are needed before any definite conclusions can be made. Currently Monte Carlo simulations are performed using the geometries employed in in-air ionization chamber scans with a build-up cap, but simulations of virtual water phantom setup can be performed in the future. Figure 4.13 shows a typical example of dose profile comparison between Monte-Carlo, EBT, in-air scan, and Starcheck. Dose profiles measured by EBT films also agreed with profiles measured by Starcheck, within the calibration uncertainty of Starcheck. Here we demonstrated the lower potential uncertainties achievable by EBT film, due to the ability to use multiple films for a single measurement and taking the average of the results to reduce the effect of poor film uniformity.

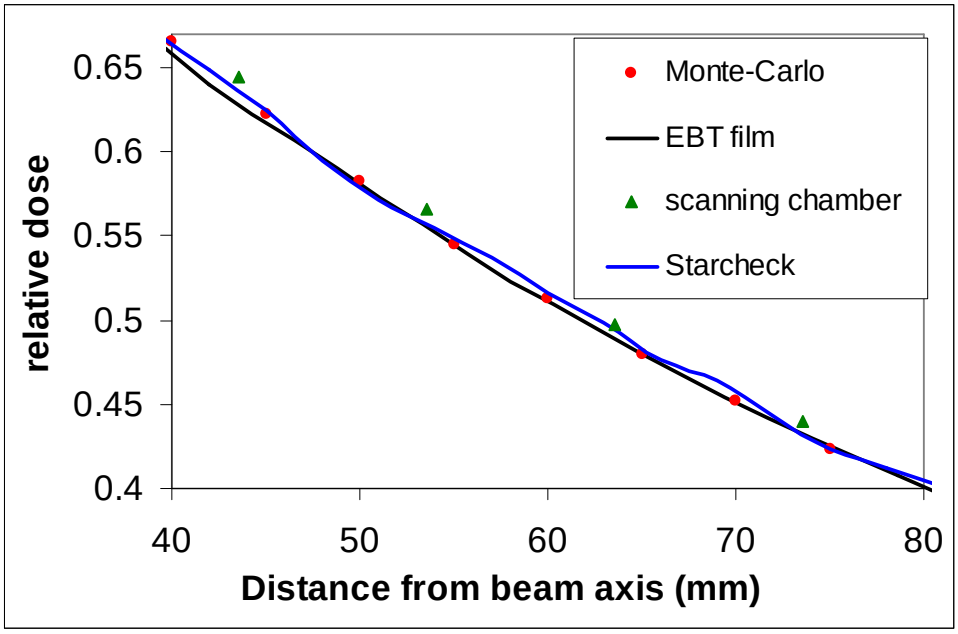

Figure 4.13. Dose profile comparison between EBT film, in-air chamber scans, Starcheck, and Monte-Carlo. All profiles are normalized to the beam axis.

4.4.5 Comparison of absolute dose per electron measurements in photon beam

As we described previously, the Vickers accelerator is capable of measuring the beam current, or the total number of electrons leaving the exit window. In this experiment, we measured the dose per electron values using both EBT film and the Starcheck beam profiler in a Virtual Water phantom. Due to the dose gradient of the Vickers X-ray beam, we used the averaged dose over a 2 mm by 8 mm area in the center of the beam to match the dimension of Starcheck's central chamber. Figure 4.14 displays a summary of dose per electron measurements using film and Starcheck for all five targets. The unit on the Y-axis is Gy per μC. Note that the absolute dose per electron increases from Be to Ta, but goes down for Pb. This variation is due to the mass-thicknesses of the different targets, which are not matched to the energy of the incident electron pencil beam. The important result of Figure 4.14 is the difference between the two data sets representing Starcheck and film. The dose difference increases with the atomic number of the target.

By taking 2 mm by 8 mm dose averages at various positions near the peak in film dose profile, we determined that a 2 mm uncertainty in Starcheck alignment results in a 0.7 % uncertainty in measured absolute dose. Therefore we estimated that the absolute dose measured by Starcheck has an uncertainty of less than 1 %. A single piece of film has a 1.5 % uncertainty in absolute dose measurement, largely due to film sensitivity fluctuations, but in this experiment, averaging of four pieces of film reduces this to 0.9 %. The observed difference between EBT film and Starcheck absolute dose per electron measurement varies from 1.3 % for Be to 5.4 % for Pb, with film showing higher doses. The observed difference in dose per electron is greater than our estimated uncertainty, and the cause of this difference requires further investigation. However, one potential cause is the beam quality dependence of Starcheck calibration. This result demonstrates the benefits of EBT film’s energy and beam modality independence, as it can be used to measure absolute dose of beams whose spectrum is unknown.

The purpose of this analysis is to demonstrate the feasibility of reference dosimetry using EBT film. To resolve the discrepancy between EBT film and Starcheck measurements, a Farmer-type ionization chamber can be placed at 5 cm depth to provide a more reliable absolute dose per electron measurement. This measurement should be a priority in future experiments.

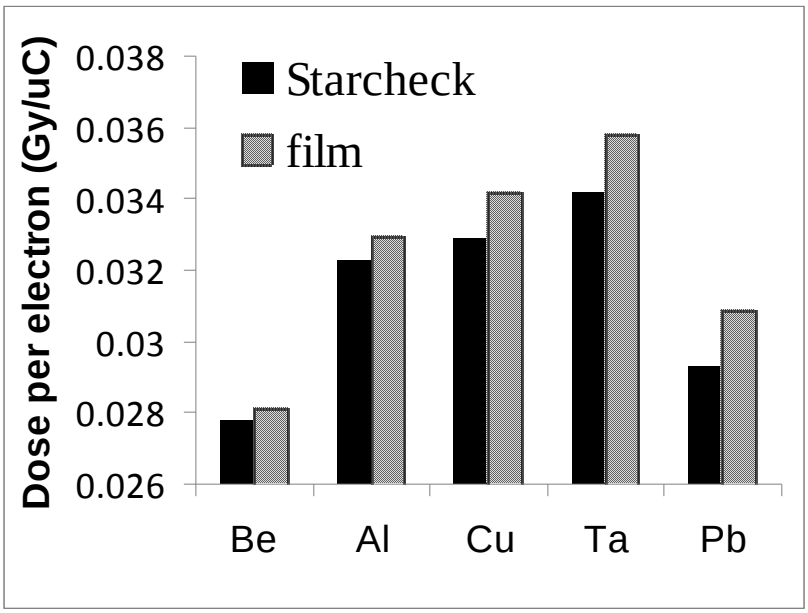

Figure 4.14. Comparison of dose per pulse measured by Starcheck and EBT film in X-ray beam produced by five different targets.

4.5 Conclusions on Vickers experiment

This EBT film dosimetry protocol was established for reference and relative dose profile measurements in Vickers electron and photon beams. Our initial results have demonstrated that EBT film provides direct experimental evidence of the circular symmetry of both electron and photon beam. For quantitative dose profile measurements, EBT film provides an alternative method of dose measurement to in-air ionization chamber scans.

For future work on this project, the effort should be concentrated on the x-ray measurements. Monte Carlo simulation of the x-ray measurements using EBT films should be performed. By matching the geometries employed in experiments and simulations, we can potentially resolve the discrepancy between simulations and ionization chamber measurements. The absolute dose per electron profiles calculated by Monte Carlo simulation can be compared to that measured by EBT film, rather than normalizing both profiles to the center of the beam. The direct comparison of absolute dose profiles in simulation and measurement can help shed light on the currently unresolved discrepancy between ionization chamber scans and Monte Carlo simulations.

The two drawbacks of EBT films are the high cost and limited size of the film. The high cost can be reduced by using a single strip of film rather than a whole sheet of film, but reliable spatial positioning techniques need to be developed before thin strips of film can replace whole sheets of film. The limited size of the film can be partially offset by mounting a square sheet of EBT film diagonally, so that the width of the dose profiles measured can be increased by a factor of 1.4. The geometric accuracy of such approach should be verified before the result can be trusted.

Chapter 5 Conclusion

We successfully commissioned a GafChromic EBT protocol at NRC. Several aspects of EBT film dosimetry presented in the literature have been investigated. An EBT film dosimetry system consists of the EBT films and a scanner. We purchased the Epson Expression 10000XL scanner, which is recommended by the vendor of EBT film, and our measurements revealed that the 10000XL showed equal or better performances than that reported for the Epson 1680Pro scanner, which is the most widely reported scanner in the literature. We confirmed that the scanner lamp does not permanently darken the EBT film in any measurable way, and any apparent darkening during repeated scanning can be attributed to the effect of rising temperature of the scanner bed. For the Epson 10000XL scanner, this temperature effect can be ignored at our chosen scanning resolution. By repeatedly scanning a single piece of EBT film, we characterized the scanner fluctuation described in the literature, and found it to be a two-state process that can be corrected with a reference piece procedure. Such correction allowed us to achieve a 0.3 % or better reproducibility in scanning the same piece of film. This excellent reproducibility in scanning allowed us to investigate the darkening of EBT film in both the first 24 hours and up to three months after irradiation. We confirmed that most of the darkening of EBT film occurs during the first 24 hours, as reported in literature. We also showed that up to a 5 % increase in net optical density can be observed after the first 24 hours, and this long-term darkening appears to be dependent on the environmental history of EBT film after irradiation. The good reproducibility in scanning a single piece of film also allowed the accurate characterization of the scanner uniformity, a topic that has been extensively reported in literature but no consensus has been reached. We reported that longitudinal correction of scanner is negligible at the 0.2 % level. The lateral correction of the scanner was found to be non-symmetric, which is contrary to current assumptions. We also discovered that a single equation can be used to describe the lateral corrections for all dose levels between 1 Gy and 8 Gy, and this allowed us to implement a scanner uniformity correction protocol with a single equation. We established a calibration protocol similar to ones reported in

the literature, and confirmed that a four parameter polynomial can be used to accurately describe the calibration curve. We confirmed the energy and beam modality independence of EBT film in megavoltage x-ray and electron beams, which was assumed in the literature and claimed by the vendor. This energy independence allowed us to apply EBT films calibrated in the Elekta accelerator to Vickers accelerator experiments. After applying all corrections reported in the literature, we concluded that the dominant limit to the accuracy of EBT film dosimetry is the uniformity of EBT film's sensitive layer. This fluctuation in EBT film's sensitivity is at the 2 % level and can not be reduced through pre-scanning. Currently the solution to this sensitivity fluctuation is irradiating multiple pieces of EBT films and averaging of the results.

Having established a protocol, we applied it in several situations: Cobalt Junior QA work and Vickers accelerator experiments in Monte Carlo benchmarking. In Vickers experiments, EBT films provided direct validation of circular symmetry of both electron and photon beams produced by the accelerator, which has been assumed in Monte Carlo simulations. In addition, EBT film measurements provided an alternative method of measuring relative dose profiles of the Vickers accelerator, serving as a complement to ionization chamber based measurements.

Bibliography

P. R. Almond, P. J. Biggs, B. M. Coursey, W. F. Hanson, M. Saiful Huq, R. Nath, and D. W. O. Rogers, "AAPM's TG-51 protocol for clinical reference dosimetry of high-energy photon and electron beams", Med. Phys. **26,** 1847-1870 (1999)

M. Anton, R. Peter Kapsch, M. Krystek and F. Renner, "Response of the alanine /ESR dosimetry system to MV x-rays relative to ^{60}Co radiation", Phys. Med. Biol. **53** 2753-2770 (2008)

L. J. van Battum, D. Hoffmans, H. Piersma, and S. Heukelom, "Accurate dosimetry with GafChromicTM EBT film of a 6 MV photon beam in water: What level is achievable?", Med. Phys. **35,** 704-716 (2008)

H. Bouchard, F. Lacroix, G. Beaudoin, J. Carrier, and I. Kawrakow, "On the characterization and uncertainty analysis of radiochromic film dosimetry", Med. Phys. **36,** 1931-1946 (2009)

M. J. Butson, T. Cheung, and P. K. N. Yu, "Absorption spectra variations of EBT radiochromic film from radiation exposure," Phys. Med. Biol. **50**, N135–N140 (2005).

M. J. Butson, T. Cheung, and P. K. N. Yu, "Weak energy dependence of EBT gafchromic film dose response in the 50 kVp-10 MVp x-ray range," Appl. Radiat. Isot. **64**, 60–62 (2006).

S. Chiu-Tsao, T. Duckworth, C. Zhang, N. S. Patel, C. Hsiung, L. Wang, J. A. Shih, and L. B. Harrison, "Dose response characteristics of new models of GafCHromic films: Dependence on densitometer light source and radiation energy," Med. Phys. **31**, 2501–2508 (2004).

S. Chiu-Tsao, Y. Ho, R. Shankar, L. Wang, and L. B. Harrison, "Energy dependence of response of new high sensitivity radiochromic films for megavoltage and kilovoltage radiation energies," Med. Phys. **32**, 3350– 3354 (2005).

S. Chiu-Tsao, Medich, and Munro III, “GAFCHROMIC® EBT film for ^{125}I seed dosimetry” Med. Phys. **35,** 704-716 (2008).

S. Chiu-Tsao and M Chan, “Depth Dose and Profile Characteristics in the Superficial Buildup Region Near Air Interface”, Med. Phys. **35** 2727 (2008)

H Chung, B Lynch, and S Samant, “High precision GafChromic based clinical dosimetry using standard flat bed scanner”, Med. Phys. **35** 2786 (2008)

F Crop, B Van Rompaye, L Paelinck, L Vakaet, H Thierens and C De Wagter, “On the calibration process of film dosimetry: OLS inverse regression versus WLS inverse prediction”, Phys. Med. Biol. **53**, 3971-3984 (2008)

S. Devic, J. Seuntjens, G. Hegyi, E. B. Podgorsak, C. G. Soares, A. S. Kirov, I. Ali, J. F. Williamson, and A. Elizondo, “Dosimetric properties of improved GafChromic films for seven different digitizers”, Med. Phys. **31**, 2392–2401 (2004).

S. Devic, J. Seuntjens, E. Sham, E. B. Podgorsak, C. Ross Schmidtlein, A. S. Kirov, and C. G. Soares, “Precise radiochromic film dosimetry using a flat-bed document scanner”, Med. Phys. **32**, 2245–2253 (2005)

S. Devic, J. Seuntjens, W. Abdel-Rahman, M. Evans, M. Olivares, E. B. Podgorsak, Té Vuong, and C. G. Soares, “Accurate skin dose measurements using radiochromic film in clinical applications,” Med. Phys. **33**, 1116–1124 (2006).

S. Devic, N. Tomic, Z. Pang, J. Seuntjens, E. B. Podgorsak, and C. G. Soares, “Absorption spectroscopy of EBT model GafChromic film,” Med. Phys. **34**, 112–118 (2007).

C. Fiandra, U. Ricardi, R. Ragona, S. Anglesio, F. R. Giglioli, E. Calamia, and F. Lucio, “Clinical use of EBT model GafChromic film in radiotherapy,” Med. Phys. **33**, 4314–4319 (2006).

M. Fuss, E. Sturtewagen, C. deWagter, and D. Georg, “Dosimetric characterization of GafChromic EBT film and its implication on film dosimetry quality assurance,” Phys. Med. Biol. **52**, 4211–4225 (2007).

P. W. Hoban, M. Heydarian, W. A. Beckham and A. H. Beddoe, “Dose rate dependence of a PTW diamond detector in the dosimetry of a 6 MV photon beam”, Phys Med Biol. **39,** 1219-1229 **(**1994)

B. M. Keller, C. Peressotti, and J. Pignol, “Optical imaging analysis of microscopic radiation dose gradients in Gafchromic EBT film using a digital microscope”, Med. Phys. **35**, 3740-3747 (2008)

I. Kawrakow, "Accurate condensed history Monte Carlo simulation of electron transport. I. EGSnrc, the new EGS4 version", Med. Phys. **27,** 485-498 (2000)

N. V. Klassen , L. van der Zwan, and J. Cygler, “GafChromic MD-55: Investigated as a precision dosimeter”, Med. Phys. **24,** 1924-1934 (1997)

D. Lewis, “Gafchromic® EBT self-developing film for radiotherapy dosimetry,” International Specialty Products, Wayne, NJ, accessed August 2007, http://www.ispcorp.com

D. Lewis, “From EBT to EBT2”, invited talk at Ottawa General Hospital, April 2009

D. A. Low and J. F. Dempsey, “Evaluation of the gamma dose distribution comparison method,” Med. Phys. **30**, 2455–2464 (2003).

B. D. Lynch, J. Kozelka, M. K. Ranade, J. G. Li, W. E. Simon, and J. F. Dempsey, “Important considerations for radiochromic film dosimetry with flatbed CCD scanners and EBT GafChromic film,” Med. Phys. **33**, 4551–4556 (2006)

M. Martišíková, B. Ackermann and O. Jäkel, “Analysis of uncertainties in Gafchromic® EBT film dosimetry of photon beams”, Phys Med Biol, **53** 7013-7027 (2008)

M. R. McEwen and D. Niven, “Characterization of the phantom material Virtual Water in high-energy photon and electron beams”, Med. Phys. **33**, 876–887 (2006).

L. Menegotti, A. Delana and A. Martignano, “Radiochromic film dosimetry with flatbed scanners: A fast and accurate method for dose calibration and uniformity correction with single film exposure”, Med. Phys. **35**, 3078-3085 (2008)

L. Paelinck, W. De Neve and C. De Wagter, “Precautions and strategies in using a commercial flatbed scanner for radiochromic film dosimetry”, Phys. Med. Biol. **52**, 231–242 (2007).

C. K. Ross, M. R. McEwen, A. F. McDonald, C. D. Cojocaru and B. A. Faddegon, “Measurement of multiple scattering of 13 and 20 MeV electrons by thin foils", Med. Phys. **35**, 4121-4131 (2008)

A. Rink, I. Alex Vitkin, and D. A. Jaffray, “Energy dependence (75 kVp to 18 MV) of radiochromic films assessed using a real-time optical dosimeter” Med. Phys. **34**, 458–463 (2007)

A. Rink, D. F. Lewis, S. Varma, I. Alex Vitkin and D. A. Jaffray, “Temperature and hydration effects on absorbance spectra and radiation sensitivity of a radiochromic medium” Med. Phys. **35**, 4545-4555 (2008)

S. Saur and J. Frengen, “GafChromic EBT film dosimetry with flatbed CCD scanner: A novel background correction method and full dose uncertainty analysis” Med. Phys. **35**, 3094-3101 (2008)

F. Su, Y. Liu, S. Stathakisa, C. Shia, C. Esquivela, and N. Papanikolaoua, "Dosimetry characteristics of GAFCHROMICs EBT film responding to therapeutic electron beams", Applied Radiation and Isotopes **65**, 1187–1192 (2007)

E Wilcox, G Daskalov, and L Nedialkova, “The Influence of Scanner Parameters On the Accuracy of Film Dosimetry: A Comparison of the Epson Expression 1680 Flatbed and the Vidar VXR-16 Dosimetry PRO Film Scanners” Med. Phys. **34**, 2496-2496 (2007).

O. A. Zeidan, S. Stephenson, S. Meeks, T. Wagner, T. Willoughby, P. Kupelian, and K. Langen, “Characterization and use of EBT radiochromic film for IMRT dose verification,” Med. Phys. **33**, 4064–4072 (2006).